

International Journal of Modern Physics A
© World Scientific Publishing Company

DARK MATTER DETECTION IN THE LIGHT OF RECENT EXPERIMENTAL RESULTS

CARLOS MUÑOZ

*Departamento de Física Teórica C-XI and Instituto de Física Teórica C-XVI,
Universidad Autónoma de Madrid, Cantoblanco, 28049 Madrid, Spain.*

The existence of dark matter was suggested, using simple gravitational arguments, seventy years ago. Although we are now convinced that most of the mass in the Universe is indeed some non-luminous matter, we still do not know its composition. The problem of the dark matter in the Universe is reviewed here. Particle candidates for dark matter are discussed with particular emphasis on Weakly Interacting Massive Particles (WIMPs). Experiments searching for these relic particles, carried out by many groups around the world, are also reviewed, paying special attention to their direct detection by observing the elastic scattering on target nuclei through nuclear recoils. Finally, we concentrate on the theoretical models predicting WIMPs, and in particular on supersymmetric extensions of the standard model, where the leading candidate for WIMP, the neutralino, is present. There, we compute the cross section for the direct detection of neutralinos, and compare it with the sensitivity of detectors. We mainly discuss supergravity, superstring and M-theory scenarios.

Keywords: dark matter; supersymmetry; supergravity; superstrings, M-Theory.

1. Introduction

One of the most evasive and fascinating enigmas in physics is the problem of the dark matter in the Universe. Substantial evidences exist suggesting that at least 90% of the mass of the Universe is due to some non-luminous matter, the so-called ‘dark matter’. However, although the existence of dark matter was suggested 70 years ago, we still do not know its composition.

In 1933, the astronomer Fritz Zwicky¹ provided evidence that the mass of the luminous matter (stars) in the Coma cluster, which consists of about 1000 galaxies, was much smaller than its total mass implied by the motion of cluster member galaxies. However, only in the 1970s the existence of dark matter began to be considered seriously. Its presence in spiral galaxies was the most plausible explanation for the anomalous rotation curves of these galaxies, as we will discuss in detail in Section 2. In summary, the measured rotation velocity of isolated stars or gas clouds in the outer parts of galaxies was not as one should expect from the gravitational attraction due to the luminous matter. This led astronomers to assume that there was dark matter in and around galaxies. We will see that nowadays there is overwhelming observational evidence for the presence of dark matter. It

not only clusters with stellar matter forming the galactic halos, but also exists as a background density over the entire Universe. Thus the problem is no longer to explain the rotation curves but to decipher the nature of the dark matter. In any case, it is fair to say that some authors still suggest that dark matter is not necessary to explain the rotation curves. They try to avoid the introduction of this hypothesis modifying the Newton's law at galactic scales. Although these attempts are not very convincing, we will briefly discuss them

As we will explain in detail in Section 3, the search of the dark matter provides a potentially important interaction between particle physics and cosmology, since only elementary particles are reliable candidates for the dark matter in the Universe. In particular we will see that baryonic objects, such as e.g. gas, brown dwarfs, etc., can be components of the dark matter, but more candidates are needed. The reason being that they cannot be present in the right amount to explain the observed matter density of the Universe, $0.1 \lesssim \Omega h^2 \lesssim 0.3$. Fortunately, particle physics, and mainly extensions of the standard model offer candidates for dark matter. Indeed, detecting non-baryonic dark matter in the Universe might be a signal for new physics beyond the Standard Model. It is fair to say that many of these candidates are quite exotic and most of them are ephemeral. However, we will also see that very interesting and plausible candidates for dark matter are Weakly Interacting Massive Particles (WIMPs), since long-lived or stable WIMPs can be left over from the Big Bang in sufficient number to account for a significant fraction of relic matter density. As suggested in 1985 by Goodman and Witten², and also by Wasserman³, this raises the hope of detecting relic WIMPs directly.

WIMPs cluster gravitationally with ordinary stars in galactic halos, and therefore they must be present in our own galaxy, the Milky Way. As a consequence there will be a flux of these dark matter particles on the Earth, and experiments can be carried out to detect this flux by observing its elastic scattering on target nuclei through nuclear recoils. As we will mention, inelastic scattering is also possible but the event rates seem to be suppressed. Thus in Section 4 we will review the current and projected experiments for detecting WIMPs directly in underground laboratories. In fact, a dark matter experiment of this type, the DAMA collaboration^{4,5}, has reported data recently favouring the existence of a WIMP signal. It was claimed that the preferred range of the WIMP-nucleon cross section is $\approx 10^{-6} - 10^{-5}$ pb for a WIMP mass of about 100 GeV. Although this could be a great discovery, it is fair to say that this experiment is controversial, mainly because other collaborations reported negative search results. In particular, CDMS⁶, and more recently EDELWEISS⁷ and ZEPLIN I⁸, claim to have excluded important regions of the DAMA parameter space. In any case, the whole region allowed by DAMA will be covered by these and other experiments in the near future. Besides, there are projected experiments which will be able to measure a cross section as small as 10^{-9} pb. In addition, there are also promising methods for the indirect detection of WIMPs by looking for evidence of their annihilation, as we will briefly discuss. Thus it seems plausible that the dark matter will be found in the near future. Given this

situation, it is crucial to analyze in detail the present theoretical models predicting WIMPs.

In Section 5 we will review the situation concerning this point. In particular, we will concentrate on the leading candidate for WIMP, the lightest supersymmetric particle (LSP). As is well known, supersymmetry (SUSY)^{9,10} is a new type of symmetry, since it relates bosons and fermions, and this ensures the stability of the hierarchy between the weak and the Planck scales. This is the most relevant theoretical argument in its favour. In SUSY models the so-called R-parity is often imposed in order to avoid fast proton decay or lepton number violation. This yields important phenomenological implications. SUSY particles are produced or destroyed only in pairs and therefore the LSP is absolutely stable, implying that it might constitute a possible candidate for dark matter. So SUSY, whose original motivation has nothing to do with the dark matter problem, might solve it.

The first discussion of SUSY dark matter was by Goldberg¹¹ in 1983. He considered the SUSY fermionic partner of the photon, the photino, as the LSP and pointed out the strong constraints on its mass from its relic abundance. Soon followed two works considering also this possibility^{12,13}, but it was in Ref. 14 where the analysis of the most general case was carried out. In particular, one has to take into account that in SUSY the photino mixes with the fermionic partners of the Z^0 and the two neutral Higgs bosons. Therefore one has four particles called neutralinos, $\tilde{\chi}_i^0$ ($i = 1, 2, 3, 4$). Obviously, the lightest neutralino, $\tilde{\chi}_1^0$, will be the dark matter candidate. The fact that the LSP is chosen to be an electrically neutral particle (also with no strong interactions) is welcome since otherwise it would bind to nuclei and would be excluded as a candidate for dark matter from unsuccessful searches for exotic heavy isotopes. It is remarkable that in large regions of the parameter space of the simplest SUSY extension of the standard model, the so-called Minimal Supersymmetric Standard Model (MSSM), the LSP is indeed the lightest neutralino.

It is worth noticing here that several accelerator experiments are in preparation in order to detect SUSY particles. For example, LHC at CERN will probably start operations in 2007 producing energies about 1 TeV. Concerning the LSP, one will be able to detect events with SUSY particle decays which produce lots of missing energy. However, let us remark that, even if neutralinos are discovered in this way, only their direct detection in underground experiments due to their presence in our galactic halo will confirm that they are the sought-after dark matter of the Universe. As a matter of fact, given the present and projected experiments in underground laboratories in order to detect WIMPs, there may be a competition between these experiments and those in accelerators in the hunt for the first SUSY particle.

Thus we will review how big the cross section for the direct detection of neutralinos can be, in the generic context of the MSSM. In fact, the cross section for the elastic scattering of $\tilde{\chi}_1^0$ on nucleons has been examined exhaustively in the literature since many years ago¹⁵. Obviously, this computation is crucial to analyze the compatibility of the neutralino as a dark matter candidate, with the sensitivity

of detectors. In the light of the recent experimental results mentioned above, many theoretical works studying possible values of the cross section in different scenarios have appeared. Here we will concentrate on the most recent results in supergravity (SUGRA), superstring and M-Theory scenarios^{16–65}.

Let us recall that in the framework of SUGRA⁹ the scalar and gaugino masses and the bilinear and trilinear couplings are generated once SUSY is softly broken through gravitational interactions, and in addition radiative electroweak symmetry breaking is imposed. First, we will analyse this framework in the usual context of a Grand Unified Theory (GUT) with scale $M_{GUT} \approx 2 \times 10^{16}$ GeV and universal soft terms^{18,19,21,22,23,24,26,28,29,31,36,39,40,41,44,45,46,47,48,49,50,51,52,55,57,58,59,60,63,64,65}, the so-called minimal supergravity (mSUGRA) scenario. Second, we will discuss how the results are modified when the GUT condition is relaxed. In particular, we will consider the case of an intermediate scale^{33,35,42,46,51,63}, a possibility inspired by experimental observations and also by some superstring constructions. Then, a more general situation in the context of SUGRA, non-universal scalar^{18,21,29,34,39,44,46,49,51,55,61,63,64} and gaugino^{30,46,51,54,55,56,62,63} masses, will be studied. On the other hand, a phenomenological SUSY model, with parameters defined directly at the electroweak scale, the so-called *eff*MSSM, has also been studied in the literature^{16,25,36,37,38}. We will discuss this approach briefly.

Let us remark that in these analyses to reproduce the correct phenomenology is crucial. In this sense it is important to check that the parameter space of the different scenarios fulfills the most recent experimental and astrophysical constraints. Concerning the former, the lower bound on the Higgs mass⁶⁶, the $b \rightarrow s\gamma$ branching ratio⁶⁷, and the muon⁶⁸ $g - 2$ will be taken into account. The astrophysical bounds on the dark matter density mentioned above will also be imposed on the theoretical computation¹⁵ of the relic neutralino density, assuming thermal production. In addition, the constraints that the absence of dangerous charge and colour breaking minima imposes on the parameter space⁶⁹ will also be taken into account.

Finally, since generically the low-energy limit of superstring theory⁷⁰ is 4-dimensional SUGRA, the neutralino is also a candidate for dark matter in superstring constructions. Taking into account that the soft terms can in principle be computed in these constructions, we will review the associated $\tilde{\chi}_1^0$ -nucleon cross section. In particular we will discuss this first in the context of the (weakly-coupled) heterotic superstring^{17,39}. Then, we will consider D-brane configurations from the type I superstring^{27,30,32,35,42,46,51}, which are explicit scenarios where intermediate scales, and also non-universality of soft terms, may occur.

On the other hand, 4-dimensional SUGRA is also the low-energy limit of 11-dimensional M-Theory⁷¹. The latter has been proposed as the fundamental theory which contains the five 10-dimensional superstring theories, and, in particular, compactified on an orbifold is indeed the strong coupling limit of the $E_8 \times E_8$ heterotic superstring theory. Therefore, the same review for the cross section as above will be

carried out for this strongly-coupled heterotic superstring obtained from M-Theory^{20,43,53}, the so-called heterotic M-Theory. The conclusions are left for Section 6.

2. The dark matter problem

To compute the rotation velocity of stars or hydrogen clouds located far away from galactic centres is easy. One only needs to extrapolate the Newton's law, which works outstandingly well for nearby astronomical phenomena, to galactic distances. For example, for an average distance r of a planet from the center of the Sun, Newton's law implies that $v^2(r)/r = GM(r)/r^2$, where $v(r)$ is the average orbital velocity of the planet, G is the Newton's constant and $M(r)$ is the total mass inside the orbit. Therefore one obtains

$$v(r) = \sqrt{\frac{G M(r)}{r}}. \quad (1)$$

Clearly, $v(r)$ decreases with increasing radius since $M(r)$ is constant and given by the solar mass.

In the case of a galaxy, if its mass distribution can be approximated as spherical or ellipsoidal, Eq. (1) can also be used as an estimate. Thus if the mass of the galaxy is concentrated in its visible part, one would expect $v(r) = \sqrt{GM_{vis}/r} \propto 1/\sqrt{r}$ for distances far beyond the visible radius. Instead, astronomers, by means of the Doppler effect, observe that the velocity rises towards a constant value $v_c \approx 100$ to 200 km s^{-1} . An example of this can be seen in Fig. 1 (from Ref. 72), where the rotation curve of M33, one of the about 45 galaxies which form our small cluster, the Local Group, is shown. For comparison, the expected velocity from luminous disk is also shown. This phenomenon has already been observed for about a thousand spiral galaxies^{73,74,75}, and in particular also for our galaxy, the Milky Way. Although this observation is more problematic in galaxies other than spirals, such as ellipticals, dwarf irregulars, dwarf spheroidals, lenticulars, etc., they also produce similar results^{76,77,75}.

The most common explanation for these flat rotation curves is to assume that disk galaxies are immersed in extended dark matter halos. Thus for large distances $M(r)/r$ is generically constant because the mass interior to r increases linearly with r , $M_{tot}(r) = G^{-1}v_c^2 r$. In fact, a self-gravitating ball of ideal gas at an uniform temperature of $kT = \frac{1}{2}m_{\text{DM}}v_c^2$, where m_{DM} is the mass of one dark matter particle, would have this mass profile⁷⁸. In addition, dark matter is necessary to explain structure formation, as deduced from the cosmic microwave background measurements. Clumps of neutral particles arose first through gravitational attraction and later, when the neutral atoms were formed, these were gravitationally attracted by the dark matter to form the galaxies.

The above analysis of rotation curves implies that 90% of the mass in galaxies is dark. Whereas current observations of luminous matter in galaxies determine $\Omega_{\text{lum}} \lesssim 0.01$, analyses of rotation curves imply in fact $\Omega \approx 0.1$. Let us recall that $\Omega = \rho/\rho_c$ is the present-day mass density averaged over the Universe, ρ , in units

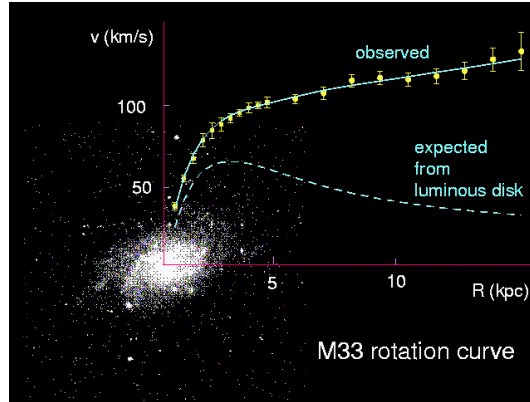


Fig. 1. Observed rotation curve of the nearby dwarf spiral galaxy M33, superimposed on its optical image.

of the critical density, $\rho_c = 10^{-5} h^2 \text{ GeV cm}^{-3}$, with $h \sim 0.7$. In fact, the previous value, $\Omega \approx 0.1$, is really a lower bound, since almost all rotation curves remain flat out to the largest values of r where one can still find objects orbiting galaxies. We do not really know how much further the dark matter halos of these galaxies extend (see e.g. Fig. 1). Thus we can conclude that galactic rotation curves imply $\Omega \gtrsim 0.1$.

Although the analysis of dark matter in cluster of galaxies becomes more involved than in galaxies, different techniques have been used to compute^{79,75} the value of Ω . For example, the conventional method of studying the motion of cluster member galaxies seems to point at values of Ω larger than those obtained in galactic scales. The high temperature of the gas detected in clusters through its X-ray emission also points at large amounts of dark matter. Finally, the more reliable method of studying the gravitational lensing confirms the previous conclusions. Here a cluster acts as a lens which distorts the light emitted by quasars and field galaxies in its background, due to the gravitational bending of light. All these analyses favour a value $\Omega \approx 0.2 - 0.3$. Moreover, measurements of velocity flows at scales larger than that of clusters favour⁷⁹ also very large amounts of dark matter: $\Omega > 0.3$. Thus the following astrophysical bounds are commonly used in the literature:

$$0.1 \lesssim \Omega_{\text{DM}} h^2 \lesssim 0.3 . \quad (2)$$

As a matter of fact, the lower part of this range seems to be preferred by comparing models with a set of cosmological observations^{80,81}. In particular, the (cold) dark matter range

$$0.094 \lesssim \Omega_{\text{DM}} h^2 \lesssim 0.129 , \quad (3)$$

can be deduced from the recent data obtained by the WMAP satellite⁸¹.

Clearly, any sensible candidate for dark matter must be able to reproduce the observations summarized by the above equations, i.e. it must be present in the right

amount to explain the observed matter density of the Universe. This is the issue that we will review in the next section.

Before finishing this section, it is fair to say that a small number of authors suggest that dark matter is not really necessary to explain rotation curves⁷⁷. Basically their approach consists of modifying the Newton's law at galactic scales. This has been done first in the pure classical theory^{82,83,84}. For example, in Ref. 83 the authors assume that the behaviour of the potential at galactic distances is $V \sim \ln r$. In the context of the relativistic theory, several authors have studied the modification induced to the scalar potential by higher-derivative gravity^{85,86}, or by a cosmological constant⁸⁷. These modifications have also been studied in other contexts, such as five dimensional gravity inspired in strings⁸⁸ (D-branes), and geodetic brane gravity⁸⁹. However, these attempts are not only rather ad hoc in general (the authors impose specific values for the free parameters of the theory in order to reproduce *some* of the rotation curves that have been observed) but also insufficient to account for the necessity of dark matter in scales larger than galactic ones⁹⁰ (values of the parameters necessary to reproduce galactic rotation curves cannot reproduce the observations at larger scales). Recently, the authors of Ref. 91, using the Sloan Digital Sky Survey, have shown the first observational evidence that the halo density decline as $1/r^3$, as predicted by cold dark matter cosmological models. Alternative theories of gravity are in contradiction with this result.

3. Dark matter candidates

Here we will review possible candidates for dark matter. Since ordinary matter is baryonic, the most straightforward possibility is to assume also this composition for the evasive dark matter. The contribution from gas is not enough, so astrophysical bodies collectively known as MAssive Compact Halo Objects (MACHOs) are the main candidates⁹². This is the case of brown and white dwarfs, Jupiter-like objects, neutron stars, stellar black hole remnants. However, the scenario of Big-Bang nucleosynthesis, which explains the origin of the elements after the Big Bang, taking into account measured abundances of helium, deuterium and lithium sets a limit to the number of baryons that can exist in the Universe, namely $\Omega_{\text{baryon}} h^2 \lesssim 0.05$. This density is clearly small to account for the whole dark matter in the Universe (see bounds (2)). The conclusion is that baryonic objects are likely components of the dark matter but more candidates are needed. This result is also confirmed by observations of MACHOs in our galactic halo through their gravitational lensing effect on the light emitted by stars. Their contribution to the dark matter density is small. Thus non-baryonic matter is required in the Universe.

Particle physics provides this type of candidate for dark matter. In principle, the three most promising are 'axions', 'neutrinos' and 'neutralinos' with masses of the order of 10^{-5} eV, 30 eV and 100 GeV, respectively. As a matter of fact, neutrinos are the only candidates which are known to exist. However, although the other

particles are not present in the standard model, they are crucial to solve important theoretical problems of this model. Thus they are well motivated by extensions of the standard model.

Before analyzing these three (standard) candidates, it is fair to say that many others have also been proposed. Although some of them are quite exotic, we will also discuss them in some detail below.

3.1. *Standard candidates*

3.1.1. *Neutrinos*

In recent years, observation of solar and atmospheric neutrinos have indicated that one flavour might change to another⁹³. As is well known, these neutrino oscillations can only happen if neutrinos have mass. The best evidence for neutrino masses comes from the SuperKamiokande experiment in Japan concerning atmospheric neutrino oscillations. The results of this experiment indicate a mass difference of order 0.05 eV between the muon neutrino and the tau neutrino. If there is a hierarchy among the neutrino masses (as it is actually the case not only for quarks but also for electron-like leptons), then such a small mass difference implies that the neutrino masses themselves lie well below 1 eV. This is not cosmologically significant as we will show below, since a light ($m_\nu \lesssim 100$ eV) neutrino has a cosmological density⁹⁴ $\Omega_\nu \approx m_\nu/30$ eV. On the other hand, there could be near mass degeneracy among the neutrino families. In this case, if neutrino masses $m_\nu \approx 30$ eV, they could still contribute significantly to the non-baryonic dark matter in the Universe.

These neutrinos left over from the Big Bang were in thermal equilibrium in the early Universe and decoupled when they were moving with relativistic velocities. They fill the Universe in enormous quantities and their current number density is similar to the one of photons (by entropy conservation in the adiabatic expansion of the Universe). In particular, $n_\nu = \frac{3}{11} n_\gamma$. Moreover, the number density of photons is very accurately obtained from the cosmic microwave background measurements. The present temperature $T \approx 2.725$ K implies $n_\gamma \approx 410.5$ cm⁻³. Thus one can compute the neutrino mass density $\rho_\nu = m_{tot} n_\nu$, where m_{tot} is basically the total mass due to all flavours of neutrino. Hence,

$$\Omega_\nu \approx \frac{m_{tot}}{30 \text{ eV}} . \quad (4)$$

Clearly, neutrinos with $m_\nu \lesssim 1$ eV cannot solve the dark matter problem, but a neutrino with $m_\nu \approx 30$ eV would give $\Omega_\nu \approx 1$ solving it. Unfortunately, due to the small energies involved, detection of these cosmological neutrinos in the laboratory is not possible.

However, even if $m_\nu \approx 30$ eV, there is now significant evidence against neutrinos as the bulk of the dark matter. Neutrinos belong to the so-called ‘hot’ dark matter because they were moving with relativistic velocities at the time the galaxies started to form. But hot dark matter cannot reproduce correctly the observed structure

in the Universe. A Universe dominated by neutrinos would form large structures first, and the small structures later by fragmentation of the larger objects. Such a Universe would produced a ‘top-down’ cosmology, in which the galaxies form last and quite recently. This time scale seems incompatible with our present ideas of galaxy evolution.

This lead to fade away the initial enthusiasm for a neutrino-dominated Universe. Hence, many cosmologists now favour an alternative model, one in which the particles dominating the Universe are ‘cold’ (non-relativistic) rather than hot. This is the case of the axions and neutralinos which we will study below.

3.1.2. Axions

Axions are spin 0 particles with zero charge associated with the spontaneous breaking of the global $U(1)$ Peccei-Quinn symmetry, which was introduced to dynamically solve the strong CP problem⁹⁵. Let us recall that this important problem arises because QCD includes in its Lagrangian the term $\frac{\theta}{16\pi^2} \text{tr}(F_{\mu\nu} \tilde{F}^{\mu\nu})$ violating CP, and therefore there are important experimental bounds against it. In particular, the stringent upper limit on neutron dipole electric moment implies the bound $\theta < 10^{-9}$. This is the problem. Why is this value so small, when a strong interaction parameter would be expected to be $\mathcal{O}(1)$?

Although axions are massless at the classical level they pick up a small mass by non-perturbative effects. The mass of the axion, m_a , and its couplings to ordinary matter, g_a , are proportional to $1/f_a$, where f_a is the (dimensionful) axion decay constant which is related to the scale of the symmetry breaking. In particular, the coupling of an axion with two fermions of mass m_f , is given by $g_a \sim m_f/f_a$. Likewise, $m_a \sim \Lambda_{\text{QCD}}^2/f_a$, i.e.

$$m_a \sim 10^{-5} \text{ eV} \times \frac{10^{12} \text{ GeV}}{f_a} . \quad (5)$$

A lower bound on f_a can be obtained from the requirement that axion emission does not over-cool stars. The supernova SN1987 put the strongest bound, $f_a \gtrsim 10^9$ GeV. On the other hand, since coherent oscillations of the axion around the minimum of its potential may give an important contribution to the energy density of the Universe, the requirement $\Omega \lesssim 1$ puts a lower bound on the axion mass implying $f_a \lesssim 10^{12}$ GeV. The combination of both constraints, astrophysical and cosmological, give rise to the following window for the value of the axion constant

$$10^9 \text{ GeV} \lesssim f_a \lesssim 10^{12} \text{ GeV} . \quad (6)$$

The lower bound implies an extremely small coupling of the axion to ordinary matter and therefore a very large lifetime, larger than the age of the Universe by many orders of magnitude. As a consequence, the axion is a candidate for dark matter⁹⁶. Axions would have been produced copiously in the Big Bang, they were never in thermal equilibrium and are always nonrelativistic (i.e. they are cold dark

matter). In addition the upper bound implies that $m_a \sim 10^{-5}$ eV if the axion is to be a significant component of the dark matter.

Since the axion can couple to two photons via fermion vacuum loops, a possible way to detect it is through conversion to photon in external magnetic field. Unfortunately, due to the small couplings to matter discussed above, we will not be able to produce axions in the laboratory. On the other hand, relic axions are very abundant (as we will discuss in Section 4, the density of dark matter particles around the Earth is about 0.3 GeV cm^{-3} , since $m_a \sim 10^{-5}$ eV there will be about 10^{13} axions per cubic centimeter) and several experiments are trying already to detect axions or are in project. For example, an experiment at Lawrence Livermore National Laboratory (California, US) has reported in 1998 its first results excluding a particular kind of axion of mass 2.9×10^{-6} eV to 3.3×10^{-6} eV as the dark matter in the halo of our galaxy.

Let us finally mention that links to web pages of axion detection experiments can be found in the web page <http://cdms.physics.ucsb.edu/others/others.html>.

3.1.3. *WIMPs*

As mentioned in the Introduction, WIMPs are very interesting candidates for dark matter in the Universe. They were in thermal equilibrium with the standard model particles in the early Universe, and decoupled when they were non-relativistic. The process was the following. When the temperature T of the Universe was larger than the mass of the WIMP, the number density of WIMPs and photons was roughly the same, $n \propto T^3$, and the WIMP was annihilating with its own antiparticle into lighter particles and vice versa. However, after the temperature dropped below the mass of the WIMP, m , its number density dropped exponentially, $n \propto e^{-m/T}$, because only a small fraction of the light particles mentioned above had sufficient kinetic energy to create WIMPs. As a consequence, the WIMP annihilation rate $\Gamma = \langle \sigma_{ann} v \rangle n$ dropped below the expansion rate of the Universe, $\Gamma \lesssim H$. At this point WIMPs came away, they could not annihilate, and their density is the same since then (freeze-out typically occurs at $T_F \approx m/20$). This can be obtained using the Boltzmann equation, which describes the time evolution of the number density $n(t)$ of WIMPs

$$\frac{dn}{dt} + 3Hn = -\langle \sigma_{ann} v \rangle [(n)^2 - (n^{eq})^2] , \quad (7)$$

where H is the Hubble expansion rate, σ_{ann} is the total cross section for annihilation of a pair of WIMPs into standard model particles, v is the relative velocity between the two WIMPs, $\langle \dots \rangle$ denotes thermal averaging, and n^{eq} is the number density of WIMPs in thermal equilibrium. One can discuss qualitatively the solution using the freeze-out condition $\Gamma = \langle \sigma_{ann} v \rangle_F n = H$. Then, the current WIMP $\Omega h^2 =$

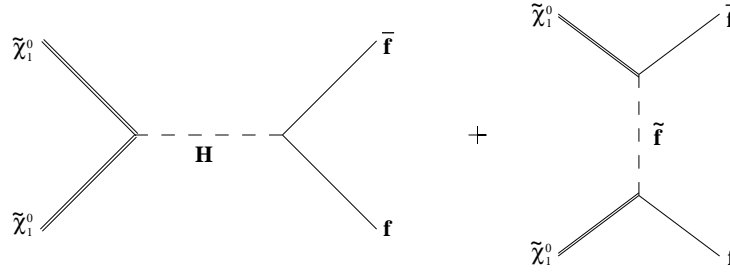


Fig. 2. Feynman diagrams contributing to early-Universe neutralino ($\tilde{\chi}_1^0$) annihilation into fermions through neutral Higgses ($H \equiv H, h, A$) and squarks and sleptons (\tilde{f}).

$(\rho/\rho_c)h^2$, turns out to be

$$\Omega h^2 \simeq \frac{3 \times 10^{-27} \text{ cm}^3 \text{ s}^{-1}}{\langle \sigma_{ann} v \rangle}, \quad (8)$$

where the number in the numerator is obtained using the value of the temperature of the cosmic background radiation, the Newton's constant, etc. As expected from the above discussion about the early Universe, the relic WIMP density decreases with increasing annihilation cross section^a.

Now we can understand easily why WIMPs are so good candidates for dark matter. If a new particle with weak interactions exists in Nature, its cross section will be $\sigma \simeq \alpha^2/m_{\text{weak}}^2$, where $\alpha \simeq \mathcal{O}(10^{-2})$ is the weak coupling and $m_{\text{weak}} \simeq \mathcal{O}(100 \text{ GeV})$ is a mass of the order of the W gauge boson. Thus one obtains $\sigma \approx 10^{-9} \text{ GeV}^{-2} \approx 1 \text{ pb}$ (recall that in natural units $1 \text{ GeV}^{-2} = 0.389 \times 10^{-27} \text{ cm}^2 = 0.389 \times 10^9 \text{ pb}$). Since at the freeze-out temperature T_F the velocity v is a significant fraction of the speed of light ($v^2 \approx c^2/20$), one obtains $\langle \sigma_{ann} v \rangle \approx 10^{-26} \text{ cm}^3 \text{ s}^{-1}$. Remarkably, this number is close to the value that we need in Eq. (8) in order to obtain the observed density of the Universe. This is a possible hint that new physics at the weak scale provides us with a reliable solution to the dark matter problem, and also a qualitative improvement with respect to the axion dark matter case, where a small mass for the axion about 10^{-5} eV has to be postulated.

SUSY is a theory that introduces new physics precisely at the weak scale, and that, as discussed in the Introduction, predict a new particle, the neutralino, which could be stable. These are the reasons to consider the neutralino as a very serious candidate for the sought-after dark matter. Concerning the annihilation cross section¹⁵ contributing to the density of the Universe in Eq. (8), there are numerous final states into which the neutralino can annihilate. The most important of these are the two body final states which occur at the tree level. Specially these are fermion-antifermion pairs^{14,98,99,100,101} ($f\bar{f}$ where f are the standard model

^aLet us remark that the theoretical computation of the relic density depends on assumptions about the evolution of the early Universe, and therefore cosmological scenarios different from the thermal production of neutralinos discussed here would give rise to different results⁹⁷.

quarks and leptons), as those shown in Fig. 2. Others are weak gauge bosons pairs ^{102,99,101} W^+W^- , Z^0Z^0 , and those containing Higgs bosons ^{102,99,103,101} such as W^+H^- , W^-H^+ , Z^0A , Z^0H , Z^0h , H^+H^- and all six combinations of A, h, H . Different subtleties of the analyses has been discussed in Refs. 104, 105. The annihilation cross section is of the form

$$\sigma_{ann} \simeq N_{ann} m_{\tilde{\chi}_1^0}^2 |\mathcal{A}_{ann}|^2, \quad (9)$$

where \mathcal{A}_{ann} is the amplitude which depends on the dynamics of the collision and N_{ann} is the number of annihilation channels. Generically $\mathcal{A}_{ann} \sim 1/\mathcal{M}^2$, where \mathcal{M} is the mass of the particles mediating the interaction. Thus $\sigma_{ann} \sim 1/m_{\tilde{\chi}_1^0}^2$, and therefore in order to satisfy the upper bound in Eq. (2), moderate values of the LSP mass are necessary. Several exceptions to this rule will be discussed in Subsection 5.2.1. Let us mention here one of them which is particularly interesting.

In principle to use the above discussed neutralino annihilation cross section is sufficient, since the effects of heavier particles are suppressed by the Boltzmann factor. However, the next to lightest supersymmetric particle (NLSP) may lie near in mass to the LSP so that both particles freeze out of equilibrium at approximately the same temperature. Thus the NLSP should be included in principle in the reaction network, since coannihilation channels NLSP-LSP (and also channels NLSP-NLSP) might be now relevant ¹⁰⁴. In fact, this is so only when $(m_{NLSP} - m_{\tilde{\chi}_1^0})/m_{\tilde{\chi}_1^0} \lesssim 0.2$, since the NLSP number density is suppressed by $e^{-(m_{NLSP} - m_{\tilde{\chi}_1^0})/T_F}$ relative to the neutralino number density, where recall that $T_F \approx m_{\tilde{\chi}_1^0}/20$. We will see in Section 5 that special regions of the parameter space of the MSSM fulfil this condition, and therefore including coannihilations is important. Coannihilation channels in SUSY, in particular $\tilde{\chi}_1^0$ -stau, $\tilde{\chi}_1^0$ -chargino and $\tilde{\chi}_1^0$ -stop, have been exhaustively studied in the literature ^{106,107,108,109,110,111,112}.

Taking into account all the above comments concerning SUSY scenarios, we will see in detail in Section 5 that significant regions of the parameter space of the MSSM produce values of the cross section in the interesting range mentioned below Eq. (8).

On the other hand, since neutralinos, or WIMPs in general, interact with ordinary matter with roughly weak strength, their presence in galactic scales, and in particular in our galaxy, raises the hope of detecting relic WIMPs directly in a detector by observing their scattering on target nuclei through nuclear recoils. This will be the subject of the next section, but before analyzing it let us briefly discuss here other candidates for dark matter.

3.2. Other candidates

The first proposed candidate for dark matter in the context of WIMPs was in fact a *heavy* (Dirac or Majorana) fourth-generation *neutrino* ¹¹³ with the usual standard model couplings. It is not easy to construct theoretical models with such a stable heavy particle, but in any case LEP limits from the Z^0 width imply $m_\nu \gtrsim m_{Z^0}/2$,

and this is not compatible with a correct relic abundance. The relic abundance can be studied as in Subsection 3.1.3 with the annihilation of the heavy neutrinos into light fermions through the exchange of Z^0 . The final result is that neutrinos with the above lower bound give rise to a too small relic abundance^{113,114}. In addition, direct¹¹⁵ and indirect¹¹⁶ detection experiments rule out $m_\nu \lesssim 1$ TeV. A recent attempt to consider massive fourth-generation neutrinos as dark matter candidates, can be found in Ref. 117.

In addition to the neutralino there are other potential SUSY candidates for dark matter. In principle one of them might be the *sneutrino*¹¹⁸ of the MSSM. One finds¹¹⁹ that the sneutrino relic density is in the region $0.1 \lesssim \Omega_{\tilde{\nu}} h^2 \lesssim 1.0$ for $550 \text{ GeV} \lesssim m_{\tilde{\nu}} \lesssim 2300 \text{ GeV}$. This is consistent with the LEP limits on $Z^0 \rightarrow$ invisible neutral particles suggesting $m_{\tilde{\nu}} \gtrsim m_{Z^0}/2$, as in the case of the heavy neutrino above. However, sneutrino-nucleus interaction is similar to the heavy neutrino-nucleus interaction, and therefore direct detection experiments¹¹⁵ impose similar limits on the sneutrino mass as above. Such a heavy sneutrino cannot be the LSP in SUSY models.

The supersymmetric partner of the graviton, the *gravitino*, has also been proposed as a candidate for dark matter¹²⁰. In the absence of inflation, it could give rise to the correct relic abundance if its mass is of order keV. This is unlikely in specific theoretical models. For example, in gravity mediated SUSY breaking the masses of the superpartners are of order the gravitino mass, and therefore this should be of order 1 TeV. Gravitinos as dark matter would be undetectable since their interactions with ordinary matter are extremely weak.

Another candidate for dark matter that can arise in SUSY is the *axino*¹²¹. Models combining SUSY and the Peccei-Quinn solution to the strong CP problem necessarily contain this particle. Unlike the neutralino and gravitino, the axino mass is generically not of order the SUSY-breaking scale and can be much smaller. For a recent work with masses in the range of tens of MeV to several GeV as corresponding to cold axino relics see e.g. Ref. 122.

The possibility that dark matter could be made of additional *scalars* in the standard model has also been analyzed¹²³. Scalar candidates have also been studied in a prototypical theory space ‘Little Higgs Model’¹²⁴, and in theories with $N = 2$ extended supersymmetry and/or extra space dimensions¹²⁵.

More (exotic) candidates can be found in the literature. Let us mention some of them. Strongly Interacting Massive Particles, *SIMPs*, have been proposed^{126,127,128}. For example, bound state of ordinary quarks and gluons with a heavy stable quark, scalar quark, gluino, or colored technibaryon.

Dark matter made of CHArged Massive Particles, *CHAMPs*, has also been proposed¹²⁹. Apparently, if their masses are larger than 20 TeV these particles will very rarely be trapped in ordinary matter, and are safe from bounds on exotic heavy isotopes.

A potential conflict between collisionless dark matter scenarios and observations motivated the authors of Ref. 130 to propose Self Interacting Dark Matter, *SIDM*,

i.e. dark matter with a large scattering cross section but negligible annihilation. On the other hand, the authors of Ref. 131 solved the problem using a mechanism of non-thermal production of WIMPs.

Instead of using WIMPs with typical masses of order a hundred GeV, the authors of Ref. 132 studied scenarios with nonthermal WIMPs in the range 10^{12} to 10^{16} GeV. They called these objects *WIMPZILLAS*.

The lightest Kaluza-Klein particle, *LKP*, in models with TeV extra dimensions has been studied as a viable dark matter candidate¹³³. It is actually a typical WIMP (the most studied possibility is a Kaluza-Klein 'photon'), with a mass in the range 400-1200 GeV.

Superweakly-interacting massive particles, *superWIMPs*, were also proposed in Ref. 134. They naturally inherit the desired relic density from late decays of metastable WIMPs. Well-motivated examples are weak-scale gravitinos in supergravity and Kaluza-Klein gravitons from extra dimensions.

In the context of the heterotic string $E_8 \times E_8$, where there is a natural hidden sector associated with the second E_8 , it was mentioned in Ref. 135 that this sector which only interacts with ordinary matter through gravitational interactions could be a *shadow world*. The astrophysical and cosmological implications of this comment were analyzed in detail in Ref. 136

Still, in the context of strings, other possibilities were also analyzed. For example, in Ref. 137 the authors proposed *Cryptons*, which are stable bound states of matter in the hidden sector. In Ref. 138 glueballs of the *hidden-sector* non-Abelian gauge group were proposed as candidates for SIDM. *Brane-world* dark matter was studied in Ref. 139.

Let us finally mention that the list of dark matter candidates discussed here is large but by no means complete. The reason being that different candidates have been proposed during many years, and therefore it is almost impossible not to forget some of them. In fact, this list is still increasing (see e.g. the works in Ref. 140).

4. Dark matter detection

Given the discussion in the previous section, one can say that there are good particle candidates for dark matter. As a matter of fact, we saw that WIMPs and axions are particularly interesting. Since the former can be left over from the Big Bang in sufficient number to account for the relic matter density in a natural way, we will concentrate on them. Thus we will review in this section the current and projected experiments for detecting WIMPs (e.g. the detection of axions was briefly discussed in Section 3.1.2). In particular we will analyze the two possible ways of detecting them: direct and indirect detection. Of course, the most clear one is the direct detection by observing their scattering on the material in a detector, and we will study it in detail. Finally, we will discuss briefly the indirect detection by looking for evidence of their annihilation.

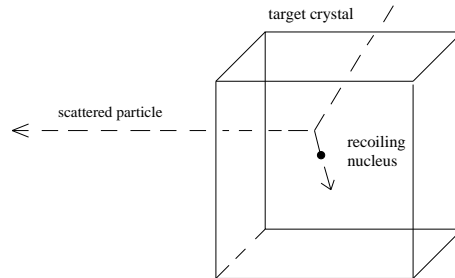


Fig. 3. Elastic scattering of a dark matter particle with an atomic nucleus in a detector.

4.1. Direct detection

As discussed in the Introduction, if neutralinos, or WIMPs in general, are the bulk of the dark matter, they will form not only a background density in the Universe, but also will cluster gravitationally with ordinary stars in the galactic halos. In particular they will be present in our own galaxy, the Milky Way. This raises the hope of detecting relic WIMPs directly, by experiments on the Earth. In particular, through scattering with the material in a detector. In fact general studies of the possibility of dark matter detection began around 1982. Since the detection will be on the Earth we need to know the properties of our galaxy in order to be sure that such a detection is feasible ^b.

As a matter of fact, rotation curves are much better known for external galaxies than for ours, due to the position of the Earth inside the galaxy. In any case, analyses have been carried out with the conclusion that indeed the Milky Way contains large amounts of dark matter ¹⁴². Besides, some observational evidence seems to point at a roughly spherical distribution of dark matter in the galaxy. At the position of the Sun, around 8.5 kpc away from the galactic center, the mean density of elementary particles trapped in the gravitational potential well of the galaxy is expected to be $\rho_0 \approx 5 \times 10^{-25} \text{ gr cm}^{-3} \simeq 0.3 \text{ GeV cm}^{-3}$. For WIMPs with masses about 100 GeV this means a number density $n_0 \approx 3 \times 10^{-3} \text{ cm}^{-3}$. In addition, their velocity will be similar to the one of the Sun since they move in the same gravitational potential well, $v_0 \approx 220 \text{ km s}^{-1}$, implying a flux of dark matter particles $J_0 = n_0 v_0 \approx 10^5 \text{ cm}^{-2} \text{ s}^{-1}$ incident on the Earth^c. Although this number

^bDirect detection of extragalactic WIMPs has also been analyzed recently ¹⁴¹. Although of much lower flux than typical galactic halo WIMPs, it seems that they have a number of interesting features for their detectability.

^cClumps of dark matter crossing the Earth with a density larger by a factor 10^8 , and with a periodicity of 30-100 Myrs, have been proposed to explain double mass extinctions of paleontology. First, the direct passage of a dark matter clump may lead to a preliminary extinction ¹⁴³ by causing lethal carcinogenesis in organisms ¹⁴⁴. Later, the accumulation of dark matter in the center of the Earth and the subsequent annihilation would produce a large amount of heat with the consequent ejection of superplumes, followed by massive volcanism leading to the second burst of more severe extinction ¹⁴⁵. For another exotic mechanism solving mass extinctions, and related

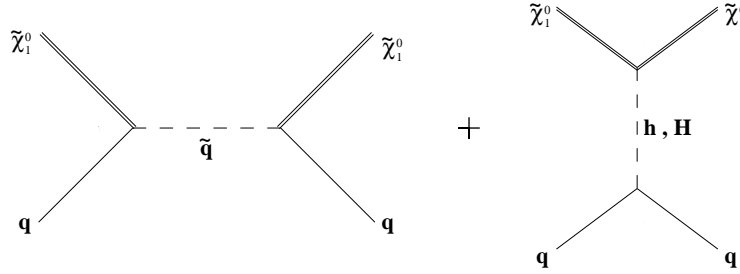


Fig. 4. Feynman diagrams contributing to neutralino-nucleon cross section through squark (\tilde{q}) exchange and CP-even light (h) and heavy (H) neutral Higgs exchange.

is apparently large, the fact that WIMPs interact weakly with matter makes their detection very difficult. Most of them will pass through matter without prevention. In any case, as suggested in 1985^{2,3}, direct experimental detection of WIMPs is in principle possible. The two types of direct detection experiments will be discussed below.

(i) *Elastic scattering*

The detection of WIMPs through elastic scattering with nuclei in a detector is shown schematically in Fig. 3. As we can see the nucleus recoils as a whole. A very rough estimate of the rate R in a detector is the following. A particle with a mass of order 100 GeV and electroweak interactions will have a cross section $\sigma \approx 1$ pb, as discussed in Subsection 3.1.3. Thus for a material with nuclei composed of about 100 nucleons, i.e. $M_N \sim 100 \text{ GeV} = 177 \times 10^{-27} \text{ kg}$, one obtains $R \sim J_0 \sigma / M_N \approx 10$ events $\text{kg}^{-1} \text{ yr}^{-1}$. This means that every day a few WIMPs, the precise number depending on the number of kilograms of material, will hit an atomic nucleus in a detector.

Of course the above computation is just an estimate and one should take into account in the exact computation the interactions of WIMPs with quarks and gluons, the translation of these into interactions with nucleons, and finally the translation of the latter into interactions with nuclei. In the case of neutralinos as WIMPs, diagrams contributing to neutralino-quark cross section are shown in Fig. 4. The relevant (scalar) $\tilde{\chi}_1^0$ -nucleus cross section is of the form

$$\sigma_{\text{scat}} \simeq M_r^2 |\mathcal{A}_{\text{scat}}|^2, \quad (10)$$

where $M_r = M_N m_{\tilde{\chi}_1^0} / (M_N + m_{\tilde{\chi}_1^0})$ is the reduced mass with M_N the mass of the nucleus, and $\mathcal{A}_{\text{scat}}$ is the amplitude which depends on the dynamics of the collision. In particular, the quarks masses m_q , the hadronic matrix elements $f_{T_q}^{(p)}$, the proton mass m_p , and the masses of the particles mediating the interaction, such as $m_{\tilde{q}}$, m_H , m_h , enter in $\mathcal{A}_{\text{scat}}$. We will check in Section 5 that significant regions of the

parameter space of the MSSM produce values of the neutralino-nucleus cross section $\sigma_{\text{scat}} \simeq 1$ pb, and therefore giving rise to a reasonable number of events. As a matter of fact, in the experimental results that one finds in the literature the authors prefer to give the WIMP-nucleon cross section. As will be discussed in Section 5, this is about eight orders of magnitude smaller than the WIMP-nucleus cross section, and therefore a typical value is $\approx 10^{-8}$ pb. In the next Sections, when talking about scattering cross section, we will always consider this one.

Let us finally remark that the diagrams for neutralino annihilation (see Fig. 2) are related to these by crossing symmetry. Thus, provided that the main annihilation channel is into fermions, the amplitudes of annihilation and scattering with nucleons are similar, and this leads for the amplitudes with the nucleus to the relation $|\mathcal{A}_{\text{scat}}|^2 \simeq c^2 A^2 |\mathcal{A}_{\text{ann}}|^2$, where A is the atomic weight and c^2 is a constant (we can deduce from Section 5 that $c \simeq f_{T_s}^{(p)} m_p / m_s = \mathcal{O}(1)$). From Eqs. (9) and (10) it is obvious that $\sigma_{\text{scat}} / \sigma_{\text{ann}} \simeq \text{const.}$ However, if the neutralinos are heavy they have other annihilation channels, such as Higgs bosons or vector boson pairs, and therefore the crossing argument does not apply.

(ii) Inelastic scattering

There are two possible ways of detecting WIMPs directly through inelastic scattering. These can be with nuclei in a detector¹⁴⁷ or with orbital electrons¹⁴⁸. The former produces an excited nuclear state, and has the double signature of recoil energy followed ~ 1 ns later by the emission of a decay photon. However, the event rates seem to be suppressed and problems of natural radioactivity and expense disfavour the materials that might be used for the detector^d. A similar conclusion concerning the event rates was obtained for the case of scattering of WIMPs from orbital electrons. These could leave an excited state emitting a photon by the deexcitation.

4.1.1. Experiments around the world

More than 20 experiments for the direct detection of dark matter are running or in preparation around the world. Given the above results, all of them use the elastic-scattering technique. For example, Germanium is a very pure material and has been used for many years for detecting dark matter in this way. In this type of experiments, in order to detect the nuclear recoil energy, they measure the ionization produced by collision with electrons. In fact, ^{76}Ge ionization detectors has been applied to WIMP searches since 1987¹¹⁵. In 2000 the situation was the following. The best combination of data from these experiments, together with the last data from the Heidelberg-Moscow¹⁵⁰ and IGEX experiments¹⁵¹ located at the Gran Sasso (L'Aquila, Italy) and Canfranc (Huesca, Spain) Underground Laboratories,

^dFor a recent analysis with a different conclusion, see Ref. 149.

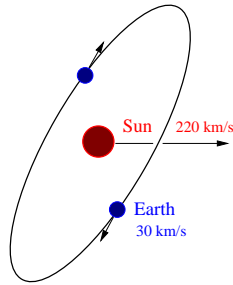


Fig. 5. Earth's motion around the Sun.

respectively, were able to exclude a WIMP-nucleon cross section larger than about 10^{-5} pb for masses of WIMPs ~ 100 GeV, due to the negative search result. Although this was a very interesting bound, it was still well above the expected value $\sim 10^{-8}$ pb.

Let us remark that it is convenient to carry the experiments out in the deep underground. For a slow moving (~ 300 km s $^{-1}$) and heavy ($\sim 100 - 1000$ GeV) particle forming the dark matter halo, the kinetic energy is very small, around 100 keV, and in fact the largest recoil energy transfer to a nucleus in the detector will only be a few keV. Since cosmic rays with energies \sim keV-MeV bombard the surface of the Earth, the experiments must have an extremely good background discrimination. In particular, neutrons coming from collisions between cosmic-ray muons and nuclei produce nuclear recoils similar to those expected from WIMPs at a rate $\sim 10^3$ events kg $^{-1}$ day $^{-1}$. Thus detectors located in the deep underground, reduce the background by orders of magnitude in comparison with the sea level intensity.

In fact, this is still not enough since the detector has to be protected also against the natural radioactivity from the surroundings (e.g. the rocks) and the materials of the detector itself. This produces again neutrons but also X rays, gamma rays and beta rays giving rise to electron recoils. The latter may be a problem for detectors based only on ionization or scintillation light since nuclear recoils with energies of a few keV are much less efficient in ionizing or giving light than electrons of the same energy. Various protections aim to reduce these backgrounds. In particular, low radioactive materials, such as e.g. high-purity copper or aged lead, are used for the shielding. In addition, high-purity materials for the detector are also used.

Summarizing, with this type of experiments the WIMP nuclear recoil signal will appear as an excess of recoil events above the expected background rate. However, it would be very interesting to also look for some additional feature of the WIMP signal that positively identifies it as galactic in origin. In this sense a different method for discriminating a dark matter signal from background is the so-called

annual modulation signature^{152,e}. As it is shown schematically in Fig. 5, as the Sun orbits the galaxy with velocity $v_0 \approx 220 \text{ km s}^{-1}$, the Earth orbits the Sun with velocity $\approx 30 \text{ km s}^{-1}$ and with the orbital plane inclined at an angle of 60° to the galactic plane. Thus e.g. in June the Earth's rotation velocity adds to the Sun's velocity through the halo with a maximum around June 2, whereas in December the two velocities are in opposite directions. When this is taken into account the Earth velocity is given by

$$v_E = v_0 \left\{ 1.05 + 0.07 \cos \left[\frac{2\pi(t - t_m)}{1 \text{ year}} \right] \right\}, \quad (11)$$

where $t_m = \text{June } 2 \pm 1.3 \text{ days}$. This fluctuation produces a rate variation between the two extreme conditions. The variation is so small $\approx 7\%$ that the experiment can only work if large number of events are found, implying that large mass apparata are necessary.

The DArk MATter (DAMA) experiment^{4,5} investigates the annual modulation of this signature rather than discriminating signal events against background. It consists of about 100 kg of material in a small room at the Gran Sasso National Laboratory located beside the Gran Sasso Tunnel on the highway connecting Teramo to Rome (see Fig. 8 for a similar experiment DAMA/LIBRA). The maximum thickness of the rock overburden is 1400 m. In the experiment they use nine 9.70 kg NaI crystal scintillators which measure the ionization produced by the nuclear recoil through the emission of photons. Remarkably, they found that their detectors flashed more times in June than in December. The data collected⁴ over four yearly cycles, DAMA/NaI-1,2,3,4, until the second half of August 1999, strongly favour the presence of a yearly modulation of the rate of the events. Moreover, very recently, more data have been reported⁵ confirming this result. In particular the DAMA/NaI-5 data have been collected from August 1999 to end of July 2000. Afterwards, the DAMA/NaI-6 data have been collected from November 2000 to end of July 2001, while the DAMA/NaI-7 data have been collected from August 2001 to July 2002. The analysis of the data of the seven annual cycles offers an immediate evidence of the presence of an annual modulation of the rate of the events in the lowest energy region as shown in Fig. 6 (from Ref. 5), where the time behaviours of the (2–4), (2–5) and (2–6) keV residual rates are depicted. This signal is compatible⁴ with WIMP masses up to 100 GeV and WIMP-nucleon cross sections in the interval $10^{-6} - 10^{-5} \text{ pb}$, as shown with a dark shaded area in Fig. 7, where the data¹⁵⁴ from DAMA/NaI-0 have also been taken into account. The lower bound of 30 GeV in the figure is purely theoretical, and inspired by the lower bound on the lightest neutralino of SUSY models, as derived from the LEP data using GUT conditions.

^eAnother novel possibility to search for characteristic signatures has recently been proposed, namely by observing the electrons which follow the ionization of the atom during the WIMP-nucleus collision¹⁵³.

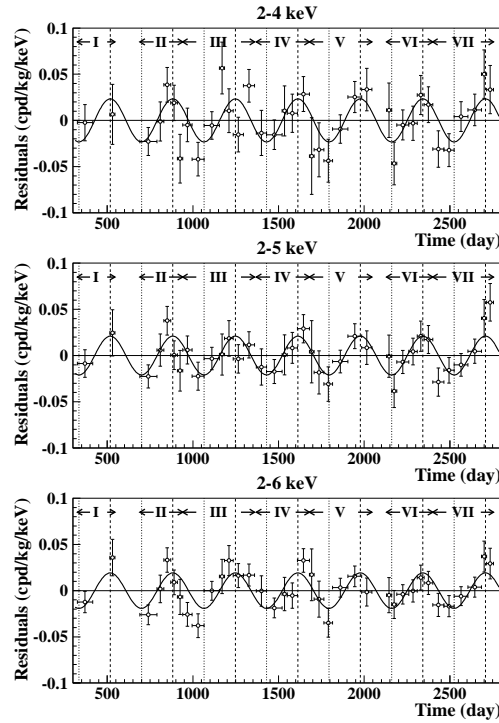


Fig. 6. Model independent residual rate for events in the (2–4), (2–5) and (2–6) keV energy intervals as a function of the time elapsed since January 1-st of the first year of data taking. The experimental points present the errors as vertical bars and the associated time bin width as horizontal bars. The superimposed curves represent the cosinusoidal behaviours expected for a WIMP signal with a period equal to 1 year and phase at 2nd June.

It is worth remarking that this result has been obtained assuming the simple isothermal sphere halo model with dark-matter density $\rho_0 = 0.3 \text{ GeV cm}^{-3}$ and WIMP velocity $v_0 = 220 \text{ km s}^{-1}$ (to be precise one assumes a Maxwell-Boltzmann local velocity distribution $f(v) \propto e^{-v^2/v_0^2}$ producing a velocity dispersion $\bar{v} = \langle v^2 \rangle^{1/2} = (3/2)^{1/2} v_0 \approx 270 \text{ km s}^{-1}$). However, when uncertainties on the halo model are taking into account, the signal is consistent with a larger region of the parameter space. In particular, in Refs. 4 and 155 modifications in the velocity distribution function for different galactic halo models were considered, using in addition the allowed ranges for v_0 and ρ_0 in each model (see Ref. 156 for other studies of uncertainties on the halo model). The final result of the analyses is shown in Fig. 7 with a light shaded area. One sees that the signal is compatible with larger values of the parameters (for a different opinion see Ref. 157), i.e. WIMP masses up to 270 GeV, and WIMP-nucleon cross sections in the interval $10^{-7} - 6 \times 10^{-5} \text{ pb}$. This result corresponds at a rate of about 1 event per kg per day. In fact, as discussed in Ref. 155 (see also Ref. 5), when co-rotation of the galactic halo is also

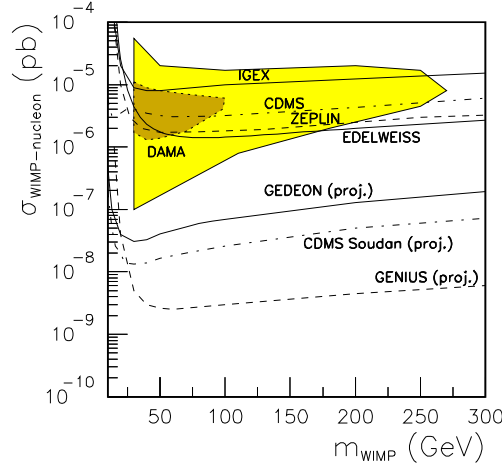


Fig. 7. Areas allowed by the different experiments for the direct detection of dark matter in the parameter space $(\sigma_{\text{WIMP-nucleon}}, m_{\text{WIMP}})$, where $\sigma_{\text{WIMP-nucleon}}$ is the WIMP-nucleon cross section and m_{WIMP} is the WIMP mass. The light shaded (yellow) area is allowed by the DAMA experiment, including uncertainties on the halo model. The dark shaded (brown) area inside the previous one corresponds to the simple case of an isothermal sphere halo model. This case is also the one analyzed by the other experiments: The (lower) areas bounded by solid, dot-dashed, dashed and (again) solid lines are allowed by IGEX, CDMS, ZEPLIN I and EDELWEISS current experimental limits. The (upper) areas bounded by solid, dot-dashed and dashed lines will be analyzed by the projected GEDEON, CDMS Soudan and GENIUS experiments.

considered, the mass range extends further to 500 – 900 GeV, for cross sections in the interval $\text{few} \times 10^{-6} - 2 \times 10^{-5}$ pb.

Although the DAMA group is confident about the data, since they claim to have ruled out systematic effects which could fake the signature^{158,159}, as e.g. temperature changes, it is worth remarking that the above values for the cross section are generically above the expected weak-interaction value, and therefore they are not easy to obtain in SUSY models with neutralino dark matter, as we will discuss in Section 5. But in fact, the DAMA result is controversial, mainly because the negative search result obtained by other recent experiments. The first of these was the Cryogenic Dark Matter Search (CDMS) experiment⁶ in the US. This was located just 10 metres below ground at Stanford University in California, and therefore it must discriminate WIMPs signals against interactions of background particles. Two detection techniques are used for this discrimination, both the ionization and the temperature rise produced during a recoil are measured. The latter can be observed since the recoiling nucleus is stopped within $10^{-7} - 10^{-6}$ cm ($\sim 10^{-14}$ s) releasing a spherical wave of phonons traveling at $\sim 5 \times 10^5$ cm s⁻¹, and subsequently converted to a thermal distribution. These two techniques allow to discriminate electron recoils caused by interactions of background particles from WIMP-induced nuclear recoils. The ratio of deposited energies heat/ionization would be $\sim 2 - 3$

for the former and larger than 10 for the latter. However, although neutrons are moderated by a 25-cm thickness of polyethylene between the outer lead shield and cryostat, an unknown fraction of them still survives. Two data sets were used in this analysis: one consisting of 33 live days taken with a 100-g Si detector between April and July 1998, and another consisting of 96 live days taken with three 165-g Ge detectors between November 1998 and September 1999. Although four nuclear recoils are observed in the Si data set, they cannot be due to WIMPs, they are due in fact to the unvetted neutron background. On the other hand, in the Ge detector thirteen nuclear recoils are observed in the 10.6 kg per day exposure between 10 and 100 keV, which is a similar rate to that expected from the WIMP signal claimed by DAMA. However, the CDMS group concludes that they are also due to neutrons. These data exclude (see also Ref. 160 for more recent data) much of the region allowed by the DAMA annual modulation signal^f, as shown in Fig. 7 ^g.

In addition, a small part of the region excluded by CDMS has also been excluded by IGEX ¹⁶³, as shown in Fig. 7. To obtain this result, 40 days of data from the IGEX detector were analyzed. Let us recall that this experiment is located at the Canfranc Tunnel Astroparticle Laboratory in the international railway tunnel of Somport at Canfranc (Spanish pyrenees), under a 860 m rock overburden, and that consists of 2 kg Germanium ionization detector. A region similar to the one excluded by IGEX has also been excluded by the Heidelberg Dark Matter Search (HDMS) experiment ¹⁶⁴. This operates two ionization Ge detectors in a unique configuration, and was installed at Gran Sasso in August 2000. The data used for the analysis were taken from February 2001 to September 2001.

But more disturbing are the recent results from EDELWEISS and ZEPLIN I collaborations excluding even larger regions than CDMS, as shown also in Fig. 7. The EDELWEISS experiment ⁷ is located at the Frejus Underground Laboratory in the Fréjus Tunnel under the French-Italians Alps, under a 1780 m rock overburden. As CDMS, this experiment also uses a heat-and-ionization cryogenic Ge detector, although they differ by their mass, geometry and electrode implantation scheme. First, this collaboration was using a 320 g detector, 70 mm in diameter and 20 mm in height, but this was not sufficient to extend the sensitivity to the values obtained by DAMA. Following this result, three new detectors with the same characteristics as the first one were put in operation simultaneously. The data consists of all physics runs recorded over a period from February to May 2002.

On the other hand, the ZEPLIN project ⁸ at the Boulby salt mine (Yorkshire, UK) consists of a series of liquid Xenon detectors operating some 1100 m under-

^fFor some attempts to show that both experiments, DAMA and CDMS, might not be in conflict, see Ref. 161.

^gAs mentioned in the caption of Fig. 7, unlike DAMA for CDMS and for the other experiments analyses taking into account the uncertainties in the galactic halo are not shown and we only see the effect of the standard halo model on their results. Including those uncertainties, the light shaded area favoured by DAMA and not excluded by the null searches would be in principle smaller than the one shown here (for an analysis of this see Ref. 162).



Fig. 8. Left picture: during the LIBRA detectors installation in HP Nitrogen atmosphere. Right picture: view at end of the detectors installation. All the used materials have been deeply selected for radiopurity (see for example the cables with teflon envelop).

ground, where the nuclear recoil produces both an ionization and a scintillation signal, potentially capable of providing much greater signal discrimination than NaI. The ZEPLIN I detector has been running for approximately one year with a mass of about 4 kg. The collaboration is concentrating on new developments for future ZEPLIN detectors.

4.1.2. Future dark matter searches

Owing to this controversy between DAMA and the other experiments, one cannot be sure whether or not the first direct evidence for the existence of dark matter has already been observed. Fortunately, the complete DAMA region will be tested by current dark matter detectors. This is for example the case of the IGEX experiment mentioned above, with a moderate improvement of the detector performances¹⁶³. In addition, a new experimental project, GERmanium DETectors in ONe cryostat (GEDEON), is planned¹⁶⁵. It will use the technology developed for the IGEX experiment and it would consist of a set of ~ 1 kg Germanium crystals, of a total mass of about 28 kg, placed together in a compact structure inside one only cryostat. GEDEON would be massive enough to search for the annual modulation effect and explore positively a WIMP-nucleon cross section $\sigma \gtrsim 3 \times 10^{-8}$ pb (see Fig. 7). Likewise an improved HDMS experiment should be able to test the DAMA evidence region within about two years¹⁶⁴.

DAMA and CDMS collaborations also plan to expand their experiments. The DAMA collaboration dismantled the 100 kg NaI set-up and installed the new LIBRA set-up. The latter consisting of about 250 kg of NaI made of 25 detectors, 9.70 kg each one. This will make the experiment more sensitive to the annual modulation signal. Some pictures taken during the installation can be seen in Fig. 8 (from Ref. 159). This was completed at the end of 2002. On the other hand, the CDMS collaboration is moving its detector to the abandoned Soudan mine in Minnesota

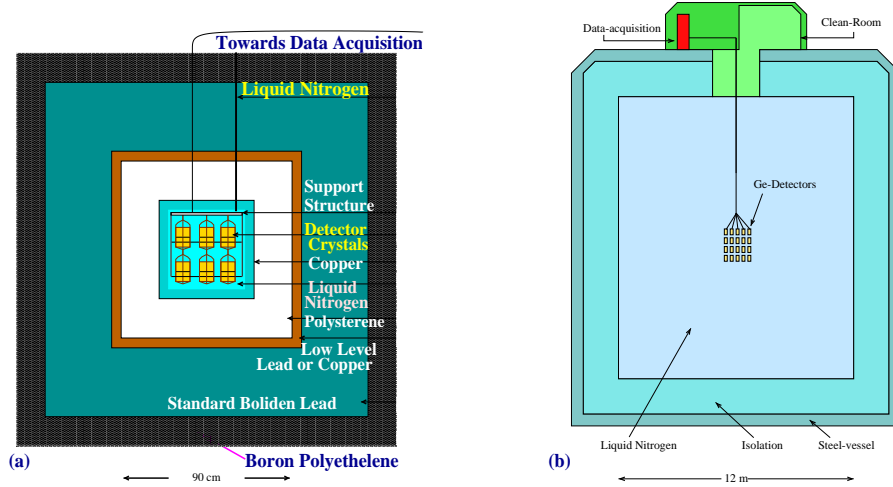


Fig. 9. (a): Conceptual design of the Genius TF. Up to 14 detectors will be housed in the inner detector chamber, filled with liquid nitrogen. As a first shield 5 cm of zone refined Germanium, or extremely low-level copper will be used. Behind the 20 cm of polystyrene isolation another 35 cm of low level lead and a 15 cm borated polyethylene shield will complete the setup. (b): GENIUS - 100 kg of Ge detectors are suspended in a large liquid nitrogen tank.

(approximately 700 metres below ground), increasing also the mass of its Ge/Si targets to about 10 kg by 2006. This experiment, CDMS Soudan, will be able to test a WIMP-nucleon cross section $\sigma \gtrsim 10^{-8}$ pb (see Fig. 7).

But this is not the end of the story, since a new generation of very sensitive experiments have been proposed all over the world. For instance, only in the Gran Sasso laboratory there will be five experiments searching for WIMPs. Apart from the two already discussed DAMA and HDMS, there are three other experiments in prospect, CRESST, CUORE and GENIUS. For example, the Cryogenic Rare Event Search using Superconducting Thermometers (CRESST) experiment ¹⁶⁶ measures simultaneously phonons and scintillation light distinguishing the nuclear recoils from the electron recoils cause by background radioactivity. In contrast to other experiments, CRESST detectors allow the employment of a large variety of target materials, such as e.g. sapphire or tungsten. This allows a better sensitivity for detecting the WIMPs. Although they are already using sapphire, for the next project, CRESST II, it is planned to install a mass of about 10 kg, consisting of 33 modules of 300 g tungsten crystals. With 3 years of measurement time the experiment will be able to test a WIMP-nucleon cross section slightly smaller than the CDMS Soudan discussed above.

The most sensitive detector will be the GERmanium in liquid NITrogen Underground Setup (GENIUS) ¹⁶⁷ shown in Fig. 9b (from Ref. 168), which will be able to test a WIMP-nucleon cross section as low as $\sigma \approx 10^{-9}$ pb (see Fig. 7). Indeed such a sensitivity covers a large range of the parameter space of SUSY models with neutralinos as dark matter, as we will see in the next section. The GENIUS

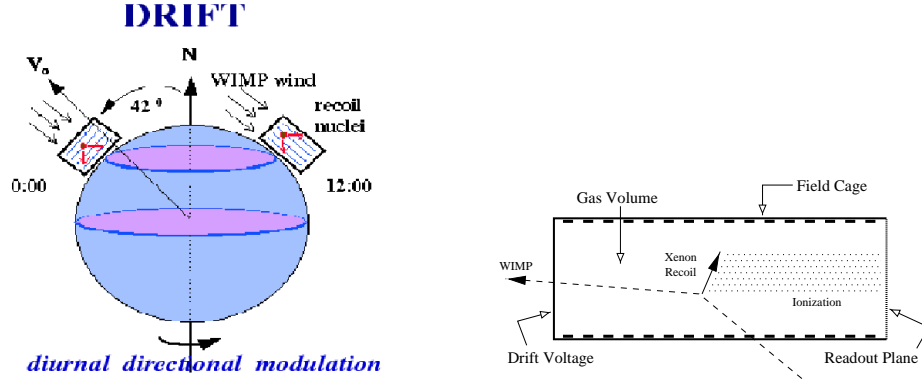


Fig. 10. Left picture: DRIFT detector sited on the Earth through the WIMP halo. Right picture: Schematic of TPC

project is based on the idea to operate an array of 100 kg of Ge crystals directly in liquid nitrogen. The latter, which is very clean with respect to radiopurity, can act simultaneously as cooling medium and shield against external activities, using a sufficiently large tank ~ 12 metres in diameter at least. It has been shown using Monte Carlo simulations that with this approach the unwanted background is reduced by three to four orders of magnitude. In order to demonstrate the feasibility of the GENIUS project a GENIUS Test-Facility (GENIUS-TF), shown in Fig. 9a, is under installation since March 2001 with 40 kg of detectors¹⁶⁹. It could test the DAMA evidence for dark matter by the annual modulation signature (similarly to the GEDEON project mentioned above) within about two years of measurement.

Other experiments are e.g. the French project MACHe3 at the Joseph Fourier University, the PICASSO project at the University of Montreal, or the ORPHEUS project at the University of Bern,

Efforts to build detectors sensitive to the directional dependence, i.e. recoil away from direction of Earth motion, has also been carried out. This is an extension of the idea of annual modulation, but clearly more powerful^{170,171}. A detector sited on the Earth can look for the signal as shown in the left frame of Fig. 10 (from Ref. 168). The detector will see the mean recoil direction rotate and back again over one day. Studies indicate that a WIMP signal could be identified with high confidence from as few as 100 detected WIMP-nucleus scattering events, compared with thousands for an annual modulation.

Of course, to reconstruct such a three-dimensional direction is not simple, but a standard Time Projection Chamber (TPC) where the arrival time of the ionization signal is measured may be used for it. Although the energies of WIMP induced nuclear recoils are smaller than 100 keV, implying short ranges for the ionization tracks, this problem can be attacked using a gas such as Xenon or Argon at low pressure to extend these ranges to a few millimetres. The recoil energy and direction can be measured by drifting the ionisation created along the recoil track to a

suitable readout plane, as shown in the right frame of Fig. 10 (from Ref. 172). The low pressure and therefore the low target mass is not a problem, since as mentioned above only a small number of WIMP events are needed. Another advantage of this technique is that its resolution should allow virtually all Compton electrons to be rejected, since the electron range at a given total ionization is predicted to be many times longer than for a Xenon recoil. The Directional Recoil Identification From Tracks (DRIFT) project¹⁷² is precisely using this technique to detect dark matter. For the moment they are using a detector, DRIFT I, consisting of Carbon Disulfide CS₂ with 1 m³ volume. It was installed at the Boulby mine in summer 2001. Although DRIFT-I is currently taking data, the next stage in the DRIFT project, DRIFT-II, is being planned. In order to achieve sensitivity to scattering cross sections below 10⁻⁶ pb, a scale up in mass is needed. DRIFT-II is thus proposed to have increased volume.

Let us finally mention that links to web pages of the direct detection experiments mentioned in this section, and others experiments, can be found in the Dark Matter Portal <http://lpsc.in2p3.fr/tep/fred/dm.html>. The same web page can be used to look for indirect detection experiments. This is precisely the subject of our next discussion.

4.2. *Indirect detection*

There are promising methods for the indirect detection of WIMPs in the halo^{173,174}. For example, WIMPs passing through the Sun and/or Earth may be slowed below escape velocity by elastic scattering. From subsequent scattering they will sink to the center and accumulate there, annihilating with another WIMP into quarks and leptons (see Fig. 2), gauge bosons, etc. Decays of these annihilation products will produce energetic neutrinos that can be detected^h. In particular, in underground, underwater and under-ice experiments through the ‘up-going’ muons produced by their interactions in the rock, water, and ice respectively. Although some underground neutrino telescopes, such as e.g. Kamiokande or MACRO, have already reported null results, in the next years underwater (e.g. NESTOR, ANTARES) and under-ice (e.g. AMANDA) experiments with sizes of about 10^{3,4} m² (10⁶ m² in the case ICECUBE, a proposed expansion of AMANDA) will have a much greater sensitivity.

Another way of detecting WIMPs indirectly is through anomalous cosmic rays produced by their annihilations in the galactic haloⁱ. Whereas positrons produced in this way are difficult to distinguish from the standard background of typical cosmic-ray positrons, there are other products of annihilation that can be distinguished. In particular, the most promising are cosmic-ray antiprotons and cosmic gamma

^hAnother proposal for studying the WIMPs accumulated in the center of the Sun is through helioseismology¹⁷⁵.

ⁱDetection of extragalactic cosmic gamma rays has also been analyzed recently¹⁷⁶.

rays. As discussed above, WIMPs annihilate into quarks, leptons, gauge bosons, etc. These will hadronize and produce, among other products, antiprotons. Unlike the usual cosmic-ray antiprotons, the flux of these does not decrease dramatically at energies less than a GeV. Space-based antimatter experiments, such as PAMELA and AMS, will study this possibility. On the other hand, two WIMPs can annihilate into gamma rays through loop diagrams, and this might be detected^j using atmospheric Cherenkov telescopes (e.g. CELESTE, MAGIC) or space-based γ ray detectors (e.g. AMS, GLAST). In particular through the observation of monochromatic photons at an energy equal to the WIMP mass. No typical cosmic gamma rays are monochromatic at energies about 100 GeV. Another contribution of photons is the continuum emission from all gamma rays produced by the cascade decays of other primarily annihilation products (e.g. from the π^0 decay originated by the fragmentation of quarks). Although the signal is less distinctive than the previous one, it has the advantage of being unsuppressed by loop effects, and therefore large flux of photons might be observed.

Finally, it is worth noticing that in some regions of SUGRA scenarios, experiments such as AMANDA, NESTOR, ANTARES, MAGIC, GLAST, AMS, might be competitive with direct detection experiments such as CDMS Soudan¹⁷³.

5. Theoretical models

As discussed in the Introduction and Subsection 3.1.3, the leading candidate for WIMP is the neutralino, a particle predicted by SUSY extensions of the standard model. In this section we will review the known SUSY scenarios based on neutralinos as dark matter candidates, in the context of the MSSM. In particular, we will discuss how big the cross section for the direct detection of these neutralinos can be. Obviously, this analysis is crucial in order to know the possibility of detecting the dark matter in current and projected experiments (see Fig. 7).

Since in the MSSM there are four neutralinos, $\tilde{\chi}_i^0$ ($i = 1, 2, 3, 4$), the lightest, $\tilde{\chi}_1^0$, will be the dark matter candidate. The neutralinos are the physical superpositions of the fermionic partners of the neutral electroweak gauge bosons, called bino (\tilde{B}^0) and wino (\tilde{W}_3^0), and of the fermionic partners of the neutral Higgs bosons, called Higgsinos ($\tilde{H}_u^0, \tilde{H}_d^0$). The neutralino mass matrix with the conventions for gaugino and Higgsino masses in the Lagrangian, $\mathcal{L} = \frac{1}{2} \sum_a M_a \lambda_a \lambda_a + \mu \tilde{H}_u^0 \tilde{H}_d^0 + \text{h.c.}$, is given by

$$\begin{pmatrix} M_1 & 0 & -M_Z \cos \beta \sin \theta_W & M_Z \sin \beta \sin \theta_W \\ 0 & M_2 & M_Z \cos \beta \cos \theta_W & -M_Z \sin \beta \cos \theta_W \\ -M_Z \cos \beta \sin \theta_W & M_Z \cos \beta \cos \theta_W & 0 & -\mu \\ M_Z \sin \beta \sin \theta_W & -M_Z \sin \beta \cos \theta_W & -\mu & 0 \end{pmatrix}, \quad (12)$$

^jIt is worth noticing that the EGRET telescope has identified a gamma-ray source at the galactic center that, apparently, has no simple explanation with standard processes¹⁷⁷. Likewise, the HEAT balloon experiment has confirmed an excess of cosmic ray positrons¹⁷⁸.

in the above basis ($\tilde{B}^0 = -i\lambda'$, $\tilde{W}_3^0 = -i\lambda^3$, \tilde{H}_u^0 , \tilde{H}_d^0). Here $\tan\beta = \langle H_u^0 \rangle / \langle H_d^0 \rangle$ is the ratio of Higgs vacuum expectation values (VEVs), M_1 and M_2 are the soft bino and wino masses respectively, and μ is the Higgsino mass parameter determined by the minimization of the Higgs effective potential

$$\mu^2 = \frac{m_{H_d}^2 - m_{H_u}^2 \tan^2\beta}{\tan^2\beta - 1} - \frac{1}{2}M_Z^2. \quad (13)$$

Thus one parameterizes the gaugino and Higgsino content of the lightest neutralino according to

$$\tilde{\chi}_1^0 = N_{11}\tilde{B}^0 + N_{12}\tilde{W}_3^0 + N_{13}\tilde{H}_d^0 + N_{14}\tilde{H}_u^0. \quad (14)$$

It is commonly defined that $\tilde{\chi}_1^0$ is mostly gaugino-like if $P \equiv |N_{11}|^2 + |N_{12}|^2 > 0.9$, Higgsino-like if $P < 0.1$, and mixed otherwise.

The relevant effective Lagrangian describing the elastic $\tilde{\chi}_1^0$ -nucleon scattering in the MSSM has been examined exhaustively in the literature^{15,179}. It is given by

$$\mathcal{L}_{eff} = \alpha_{2i}\bar{\chi}\gamma^\mu\gamma^5\chi\bar{q}_i\gamma_\mu\gamma^5q_i + \alpha_{3i}\bar{\chi}\chi\bar{q}_iq_i. \quad (15)$$

The Lagrangian is to be summed over the quark generations, and the subscript i refers to up-type quarks ($i=1$) and down-type quarks ($i=2$). The couplings $\alpha_{2,3}$ can be found e.g. in Ref. 28 with the sign conventions for Yukawa couplings in the Lagrangian, $\mathcal{L} = -\lambda_u H_u^0 \bar{u}_L u_R - \lambda_d H_d^0 \bar{d}_L d_R - \lambda_e H_d^0 \bar{e}_L e_R + \text{h.c.}$ In particular, the coupling α_{3i} associated to the scalar (spin-independent) interaction include contributions from squark (\tilde{q}) exchange and CP-even light (h) and heavy (H) neutral Higgs exchange, as illustrated in Fig. 4, and can be approximated as²³

$$\begin{aligned} \alpha_{3i} \simeq & \frac{1}{2(m_{1i}^2 - m_{\tilde{\chi}_1^0}^2)} \left(g'^2 N_{11}^2 \eta_{11} \eta_{12} e_i \frac{y_i}{2} \right) + \frac{1}{2(m_{2i}^2 - m_{\tilde{\chi}_1^0}^2)} \left(g'^2 N_{11}^2 \eta_{21} \eta_{22} e_i \frac{y_i}{2} \right) \\ & + \frac{gg'm_{q_i}}{4m_W B_i} \left[\delta_{1i} N_{11} D_i C_i \left(\frac{1}{m_h^2} - \frac{1}{m_H^2} \right) + \delta_{2i} N_{11} \left(\frac{D_i^2}{m_h^2} + \frac{C_i^2}{m_H^2} \right) \right], \end{aligned} \quad (16)$$

where we are neglecting CP-violating phases^k. Here, δ_{1i} is N_{13} (N_{14}), δ_{2i} is N_{14} ($-N_{13}$), B_i is $\sin\beta$ ($\cos\beta$), C_i is $\sin\alpha$ ($\cos\alpha$) with α is the Higgs mixing angle, and D_i is $\cos\alpha$ ($-\sin\alpha$) for up (down) type quarks. y_i is the hypercharge defined by $e_i = T_{3i} + y_i/2$. m_{q_i} are the masses of the quarks, and the masses m_1 and m_2 correspond to the two squark mass eigenstates, and the η 's are the entries of the matrix diagonalizing the sfermion squared mass matrix which can be parameterized by an angle θ_f

$$\begin{pmatrix} \cos\theta_f & \sin\theta_f \\ -\sin\theta_f & \cos\theta_f \end{pmatrix} \equiv \begin{pmatrix} \eta_{11} & \eta_{12} \\ \eta_{21} & \eta_{22} \end{pmatrix}.$$

^kAnalyses of the effects of the CP phases on the cross section can be found in Refs. 19, 22, 23 and 24.

The first two terms in Eq. (16) arise from interactions of the type $g'q\tilde{q}\tilde{B}^0 \propto g'N_{11}q\tilde{q}\tilde{\chi}_1^0$, and the last two from $\lambda_q H_{u,d}^0 \bar{q}q$ (note that $gm_{q_i}/(m_W B_i) = \sqrt{2}\lambda_{q_i}$), $g' H_{u,d}^0 \tilde{H}_{u,d}^0 \tilde{B}^0 \propto g'N_{13,14}N_{11}H_{u,d}^0 \tilde{\chi}_1^0 \tilde{\chi}_1^0$. Due to the relative size of the lightest Higgs mass to the squark masses, and the smallness of η_{12} to η_{11} , the Higgs exchange term can dominate in α_3 23,180. Note also that the heavy Higgs can make a significant contribution to the down-type-quark part of α_3 . The reason being that the latter is proportional to $C_d^2 = \cos^2 \alpha$ whereas the light Higgs contribution is proportional to $D_d^2 = \sin^2 \alpha$, and for a wide range of parameters one finds $\tan \alpha = O(1/10)$. In addition, as we will discuss in Subsection 5.2.1, m_H may decrease significantly for large $\tan \beta$.

The contribution of the scalar interaction to the $\tilde{\chi}_1^0$ -nucleus cross section, $\sigma_{\tilde{\chi}_1^0-N}$, is given by 15,181

$$\sigma_{3N} = \frac{4M_r^2}{\pi} [Zf_p + (A-Z)f_n]^2, \quad (17)$$

where the reduced mass $M_r = M_N m_{\tilde{\chi}_1^0} / (M_N + m_{\tilde{\chi}_1^0})$, with M_N the mass of the nucleus, and the relevant contributions to f_p are

$$\frac{f_p}{m_p} = \sum_{q=u,d,s} f_{Tq}^{(p)} \frac{\alpha_{3q}}{m_q} + \frac{2}{27} f_{TG}^{(p)} \sum_{c,b,t} \frac{\alpha_{3q}}{m_q}, \quad (18)$$

where m_p is the mass of the proton, m_q the masses of the quarks, the parameters $f_{Tq}^{(p)}$ are defined by $\langle p | m_q \bar{q}q | p \rangle = m_p f_{Tq}^{(p)}$, while $f_{TG}^{(p)} = 1 - \sum_{q=u,d,s} f_{Tq}^{(p)}$. f_n has a similar expression. Typical numerical values of the hadronic matrix elements $f_{Tq}^{(p,n)}$ can be found e.g. in Ref. 28. These are:

$$\begin{aligned} f_{Tu}^{(p)} &= 0.020 \pm 0.004, & f_{Td}^{(p)} &= 0.026 \pm 0.005, & f_{Ts}^{(p)} &= 0.118 \pm 0.062, \\ f_{Tu}^{(n)} &= 0.014 \pm 0.003, & f_{Td}^{(n)} &= 0.036 \pm 0.008, & f_{Ts}^{(n)} &= 0.118 \pm 0.062, \end{aligned} \quad (19)$$

and we will use throughout this review the central values¹. We see that $f_{Ts}^{(n)} = f_{Ts}^{(p)}$ and much larger than f_{Tq} for u and d quarks, and therefore f_p and f_n are basically equal (note that the relevant part of the couplings α_{3q} are proportional to m_q , so the fraction α_{3q}/m_q does not become large for small m_q). Thus we can write^m

$$\sigma_{3N} \simeq \frac{4M_r^2}{\pi} A^2 f_p^2. \quad (20)$$

It is worth noticing here that the spin-independent scattering adds coherently giving rise to a cross section proportional to the squared of the atomic weight, A . However, the axial-vector (spin-dependent) interaction, the one proportional to α_{2i} in Eq. (15), which is nonzero only if the nucleus has a non-vanishing spin, is

¹Larger values of the hadronic matrix elements have also been considered in the literature. For analyses of the effect induced on the cross section by the present uncertainties in these values, see e.g. Refs. 26 and 29. A rough estimate can be obtained from Eq. (23) below.

^mThe contribution to this cross section from two-nucleon currents from pion exchange in the nucleus has recently been discussed in the last work of Ref. 161.

incoherent. Thus, for heavy targets, the scalar cross section is generically larger implying $\sigma_{\tilde{\chi}_1^0-N} \simeq \sigma_{3N}$. Recall that this is the case of the experiments discussed in Section 4. For example, Ge with a mass ~ 73 GeV and NaI with masses ~ 23 GeV for Na and ~ 127 GeV for I are used. In what follows we will concentrate on the scalar cross sectionⁿ, and in particular on the one for protons

$$\sigma_{3p} \equiv \sigma_{\tilde{\chi}_1^0-p} = \frac{4m_r^2}{\pi} f_p^2, \quad (21)$$

where $m_r = m_p m_{\tilde{\chi}_1^0} / (m_p + m_{\tilde{\chi}_1^0}) \approx m_p$. In fact, this is the cross section shown in the experimental papers (see Fig. 7), and therefore the one that we will compute in the different theoretical models. Note that for a material with heavy nuclei, $A \approx 100$, $M_N \approx 100$ GeV $\approx m_{\tilde{\chi}_1^0}$ and therefore

$$\sigma_{\tilde{\chi}_1^0-N} \approx 10^8 \sigma_{\tilde{\chi}_1^0-p}. \quad (22)$$

For $\sigma_{\tilde{\chi}_1^0-p} \approx 10^{-8}$ pb one recovers the rough estimate of Subsection 3.1.3, $\sigma_{\tilde{\chi}_1^0-N} \approx 1$ pb, for a particle with weak interactions.

The predictions for the scalar neutralino-proton cross section, $\sigma_{\tilde{\chi}_1^0-p}$, are usually studied in the framework of SUGRA, and we will review them below. We will see that $\sigma_{\tilde{\chi}_1^0-p} \approx 10^{-8}$ pb can be obtained, but that smaller (or larger) values are also possible depending on the parameter space chosen (e.g. m , M , A , $\tan\beta$ in mSUGRA as we will discuss in Subsection 5.2.1), since very different values for m_h , m_H , N_{11} , N_{13} , etc. can arise. Note in this sense that, from the above results, the neutralino-proton cross section can be approximated as

$$\begin{aligned} \sigma_{\tilde{\chi}_1^0-p} \approx & \frac{1}{4\pi} \left(\frac{gg' f_{Ts}^{(p)} m_p^2}{m_W \cos\beta} \right)^2 \\ & \times \left[N_{11} N_{14} \sin\alpha \cos\alpha \left(\frac{1}{m_h^2} - \frac{1}{m_H^2} \right) + N_{11} N_{13} \left(\frac{\sin^2\alpha}{m_h^2} + \frac{\cos^2\alpha}{m_H^2} \right) \right]^2 \end{aligned} \quad (23)$$

For example, assuming the typical values $N_{11} \approx 1$, $N_{13} \approx 0.1$, $\tan\alpha \approx 1/10$, $\tan\beta \approx 10$, and $m_H \approx 100(500)$ GeV, one obtains $\sigma_{\tilde{\chi}_1^0-p} \approx 10^{-8}(10^{-11})$ pb.

Before analyzing in detail the cross section, it is worth remarking that in these analyses to reproduce the correct phenomenology is crucial. Thus, in the next Subsection, the most recent experimental and astrophysical constraints which can affect this computation will be discussed.

ⁿRecent analyses of the spin-dependent part of the cross section can be found e.g. in Refs. 23, 28, 34, 48 and 182. In Ref. 183 it was pointed out that for targets with spin-non-zero nuclei, as e.g. ^{73}Ge where $\text{spin} = 9/2$, it might be the spin-dependent interaction the one determining the lower bound for the direct detection rate, when the cross section of the scalar interaction drops below about 10^{-12} pb.

5.1. Experimental and astrophysical constraints

We list here the most recent experimental and astrophysical results which are relevant when computing the neutralino-nucleon cross section. They give rise to important constraints on the SUSY parameter space.

(a) Higgs mass

Whereas in the context of the standard model the negative direct search for the Higgs at the LEP2 collider implies a lower bound on its mass of about 114.1 GeV, the situation in SUSY scenarios is more involved. In particular, in the framework of mSUGRA (to be discussed in detail below), one obtains for the lightest CP-even Higgs $m_h \gtrsim 114.1$ GeV when $\tan\beta \lesssim 50$, and $m_h \gtrsim 91$ GeV when $\tan\beta$ is larger¹⁸⁴. Recall in this sense that $\sigma_{SUSY}(e^+e^- \rightarrow Zh) = \sin^2(\alpha - \beta) \sigma_{SM}(e^+e^- \rightarrow Zh)$ with α the Higgs mixing angle in the neutral CP-even Higgs sector¹⁸⁵. Thus when the ZZh coupling, $\sin^2(\alpha - \beta)$, which controls the detection of the lightest MSSM Higgs at LEP, is ~ 1 one recovers the standard model bound. However, when a suppression of $\sin^2(\alpha - \beta)$ is obtained the bound will be smaller. Such a suppression occurs with $\tan\beta > 50$. In this case, in some regions of the parameter space $m_A^2 = m_{H_d}^2 + m_{H_u}^2 + 2\mu^2$ becomes small, $m_A \lesssim 150$ GeV, because the bottom Yukawa coupling entering in the renormalization group equation (RGE) for $m_{H_d}^2$ is large. And a small m_A gives rise to $\sin^2(\alpha - \beta) < 1$, as can be understood in terms of the relations between the angles α , β and m_A ¹⁸⁶.

In any case, let us remark that generically $\tan\beta$ is constrained to be $\tan\beta \lesssim 60$, since otherwise several problems arise. For example, as mentioned above, the bottom Yukawa coupling is large and for $\tan\beta > 60$, even for moderate values of m and M , $m_{H_d}^2$ becomes negative. As a consequence m_A^2 becomes also negative unless a fine-tuning (in the sense that only certain combinations of m and M are possible) is carried out. In this review we study only cases with $\tan\beta \leq 50$. Thus for mSUGRA we will always have $\sin^2(\alpha - \beta) \sim 1$. However, we will also be interested in relaxing the mSUGRA framework and therefore $\sin^2(\alpha - \beta)$ must be computed in this case for all points of the parameter space, in order to know which bound for the lightest MSSM Higgs must be applied. For the latter one can use the plot $\sin^2(\alpha - \beta)$ versus m_h shown in Ref. 187.

Let us finally mention that a very convenient program to evaluate m_h is the so-called **FeynHiggs**¹⁸⁸ which contains the complete one-loop and dominant two-loop corrections. Higher-order corrections introduce an uncertainty of about 3 GeV in the result. In addition, there is a simplified version of the program, **FeynHiggsFast**. The value of m_h obtained with this version is approximately 1 GeV below the one obtained using **FeynHiggs**. The figures shown throughout this review were obtained using **FeynHiggsFast**, and neglecting the uncertainty due to higher-order corrections. Recently, another program to study Higgs phenomenology has been constructed. See Ref. 189 for details.

(b) Top mass

The central experimental value for the top mass, $m_t(\text{pole}) = 175$ GeV, is used throughout this review. However, let us remark that a modification in this mass by ± 1 GeV implies, basically, a modification also of ± 1 GeV in the value of m_h ¹⁸⁴.

(c) *Bottom and tau masses*

For the bottom mass the input $m_b(m_b) = 4.25$ GeV is used throughout this review, which, following the analysis of Ref. 190 with $\alpha_s(M_Z) = 0.1185$, corresponds to $m_b(M_Z) = 2.888$ GeV. In the evolution of the bottom mass the SUSY threshold corrections at M_{SUSY} ¹⁹¹ are taken into account. These are known to be significant, specially for large values of $\tan\beta$. A similar analysis must be carried out for the tau mass, using as input $m_\tau(M_Z) = 1.7463$ GeV.

(d) *SUSY spectrum*

The present experimental lower bounds on SUSY masses coming from LEP and Tevatron must be imposed. In particular, using the low-energy relation from mSUGRA, $M_1 = \frac{5}{3}\tan^2\theta_W M_2$, one obtains for the lightest chargino mass the bound¹⁹² $m_{\tilde{\chi}_1^\pm} > 103$ GeV. Likewise, one is also able to obtain the following bounds for sleptons masses¹⁹³: $m_{\tilde{e}} > 99$ GeV, $m_{\tilde{\mu}} > 96$ GeV, $m_{\tilde{\tau}} > 87$ GeV. Finally, for the masses of the sneutrino, the lightest stop, the rest of squarks, and gluinos, one can use the following bounds: $m_{\tilde{\nu}} > 50$ GeV, $m_{\tilde{t}_1} > 95$ GeV, $m_{\tilde{q}} > 150$ GeV, $m_{\tilde{g}} > 190$ GeV.

(e) *$b \rightarrow s\gamma$*

The measurements of $B \rightarrow X_s\gamma$ decays at CLEO¹⁹⁴ and BELLE¹⁹⁵ lead to bounds on the branching ratio $b \rightarrow s\gamma$. In particular we impose throughout this review: $2 \times 10^{-4} \leq BR(b \rightarrow s\gamma) \leq 4.1 \times 10^{-4}$. Let us mention that a routine to carry out this evaluation is provided e.g. by the program micrOMEGAs¹⁹⁶. A description of this procedure can be found in Ref. 197. Although the improvements of Ref. 198 are not included in this routine, they are not so important for this review since, as discussed below, only $\mu > 0$ will be considered.

(f) *$g_\mu - 2$*

The new measurement of the anomalous magnetic moment of the muon, $a_\mu = (g_\mu - 2)/2$, in the E821 experiment at the BNL¹⁹⁹ deviates by $(33.7 \pm 11.2) \times 10^{-10}$ from the recent standard model calculation of Ref. 200 using e^+e^- data. Assuming that the possible new physics is due to SUGRA, we will show in the figures throughout this review the constraint $11.3 \times 10^{-10} \leq a_\mu(\text{SUGRA}) \leq 56.1 \times 10^{-10}$ at the 2σ level. This excludes the case $\mu < 0^\circ$.

(g) *$B_s \rightarrow \mu^+\mu^-$*

^oHowever, it is worth noticing that this result for a_μ is in contradiction with the one obtained by using tau decay data (instead of e^+e^- ones) which only implies a deviation $(9.4 \pm 10.5) \times 10^{-10}$ from the standard model calculation²⁰⁰. In any case, concerning the value of μ , it is worth recalling that constraints coming from the $b \rightarrow s\gamma$ process highly reduce the $\mu < 0$ parameter space.

The branching ratio for the $B_s \rightarrow \mu^+ \mu^-$ decay has been experimentally bounded by CDF ²⁰¹ with the result $BR(B_s \rightarrow \mu^+ \mu^-) < 2.6 \times 10^{-6}$. Although in the standard model this branching ratio is very small, of order 3×10^{-9} , it might be in principle significant in the SUSY case for large $\tan \beta$, due to Higgs (A) mediated decay ²⁰². This issue has been analyzed recently in the context of dark matter. It seems that the current experimental constraint does not eliminate in fact any relevant part of the parameter space of the MSSM ⁵⁹. Analyses of other scenarios can be found in Refs. 61 and 64.

(h) LSP

As mentioned in the Introduction, the LSP, with mass of order GeV, is stable and therefore must be an electrically neutral (also with no strong interactions) particle, since otherwise it would bind to nuclei and would be detectable in the Earth as an exotic heavy isotope with abundance $n/n(\text{proton}) \sim 10^{-10}(10^{-6})$ in the case of strong (electromagnetic) interactions ¹²⁶. This is not consistent with the experimental upper limits ²⁰³ $n/n(\text{proton}) \lesssim 10^{-15}$ to 10^{-30} . Although the lightest neutralino, $\tilde{\chi}_1^0$, is the LSP in most of the parameter space of the MSSM, in some regions one of the staus, $\tilde{\tau}_1$, can be lighter. Therefore, following the above discussion, these regions must be discarded.

(i) Relic $\tilde{\chi}_1^0$ density

The preferred astrophysical bounds on the dark matter density (see Eq. (2)), $0.1 \lesssim \Omega_{\text{DM}} h^2 \lesssim 0.3$, must be imposed on the theoretical computation of the relic $\tilde{\chi}_1^0$ density, once $\Omega_{\tilde{\chi}_1^0} = \Omega_{\text{DM}}$ is assumed^P. For the sake of completeness, we also show in the figures below the bounds $0.094 \lesssim \Omega_{\text{DM}} h^2 \lesssim 0.129$ deduced from the WMAP satellite (see Eq. 3). As mentioned in footnote *a*, different cosmological scenarios give rise to different results in the computation of the relic density. We will consider throughout this review the standard mechanism of thermal production of neutralinos (see Section 3.1.3).

Let us finally mention that there are programs ^{205,196} to evaluate $\Omega_{\tilde{\chi}_1^0}$. A very convenient one used in the figures shown here is **microMEGAS** ¹⁹⁶. In this program the exact tree-level cross sections for all possible annihilation ¹⁵ and coannihilation ^{108,109,110} channels are included in the code through a link to **CompHEP** ²⁰⁶, and accurate thermal average of them is used. Also, poles and thresholds are properly handled and one-loop QCD corrected Higgs decay widths ²⁰⁷ are used. The SUSY corrections included in the latest version of the code ²⁰⁷ are not implemented yet

^PIf neutralinos do not constitute all the dark matter in the Universe, and other particles discussed in Section 3 also contribute, then $\Omega_{\tilde{\chi}_1^0} < \Omega_{\text{DM}}$. This may allow points in the parameter space which would be excluded by $\Omega_{\tilde{\chi}_1^0} h^2 < 0.1$. However, notice that in this case the density of neutralinos in the galaxy would be $\rho_{\tilde{\chi}_1^0} = \xi \cdot 0.3 \text{ GeV cm}^{-3}$ with $\xi < 1$, and therefore the results (event rates) would imply a larger value of the experimental cross section ²⁰⁴. Since the DAMA area is already difficult to reproduce in SUSY models, now the situation will be even worse. In Fig. 7 we should substitute $\sigma_{\text{WIMP-nucleon}}$ by $\xi \cdot \sigma_{\text{WIMP-nucleon}}$.

by **micrOMEGAs**. Fortunately, in our case, their effect is much smaller than that of the QCD corrections. Good agreement between **micrOMEGAs** and other independent computations of $\Omega_{\tilde{\chi}_1^0}$ including $\tilde{\chi}_1^0 - \tilde{\tau}_1$ coannihilations can be found in Ref. 208.

(j) *UFB*

The constraints that arise from imposing the absence of charge and colour breaking minima can also be considered ⁶³. As is well known, the presence of scalar fields with colour and electric charge in SUSY theories induces the possible existence of dangerous charge and colour breaking minima, which would make the standard vacuum unstable ⁶⁹. The presence of these instabilities may imply either that the corresponding model is inconsistent or that it requires non-trivial cosmology to justify that the Universe eventually fell in the phenomenologically realistic (but local) minimum ²⁰⁹. There are two types of constraints: the ones arising from directions in the field-space along which the (tree-level) potential can become unbounded from below (UFB), and those arising from the existence of charge and color breaking (CCB) minima in the potential deeper than the standard minimum. By far, the most restrictive are the UFB bounds, and therefore these are the ones used in the figures shown here. There are three UFB directions, labelled as UFB-1, UFB-2, UFB-3 in Ref. 210. It is worth mentioning here that in general the unboundedness is only true at tree-level since radiative corrections eventually raise the potential for large enough values of the fields, but still these minima can be deeper than the realistic one (i.e. the SUSY standard-model vacuum) and thus dangerous. The UFB-3 direction, which involves the scalar fields $\{H_u, \nu_{L_i}, e_{L_j}, e_{R_j}\}$ with $i \neq j$ and thus leads also to electric charge breaking, yields the strongest bound among all the UFB and CCB constraints.

5.2. *SUGRA predictions for the neutralino-nucleon cross section*

As can be deduced from the above discussion concerning the cross section in Eq. (21), the values of the SUSY parameters, such as scalar masses or gaugino masses, are crucial in the analysis. Obviously, these values are associated with the mechanism of SUSY breaking. A pragmatic attitude to this issue is the addition of explicit soft SUSY-breaking parameters of the appropriate size (of order $10^2 - 10^3$ GeV) in the Lagrangian and with appropriate flavour symmetries to avoid dangerous flavour-changing neutral currents (FCNC) transitions. The problem with this pragmatic attitude is that, taken by itself, lacks any theoretical explanation. SUGRA theories provide an attractive context that can justify such a procedure. Indeed, if one considers the SUSY standard model and couples it to $N = 1$ SUGRA, the spontaneous breaking of local SUSY in a hidden sector generates explicit soft SUSY-breaking terms of the required form in the effective low-energy Lagrangian ²¹¹. If SUSY is broken at a scale Λ_S , the soft terms have a scale of order Λ_S^2/M_{Planck} , and therefore one obtains the required size if SUSY is broken at an intermediate scale $\Lambda_S \sim 10^{11}$ GeV.

Thus one usually considers the MSSM in the framework of SUGRA. Working in

this framework the soft parameters generated once SUSY is broken through gravitational interactions, i.e., gaugino masses, scalar masses, trilinear couplings and bilinear couplings, are denoted at high energy by M_a , m_α , $A_{\alpha\beta\gamma}$, and B , respectively. Although in principle these are free parameters together with μ , when electroweak symmetry breaking is imposed μ^2 and B are determined. Finally, the renormalization group equations (RGEs) are used to derive low-energy SUSY parameters⁹. Since the SUGRA framework still allows a large number of free parameters, in order to have predictive power, one usually assumes that the above soft parameters are universal at the GUT scale, $M_{GUT} \approx 2 \times 10^{16}$ GeV, providing also for an understanding of FCNC suppression. As mentioned in the Introduction, this is the mSUGRA scenario, also called in the literature the Constrained MSSM (CMSSM). Although, apparently, this assumption about universality is arbitrary, it is worth noticing that interesting classes of SUGRA models give rise to this kind of universal soft SUSY-breaking terms²¹¹. In addition, explicit string constructions with these universality properties can be found in some limits²¹¹. We will discuss them in some detail in Subsections 5.3 and 5.4.

Let us recall that the full N=1 Supergravity Lagrangian is specified in terms of three functions which depend on the scalar fields ϕ_M of the theory: the analytic gauge kinetic function $f_a(\phi_M)$, the real Kähler potential $K(\phi_M, \phi_M^*)$ and the analytic superpotential $W(\phi_M)$. In particular, f_a determines the kinetic terms for the gauge fields and is related to the gauge couplings as $Re f_a = 1/g_a^2$, where the subindex a is associated with the different gauge groups of the theory, K determines the kinetic terms for the scalar fields, and W determines the Yukawa couplings. Thus, for example, the form of K that leads to canonical kinetic terms for the observable fields C_α , namely $K = \sum_\alpha C_\alpha C_\alpha^*$, irrespective of the SUSY-breaking mechanism gives rise to universal soft scalar masses²¹¹, $m_\alpha = m$, of the type imposed in mSUGRA.

Below we will carry out the analysis of mSUGRA concerning dark matter. We will also discuss how the results are modified when the above assumptions are relaxed. In particular, we will allow an intermediate scale instead of the usual GUT one, and also non-universal soft scalar and gaugino masses.

5.2.1. mSUGRA scenario with a GUT scale

As can be deduced from the above discussion, in this scenario there are only four free parameters^r: m , M , A , and $\tan\beta$. In addition, the sign of μ remains also

⁹Let us remark that, given the convention used throughout this review for gaugino masses in the Lagrangian, $\mathcal{L} = \frac{1}{2} \sum_a M_a \lambda_a \lambda_a + \text{h.c.}$, one has to use the (one-loop) RGEs obtained e.g. in Ref. 212, but with an opposite sign in the gaugino contributions to the RGE's of the A parameters.

^rIn fact, scenarios with less free parameters are also possible. For instance, in the above example with canonical kinetic terms, if in addition we assume that Yukawa couplings and μ are constants, i.e. that they do not depend on hidden sector fields, one obtains $B = A - m$. Scenarios with this type of constraints between soft parameters have been analyzed in the context of dark matter in Ref. 65.

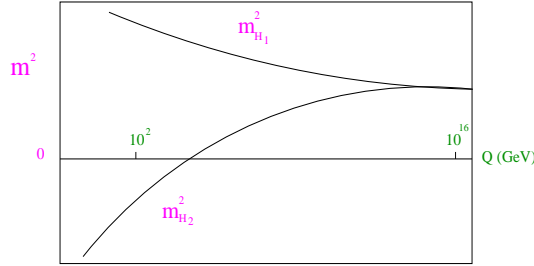


Fig. 11. Running of the soft Higgs masses-squared with energy.

undetermined (see Eq. (13)). Let us also remark that in this context the lightest neutralino is mainly bino^{213,214}. To understand this result qualitatively, we show schematically in Fig. 11 the well known evolution of $m_{H_u}^2$ (and $m_{H_d}^2$ neglecting bottom and tau Yukawa couplings) towards large and negative values with the scale. Since μ^2 given by Eq. (13), for reasonable values of $\tan\beta$, can be approximated as,

$$\mu^2 \approx -m_{H_u}^2 - \frac{1}{2}M_Z^2, \quad (24)$$

then it becomes also large (the effect of the one-loop corrections to the scalar potential can be minimized by evaluating μ at the scale $M_{SUSY} = \sqrt{m_{\tilde{t}_1} m_{\tilde{t}_2}}$). In particular, $|\mu|$ becomes much larger than M_1 and M_2 . Thus, as can be easily understood from Eqs. (12) and (14), the lightest neutralino will be mainly gaugino, and in particular bino, since at low energy $M_1 = \frac{5}{3} \tan^2 \theta_W M_2 \approx 0.5 M_2$. We show this fact in the plot on the left frame of Fig. 12, where for $\tan\beta = 10$ the gaugino-Higgsino components-squared N_{1i}^2 of the lightest neutralino as a function of its mass $m_{\tilde{\chi}_1^0}$ are exhibited. Here we are using an example with $m = 150$ GeV and $A = M$. Note that M is essentially fixed for a given $m_{\tilde{\chi}_1^0}$. Clearly, N_{11} is extremely large and therefore $P \gtrsim 0.9$.

Now, using Eq. (21) one can compute the cross section for different values of the parameters (for recent results see Refs. 18, 19, 21, 22, 23, 24, 26, 28, 29, 31, 36, 39, 40, 41, 44, 45, 46, 47, 48, 49, 50, 51, 52, 55, 57, 58, 59, 60, 63, 64, 65). As a consequence of the $\tilde{\chi}_1^0$ being mainly bino, the predicted $\sigma_{\tilde{\chi}_1^0-p}$ is well below the accessible experimental regions for low and moderate values of $\tan\beta$, since the scattering channels through Higgs exchange shown in Fig. 4 are not so important (recall that the Higgs-neutralino-neutralino couplings are proportional to N_{13} and N_{14} as shown in Eq. (16)). In addition, the (tree-level) mass of the CP-odd Higgs, A ,

$$m_A^2 = m_{H_d}^2 + m_{H_u}^2 + 2\mu^2, \quad (25)$$

will be large because μ^2 is large. Since the heaviest CP-even Higgs, H , is almost degenerate in mass with this, m_H will also be large producing a further suppression in the scattering channels. This fact is shown in Fig. 13, where contours of $\sigma_{\tilde{\chi}_1^0-p}$

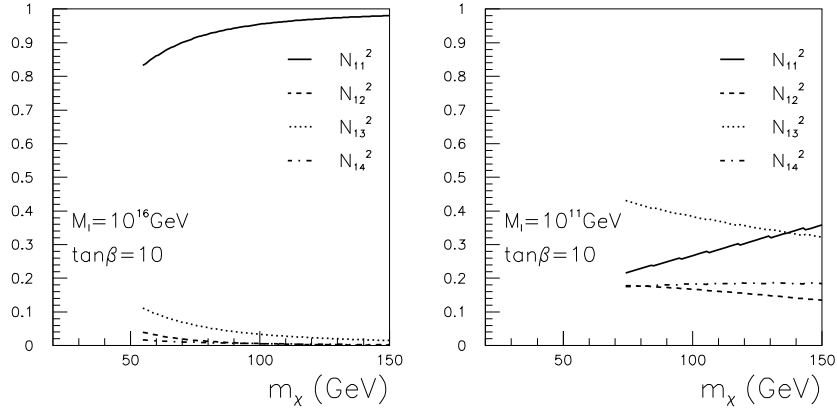


Fig. 12. Gaugino-Higgsino components-squared of the lightest neutralino as a function of its mass for the unification scale (left frame), $M_I = 10^{16}$ GeV, and for the intermediate scale (right frame), $M_I = 10^{11}$ GeV.

in the parameter space (m, M) for $\tan\beta = 10$, $A = 0$ and $\mu > 0$ ^s are plotted⁶³. Note that we can deduce the value of the $\tilde{\chi}_1^0$ mass in the plots from the value of M , since $m_{\tilde{\chi}_1^0} \simeq M_1 \simeq 0.4 M$. For the gluino mass we can also use the simple relation, $m_{\tilde{g}} \simeq 2.5 M$.

As we can see in the figure, the experimental bounds discussed in Subsection 5.1 are very important and exclude large regions of the parameter space. This is due to the combination of the Higgs mass bound with the $g_\mu - 2$ lower bound^t. One obtains from the Higgs mass the lower bound $M \gtrsim 320$ GeV, and from $g_\mu - 2$ the upper bound $M \lesssim 440$ GeV. These bounds imply for the neutralino, $128 \lesssim m_{\tilde{\chi}_1^0} \lesssim 176$ GeV, and for the gluino (and squarks) $800 \lesssim m_{\tilde{g}, \tilde{q}} \lesssim 1100$ GeV. The light shaded area in the figure shows the region allowed by the experimental bounds. There, the lower contour (double solid line) is obtained including also the constraint coming from the LSP bound, $m_{\tilde{\chi}_1^0} < m_{\tilde{\tau}_1}$. For this area $\sigma_{\tilde{\chi}_1^0-p} \approx 10^{-9}$ pb.

On the other hand, the astrophysical bounds $0.1 \lesssim \Omega_{\tilde{\chi}_1^0} h^2 \lesssim 0.3$ must be imposed in the computation. Let us recall that there are only four regions where the upper bound $\Omega_{\tilde{\chi}_1^0} h^2 \sim 1/\sigma_{ann} \lesssim 0.3$ can be satisfied. There is the *bulk region* at

^sLet us remark that the sign of the dominant contribution to the supersymmetric contribution to the $g_\mu - 2$ is given by $M_2\mu$. As discussed in Subsection 5.1, we are taking this to be positive, and therefore we will only consider $\text{sign}(M) = \text{sign}(\mu)$. Now, due to the symmetry of the RGEs, the results for $(-M, A, -\mu)$ are identical to those for $(M, -A, \mu)$, and therefore, one can cover the whole (permitted) parameter space restricting to positive values for M and μ and allowing A to take positive and negative values.

^tRecall that we are using only the limit based on e^+e^- analysis (see footnote n), otherwise the allowed region would extend towards the right hand side of the figure.

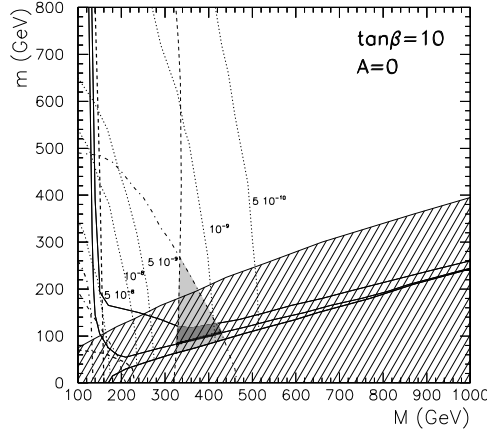


Fig. 13. Scalar neutralino-proton cross section $\sigma_{\tilde{\chi}_1^0-p}$ in the parameter space of the mSUGRA scenario (m , M) for $\tan\beta = 10$, $A = 0$ and $\mu > 0$. The dotted curves are contours of $\sigma_{\tilde{\chi}_1^0-p}$. The region to the left of the near-vertical dashed line is excluded by the lower bound on the Higgs mass $m_h > 114.1$ GeV. The region to the left of the near-vertical double dashed line is excluded by the lower bound on the chargino mass $m_{\tilde{\chi}_1^\pm} > 103$ GeV. The corner in the lower left shown also by a double dashed line is excluded by the LEP bound on the stau mass $m_{\tilde{\tau}_1} > 87$ GeV. The region bounded by dot-dashed lines is allowed by $g_\mu - 2$. The region to the left of the double dot-dashed line is excluded by $b \rightarrow s\gamma$. From bottom to top, the solid lines are the upper bounds of the areas such as $m_{\tilde{\tau}_1} < m_{\tilde{\chi}_1^0}$ (double solid), $\Omega_{\tilde{\chi}_1^0}h^2 < 0.1$ and $\Omega_{\tilde{\chi}_1^0}h^2 < 0.3$. The light shaded area is favored by all the phenomenological constraints, while the dark one fulfills in addition $0.1 \leq \Omega_{\tilde{\chi}_1^0}h^2 \leq 0.3$ (the black region on top of this indicates the WMAP range $0.094 < \Omega_{\tilde{\chi}_1^0}h^2 < 0.129$). The ruled region is excluded because of the charge and colour breaking constraint UFB-3.

moderate M and m ^{11,14}. There, since $\tilde{\chi}_1^0$ is mainly bino, the annihilation channels into leptons are important (see e.g. Fig. 2), specially those from \tilde{l}_R exchange because they have the largest hypercharge. Moreover, the mass of \tilde{l}_R only receives very small contributions from gaugino loop diagrams. Here $\Omega_{\tilde{\chi}_1^0}h^2 \lesssim 0.3$ requires specific upper bounds on $\tilde{\chi}_1^0$ and \tilde{l}_R masses ¹⁰¹. Another region is the *coannihilation region* extending to larger M ¹⁰⁴. There the tail where the LSP is almost degenerate with the NLSP, the stau, producing efficient coannihilations, is rescued ¹⁰⁸. This is true even for large values of $m_{\tilde{\chi}_1^0}$. These two regions can clearly be seen in Fig. 13. There is also the *focus-point region* at $m > 1$ TeV not shown in this figure, and that will be discussed at the end of this subsection. Finally, there is the *Higgs pole region* extending to large M and m because rapid annihilation through a direct-channel pole ^{101,215,41} when $2m_{\tilde{\chi}_1^0} \sim m_{A,H}$ (see e.g. Fig. 2). But this region occurs at large $\tan\beta$ and will be discussed below in Fig. 14.

Given the above bounds, we observe in Fig. 13 that the allowed (dark shaded) area becomes very small (extremely small if the recent WMAP data are taken into

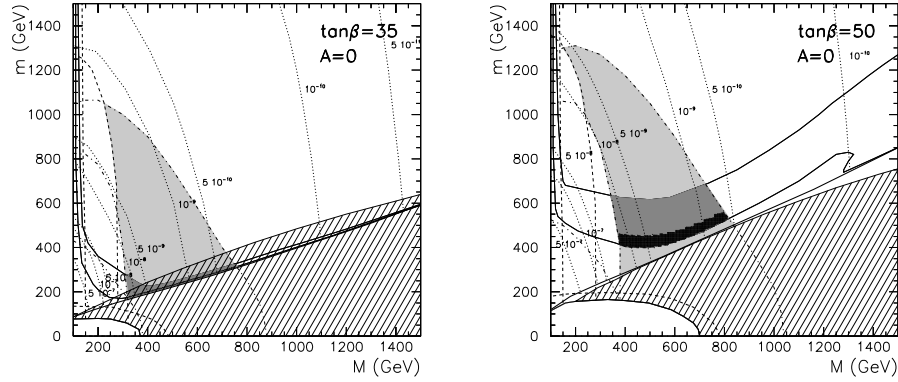


Fig. 14. The same as in Fig. 13 but for $\tan\beta = 35$ and 50 . The white region at the bottom bounded by a solid line is excluded because $m_{\tilde{\tau}_1}^2$ becomes negative.

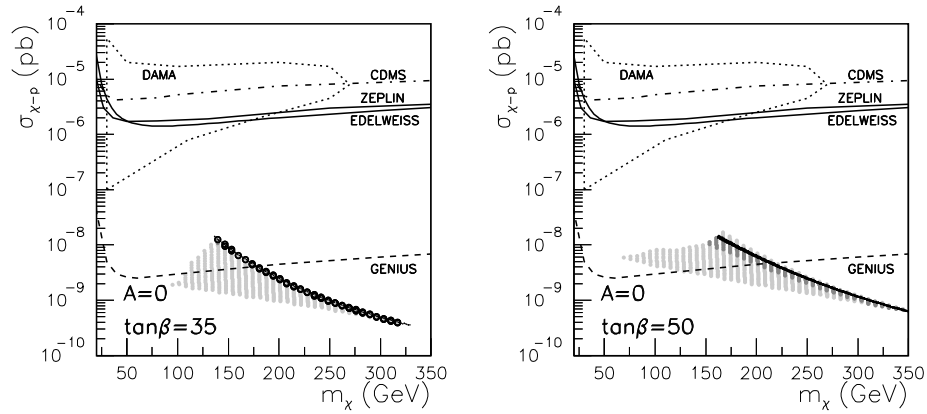


Fig. 15. Scatter plot of the scalar neutralino-proton cross section $\sigma_{\tilde{\chi}_1^0-p}$ as a function of the neutralino mass $m_{\tilde{\chi}_1^0}$ in the mSUGRA scenario, for $\tan\beta = 35$ and 50 , $A = 0$ and $\mu > 0$. The light grey dots correspond to points fulfilling all experimental constraints. The dark grey dots correspond to points fulfilling in addition $0.1 \leq \Omega_{\tilde{\chi}_1^0} h^2 \leq 0.3$ (the black dots on top of these indicate those fulfilling the WMAP range $0.094 < \Omega_{\tilde{\chi}_1^0} h^2 < 0.129$). The circles indicate regions excluded by the UFB-3 constraint. The lines corresponding to the different experiments are as in Fig. 7.

account). Only the beginning of the tail mentioned above is rescued. In addition, the restrictions coming from the UFB-3 constraint exclude also this area. In conclusion, the results indicate that the whole parameter space for $\tan\beta = 10$ is excluded on these grounds. This is also true for other values of A , as shown explicitly in Ref. 63.

The neutralino-proton cross section can be increased when the value of $\tan\beta$ is increased^{18,29,40,41}. Notice for instance that the contribution of the down-type

quark to the cross section is proportional to $1/\cos\beta$ (see e.g. Eq. (23)). In addition, the bottom Yukawa coupling increases, and as a consequence $m_{H_d}^2$ decreases, implying that m_A^2 , given by Eq. (25), also decreases. Since, as mentioned above, $m_H \approx m_A$, this will also decrease significantly. Indeed, scattering channels through Higgs exchange are more important now and their contributions to the cross section will increase it. Thus, in principle, we can even enter in the DAMA region. However, the present experimental constraints exclude this possibility^{48,49}. We show this fact for $\tan\beta = 35$ and $A = 0$ in the plot on the left frame of Fig. 14⁶³. In principle, if we only impose the LEP lower bound $m_{\tilde{\chi}_1^\pm} > 103$ GeV, the cross section can be as large as $\sigma_{\tilde{\chi}_1^0-p} \approx 10^{-6}$ pb. However, at the end of the day, the other experimental bounds (Higgs mass, $b \rightarrow s\gamma$, $g_\mu - 2$ upper bound) constrain the cross section to be $\sigma_{\tilde{\chi}_1^0-p} \lesssim 10^{-8}$ pb. The region allowed by the $g_\mu - 2$ lower bound is now larger and the cross section can be as low as $\sigma_{\tilde{\chi}_1^0-p} \approx 5 \times 10^{-10}$ pb. These bounds imply $260 \lesssim M \lesssim 750$ GeV, and therefore $104 \lesssim m_{\tilde{\chi}_1^0} \lesssim 300$ GeV, $650 \lesssim m_{\tilde{g},\tilde{q}} \lesssim 1875$ GeV. Concerning the UFB-3 constraint, it is worth noticing that the larger $\tan\beta$ is, the larger the excluded region becomes. However, unlike the case $\tan\beta = 10$, this is not sufficient to forbid the whole dark shaded area allowed also by the astrophysical bounds. In fact, one can check that with $\tan\beta > 20$ one can always find regions where all constraints are fulfilled, depending on the value of A . For example, for $\tan\beta = 35$ and $A = M$ essentially the whole dark shaded area is allowed, whereas for $A = -M, -2M$ this is forbidden. A detailed analysis of this issue can be found in Ref. 63.

The above comments, concerning the cross section, can also be applied for very large values of $\tan\beta$, as e.g. $\tan\beta = 50^u$. We show this in the plot on the right frame of Fig. 14. However, note that now, unlike the case $\tan\beta = 35$, the whole dark shaded area allowed by experimental and astrophysical bounds is not constrained by the UFB-3. This is also true for other values of A . Let us finally recall that the region allowed by $0.1 \leq \Omega_{\tilde{\chi}_1^0} h^2 \leq 0.3$ is larger because the CP-odd Higgs A becomes lighter as $\tan\beta$ increases, as discussed above. This allows the presence of resonances in the Higgs mediated annihilation channels, resulting in drastic reduction of the neutralino relic abundance. In the case of $\tan\beta = 50$, the resonant effects in the annihilation channels are felt in the whole parameter space displayed in Fig. 14. We can see as well, that the area of the parameter space where $\tilde{\chi}_1^0 - \tilde{\tau}_1$ coannihilations are relevant lead to values of $\Omega_{\tilde{\chi}_1^0} h^2 < 0.1$.

We summarize the above results for $\tan\beta = 35, 50$, and $A = 0$, in Fig. 15⁶³. There, the values of $\sigma_{\tilde{\chi}_1^0-p}$ allowed by all experimental constraints as a function of the neutralino mass $m_{\tilde{\chi}_1^0}$ are shown. Dark grey dots correspond to those points having a relic neutralino density within the preferred range $0.1 \leq \Omega h^2 \leq 0.3$. Given the narrow range of these points for the case $\tan\beta = 35$, they overlap in the figure

^uFor this very large values of $\tan\beta$ results become very sensitive to the precise values of m_t and m_b . This has been discussed e.g. in Refs. 40, 41 and 49.

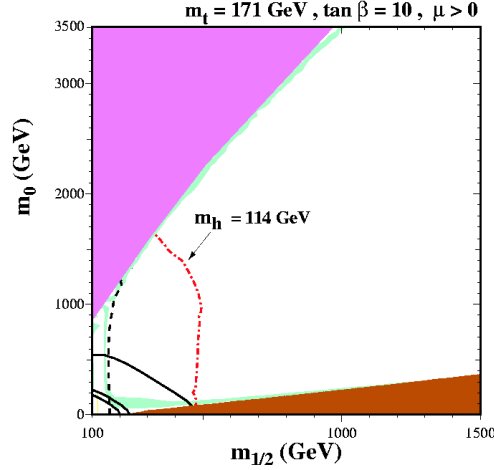


Fig. 16. An expanded view of the $M-m$ parameter plane showing the focus-point regions at large m for $\tan\beta = 10$. In the shaded (magenta) region in the upper left corner, there are no solutions with proper electroweak symmetry breaking. Note that $m_t = 171$ GeV has been chosen, in which case the focus-point region is at lower m than when $m_t = 175$ GeV, as assumed in the other figures. The position of this region is very sensitive to m_t .

with those excluded by the UFB-3 constraint (shown with circles). We observe that, generically, the cross section and the neutralino mass are constrained to be (for any value of A) $5 \times 10^{-10} \lesssim \sigma_{\tilde{\chi}_1^0-p} \lesssim 3 \times 10^{-8}$ pb and $120 \lesssim m_{\tilde{\chi}_1^0} \lesssim 320$ GeV, respectively.

Qualitatively similar results are obtained when dark matter is analyzed in the so-called focus-point supersymmetry scenario. Let us recall that this has been proposed as an alternative scenario in order to avoid dangerous SUSY contributions to flavour and CP violating effects²¹⁶. The idea is to assume the existence of squarks and sleptons with masses which can be taken well above 1 TeV (of course this scenario rules out SUSY as an explanation of the possible deviation in the $g_\mu - 2$ from the standard model prediction). It has also been argued that this situation produces no loss of naturalness. Notice that for $m^2 \gg M^2$ the electroweak scale given by Eq. (24), $M_Z^2/2 \approx -m_{H_u}^2 - \mu^2$, can easily be obtained since $m_{H_u}^2$ becomes less negative.

The implications of focus-point supersymmetry for neutralino dark matter have been considered in Ref. 31. In particular, it was pointed out that for $m > 1$ TeV the lightest neutralino is a gaugino-Higgsino mixture over much of parameter space. This can be understood from Eq. (24) since $m_{H_u}^2$ becomes less negative for $m_0 > 1$ TeV (recall Fig. 11), and therefore $|\mu|$ decreases. As a consequence, although as m increases the t -channel sfermion exchange process (see e.g. Fig. 2) is more and more suppressed, the LSP gradually acquires a significant Higgsino component and other diagrams become unsuppressed. Thus the upper bound in Eq. (2) is fulfilled.

This ‘focus-point’ region, which is adjacent to the boundary of the region where electroweak symmetry breaking is possible, is shown in Fig. 16 (from Ref. 50).

Concerning the neutralino-proton cross section, scattering channels through Higgs exchange will increase it. However, one still needs large values for $\tan \beta$ (of order 50) in order to have very large cross sections, and then experimental constraints are very important.

Obviously, in the mSUGRA scenario with a GUT scale that we have reviewed in this Subsection, where $\sigma_{\tilde{\chi}_1^0-p} \lesssim 3 \times 10^{-8}$ pb, more sensitive detectors producing further data are needed. As discussed in Subsection 4.1.2, many dark matter detectors are being projected. Particularly interesting is the case of GENIUS, where values of the cross section as low as $\approx 10^{-9}$ pb will be accessible, although this might not be sufficient depending on the values of the parameters (see Fig. 15).

5.2.2. *mSUGRA scenario with an intermediate scale*

The analysis of the cross section $\sigma_{\tilde{\chi}_1^0-p}$ carried out above in the context of mSUGRA, was performed assuming the unification scale $M_{GUT} \approx 10^{16}$ GeV. However, there are several interesting phenomenological arguments in favour of SUGRA scenarios with scales $M_I \approx 10^{10-14}$ GeV, such as to explain neutrino masses, the scale of axion physics, and others²¹⁷. In addition, the string scale may be anywhere between the weak and the Planck scale, and explicit scenarios with intermediate scales may arise in the context of D-brane constructions from type I strings, as we will discuss in Subsection 5.3. Inspired by all these scenarios, to use the value of the initial scale M_I as a free parameter for the running of the soft terms is particularly interesting. In fact, it was pointed out in Refs. 33, 35, 42 that $\sigma_{\tilde{\chi}_1^0-p}$ is very sensitive to the variation of M_I for the running of the soft terms. For instance, by taking $M_I = 10^{10-12}$ GeV rather than M_{GUT} , regions in the parameter space of mSUGRA can be found where $\sigma_{\tilde{\chi}_1^0-p}$ is two orders of magnitude larger than for M_{GUT} ^{33,46,51,63}.

Before trying to understand this result, let us discuss what we mean by an intermediate unification scale. Concerning this point two possible scenarios are schematically shown in Fig. 17 for the example $M_I = 10^{11}$ GeV. In scenario (a) the gauge couplings are non universal, $\alpha_i \neq \alpha$, and their values depend on the initial scale M_I chosen. As we will discuss in Subsection 5.3, a qualitatively similar scenario may arise in the context of type I string constructions if the gauge groups of the standard model come from different types of D-branes. Since different D-branes have associated different couplings, this implies the non universality of the gauge couplings.

On the other hand, scenario (b) with gauge coupling unification at M_I , $\alpha_i = \alpha$, can be obtained with the addition of extra fields in the massless spectrum. For the example of the figure these are doublets and singlets under the standard model gauge group. As discussed in Ref. 33, the values of the gauge coupling constants

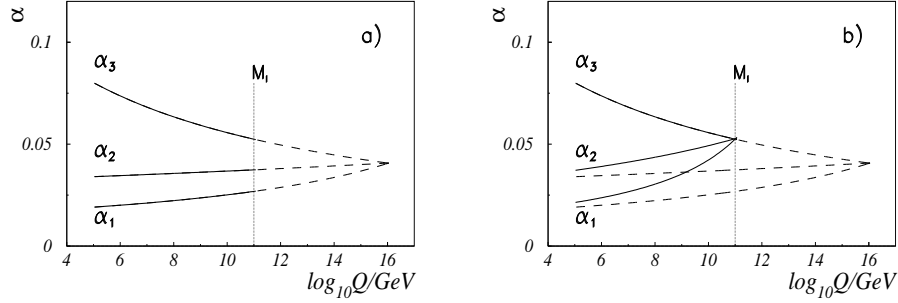


Fig. 17. Running of the gauge couplings with energy, shown with solid lines, assuming (a) non universality and (b) universality of couplings at the initial scale M_I . For comparison the usual running of the MSSM couplings is also shown with dashed lines.

at the intermediate scale are important in the computation of the cross section, and scenario (a) gives rise to larger cross sections than scenario (b). Let us then concentrate on the former.

The fact that smaller scales imply a larger $\sigma_{\tilde{\chi}_1^0-p}$ can be explained with the variation in the value of μ with M_I . One observes that, for $\tan\beta$ fixed, the smaller the initial scale for the running the smaller the numerator in the first piece of Eq. (13) becomes. This can be understood from the evolution of $m_{H_u}^2$ with the scale (see Fig. 11). Clearly, when the value of the initial scale is reduced the RGE running is shorter and, as a consequence, the negative contribution $m_{H_u}^2$ to μ^2 in Eq. (13) becomes less important. Then, $|\mu|$ decreases and therefore the Higgsino composition of the lightest neutralino increases. Eventually, $|\mu|$ will be of the order of M_1 , M_2 and $\tilde{\chi}_1^0$ will be a mixed Higgsino-gaugino state (see the plot on the frame of Fig. 12). In addition, when $|\mu|$ decreases m_A^2 , given by Eq. (25), also decreases. As mentioned in the previous Subsection when talking about increasing $\tan\beta$, H will decrease and therefore the scattering channels through Higgs exchange will increase the cross section.

Let us also remark that, for the same value of the parameters, the lightest Higgs mass m_h decreases with respect to the GUT scale scenario. This is because the value of m_h depends on the value of the gluino mass M_3 . It increases when M_3 increases at low energy. However, now the running is shorter and therefore M_3 at low energy is smaller than in the GUT scenario. Although the latter may be welcome in order to obtain larger cross sections, it may also be dangerous when confronting with the experimental result concerning the Higgs mass.

Concerning the value of the relic density, $\Omega_{\tilde{\chi}_1^0}$ is dramatically reduced with respect to the M_{GUT} case. This is due to a combination of several factors: 1) The Higgsino-gaugino composition of $\tilde{\chi}_1^0$ allows a significant increase of the $\tilde{\chi}_1^0$ annihilation cross section, due to channels with Higgs and gauge bosons in the final states; 2) The decrease of the mass of the pseudoscalar Higgs, along with the

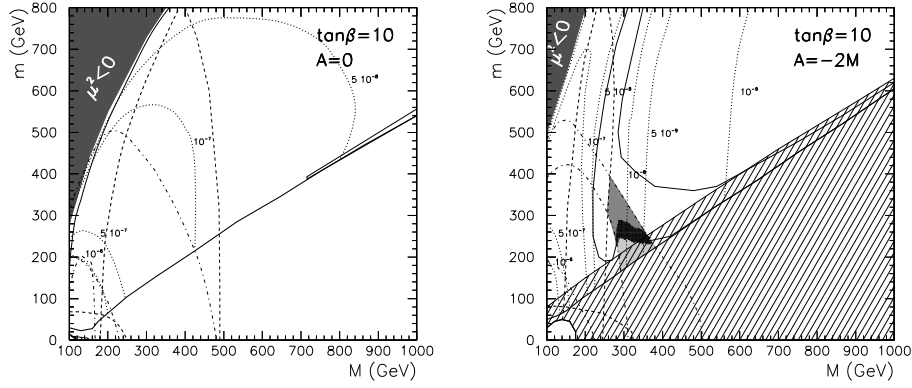


Fig. 18. The same as in Fig. 13 but for the intermediate scale $M_I = 10^{11}$ GeV, with $A = 0, -2M$. The black area is excluded because μ^2 becomes negative. The white region at the bottom bounded by a solid line is excluded because $m_{\tau_1}^2$ becomes negative.

value of the μ -term, enables the presence of resonant annihilation channels even at $\tan \beta = 10$; 3) The masses of the lightest chargino and stop are small enough to allow $\tilde{\chi}_1^0 - \tilde{\chi}_1^\pm$ ¹⁰⁹ and $\tilde{\chi}_1^0 - \tilde{t}_1$ ¹¹⁰ coannihilations in some areas of the parameter space. Although the later is less relevant, we find some areas at $\tan \beta = 50$ and $A < 0$.

We show in Fig. 18 the result for $M_I = 10^{11}$ GeV, with $\tan \beta = 10$ and $A = 0, -2M$ ⁶³. We choose A proportional to M because this relation is particularly interesting, arising naturally in several string models ²¹¹. However our conclusions will be independent on this assumption. For example, if we choose to do the plots for different constant values of A , a very common procedure in pure SUGRA analyses, the results will be qualitatively similar. The case $A = 0$ can be compared with the one in Fig. 13, where M_{GUT} is used. Now the relation $m_{\tilde{\chi}_1^0} \sim 0.4 M$ does not hold, and one has $m_{\tilde{\chi}_1^0} > 0.4M$. In any case, $m_{\tilde{\chi}_1^0} < M_1$ since the bino-Higgsino mixing is significant in this case. Clearly, for the same values of the parameters, larger cross sections can be obtained with the intermediate scale. It is worth noticing that even with this moderate value of $\tan \beta$, $\tan \beta = 10$, there are regions where the cross section enters in the DAMA area, $\sigma_{\tilde{\chi}_1^0 - p} \approx 10^{-6}$ pb. However, for $A = 0$ the whole parameter space is forbidden due to the combination of the Higgs mass bound with the $g_\mu - 2$ lower bound (for $A = M$ the situation is similar). We have checked explicitly that 114.1 GeV is the correct lower bound to be used concerning the Higgs mass, since generically $\sin^2(\alpha - \beta) \sim 1$ for the intermediate scale. Notice also that now, for $A = 0$ (and also for $A = M$), $\Omega_{\tilde{\chi}_1^0} h^2$ is smaller than 0.1 in most of the parameter space. Only tiny regions bounded by solid lines in the figure, and therefore with $0.1 \leq \Omega_{\tilde{\chi}_1^0} h^2 \leq 0.3$, can be found.

On the other hand, for $A = -2M$ (and also for $A = -M$) there are small

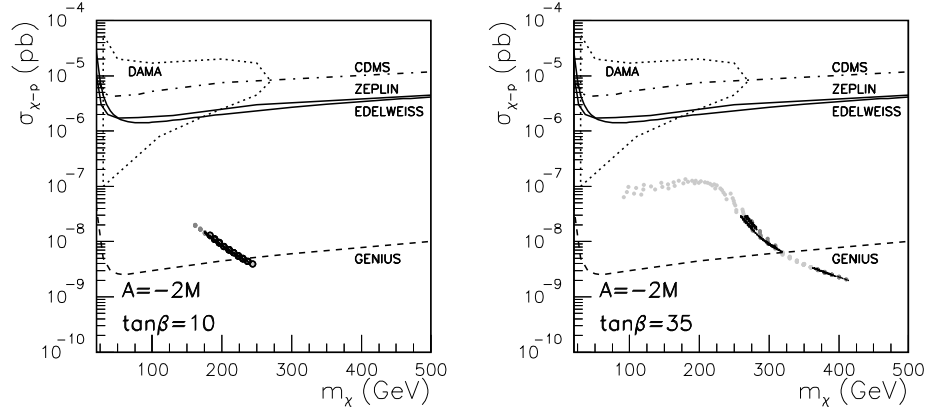


Fig. 19. The same as in Fig. 15 but for the intermediate scale $M_I = 10^{11}$ GeV, with $\tan \beta = 10, 35$ and $A = -2M$.

regions where the m_h and $g_\mu - 2$ bounds are compatible, but finally the constraint $m_h > 114.1$ GeV implies that the allowed cross sections do not enter in the DAMA area. Although now larger regions with $0.1 \leq \Omega_{\tilde{\chi}_1^0} h^2 \leq 0.3$ are present, for $A = -M$ these are not compatible with the experimental bounds.

One also finds that the regions excluded by the UFB-3 constraint are much smaller than in those cases where the initial scale is the GUT one. For example for $A = 0$ (and $A = M$) no region is excluded (see however Fig. 13 for the GUT case). For $A = -M$ the region excluded by the UFB-3 is smaller than the one forbidden by the LSP bound. We have to go to $A = -2M$ to have it larger.

In the plot on the left frame of Fig. 19 we summarize the above results for $\tan \beta = 10$, concerning the cross section $\sigma_{\tilde{\chi}_1^0-p}$, showing the values of $\sigma_{\tilde{\chi}_1^0-p}$ allowed by all experimental constraints as a function of the neutralino mass $m_{\tilde{\chi}_1^0}$, for $A = -2M$. Only in this case there are dark grey dots corresponding to points having a relic neutralino density within the preferred range $0.1 \leq \Omega_{\tilde{\chi}_1^0} h^2 \leq 0.3$. Given the narrow range of these points, they overlap in the figure with those excluded by the UFB-3 constraint. They correspond to $150 \lesssim m_{\tilde{\chi}_1^0} \lesssim 250$ GeV, and e.g. the mass of the lightest stop, \tilde{t}_1 , is between 250 and 340 GeV.

Qualitatively, similar results are obtained for larger values of $\tan \beta$. For example, for $\tan \beta = 35$ only for $A = -2M$ we obtain points allowed by all experimental and astrophysical constraints, and this is shown in the plot on the right frame of Fig. 19. The upper bound in the cross section is because of the $b \rightarrow s\gamma$ process. Points within the preferred astrophysical range correspond to $\sigma_{\tilde{\chi}_1^0-p} \lesssim 10^{-8}$ pb. Now, there are two allowed regions with $275 \lesssim m_{\tilde{\chi}_1^0} \lesssim 325$ GeV and $370 \lesssim m_{\tilde{\chi}_1^0} \lesssim 420$ GeV. For these, $570 \lesssim m_{\tilde{t}_1} \lesssim 720$ GeV. Let us finally mention that in the case of $\tan \beta = 50$, for $A = -M$ there are points allowed by all experimental and astrophysical constraints, and $\sigma_{\tilde{\chi}_1^0-p} \lesssim 10^{-7}$ pb.

It is worth noticing that in this analysis gaugino mass universality has been

assumed at the high-energy scale, although in this scenario gauge couplings do not unify. This situation is in principle possible in generic SUSY models, however it is not so natural in SUSY models from SUGRA where gaugino masses and gauge couplings are related through the gauge kinetic function. Since an explicit string construction with nonuniversal gauge couplings and gaugino masses will be analyzed in detail in Subsection 5.3, we have chosen to simplify the discussion here assuming gaugino mass universality.

Summarizing, when an intermediate scale is considered in mSUGRA, although the cross section increases significantly the experimental bounds impose $\sigma_{\tilde{\chi}_1^0-p} \lesssim 4 \times 10^{-7}$ pb. And, in fact, at the end of the day, the preferred astrophysical range for the relic neutralino density, $0.1 \leq \Omega_{\tilde{\chi}_1^0} h^2 \leq 0.3$, imposes $\sigma_{\tilde{\chi}_1^0-p} \lesssim 10^{-7}$ pb. Clearly, present experiments are not still sufficient, and more sensitive detectors producing further data are needed, as in the case of a GUT scale.

5.2.3. *SUGRA scenario with non-universal soft terms*

The general situation for the soft parameters in SUGRA is to have a non-universal structure²¹¹. For the case of the observable scalar masses this is due to the non-universal couplings in the Kähler potential between the hidden sector fields breaking SUSY and the observable sector fields. For example, $K = \sum_{\alpha} \tilde{K}_{\alpha}(h_m, h_m^*) C_{\alpha} C_{\alpha}^*$, with \tilde{K}_{α} a function of the hidden-sector fields h_m , will produce non-universal scalar masses $m_{\alpha} \neq m_{\beta}$ if $\tilde{K}_{\alpha} \neq \tilde{K}_{\beta}$. For the case of the gaugino masses this is due to the non-universality of the gauge kinetic functions associated with the different gauge groups $f_a(h_m)$. For example, non-universal gaugino masses are obtained if the f_a have a different dependence on the hidden sector fields. We will see in Subsection 5.3 that general string constructions whose low-energy limit is SUGRA, exhibit these properties²¹¹.

It was shown in the literature that the non-universality of the soft parameters allows to increase the neutralino-proton cross section with respect to the universal case. This can be carried out with non-universal scalar masses and/or gaugino masses. We will concentrate on this possibility here.

(i) *Non-universal scalar masses*

Let us analyse a SUGRA scenario with GUT scale and non-universal soft scalar masses. In fact, non-universality in the Higgs sector, concerning dark matter, was first studied in Refs. 218, 219, 18. Subsequently, non-universality in the sfermion sector was added in the analysis^{220,21,29}. Analyses of the dark matter cross section using generic non-universal soft masses were carried out in Refs. 18, 21, 29, 34, 46, 51, 55, 63, whereas in Refs. 39, 44, 49, 61, 64, 112 $SU(5)$ or $SO(10)$ GUT relations were used. In the light of the recent experimental results, one important consequence of the non-universality is that the cross section can be increased in some regions of

the parameter space.

Let us then parameterized this non-universality in the Higgs sector as follows:

$$m_{H_d}^2 = m^2(1 + \delta_1) , \quad m_{H_u}^2 = m^2(1 + \delta_2) . \quad (26)$$

Concerning squarks and sleptons, in order to avoid potential problems with FCNC, one can assume that the first two generations have a common scalar mass m at M_{GUT} , and that non-universality are allowed only for the third generation:

$$\begin{aligned} m_{Q_L}^2 &= m^2(1 + \delta_3) , & m_{u_R}^2 &= m^2(1 + \delta_4) , \\ m_{e_R}^2 &= m^2(1 + \delta_5) , & m_{d_R}^2 &= m^2(1 + \delta_6) , \\ m_{L_L}^2 &= m^2(1 + \delta_7) , \end{aligned} \quad (27)$$

where $Q_L = (\tilde{t}_L, \tilde{b}_L)$, $L_L = (\tilde{\nu}_L, \tilde{\tau}_L)$, $u_R = \tilde{t}_R$ and $e_R = \tilde{\tau}_R$. Note that whereas $\delta_i \geq -1$, $i = 3, \dots, 7$, in order to avoid an UFB direction breaking charge and colour, $\delta_{1,2} \leq -1$ is possible as long as the conditions $m_1^2 = m_{H_d}^2 + \mu^2 > 0$, $m_2^2 = m_{H_u}^2 + \mu^2 > 0$ are fulfilled.

As discussed for intermediate scales in Subsection 5.2.2, an important factor in order to increase the cross section consists in reducing the value of $|\mu|$. This value is determined by condition (24) and can be significantly reduced for some choices of the δ 's. We can have a qualitative understanding of the effects of the δ 's on μ from the following. First, when $m_{H_u}^2$ at M_{GUT} increases its negative low-energy contribution to Eq. (24) becomes less important. Second, when $m_{Q_L}^2$ and $m_{u_R}^2$ at M_{GUT} decrease, due to their contribution proportional to the top Yukawa coupling in the RGE of $m_{H_u}^2$, the negative contribution of the latter to μ^2 is again less important. Thus one can deduce that μ^2 will be reduced (and hence $\sigma_{\tilde{\chi}_1^0-p}$ increased) by choosing $\delta_{3,4} < 0$ and $\delta_2 > 0$. In fact non-universality in the Higgs sector give the most important effect, and including the one in the sfermion sector the cross section only increases slightly. Thus in what follows we will take $\delta_i = 0$, $i = 3, \dots, 7$.

Concerning the value of the relic density, $\Omega_{\tilde{\chi}_1^0}$ is affected due to the increase of the Higgsino components of $\tilde{\chi}_1^0$ with respect to the dominant bino component of the universal case. The change in μ also determines the presence of the Higgs mediated resonant channels. In contrast to Subsection 5.2.2, the most relevant coannihilation scenarios are $\tilde{\chi}_1^0-\tilde{\tau}_1$, in particular $\tilde{\chi}_1^0-\tilde{\chi}_1^\pm$ coannihilations are only sizeable for $\tan\beta = 35$ in Fig. 20 (see the discussion below), when the μ -parameter becomes small. However, even in this case the area inside the WMAP bounds corresponds to neutralino annihilations, which are enhanced due to enlargement of its Higgsino components.

On the other hand, there is another relevant way of increasing the cross section using the non-universality of the Higgs sector. Note that decreasing $m_{H_d}^2$, i.e. choosing $\delta_1 < 0$, leads to a decrease in m_A^2 given by Eq. (25), and therefore in the mass of the heaviest Higgs H (on the contrary, the lightest Higgs mass, m_h , is almost unaltered, it only decreases less than 1%). This produces an increase in the

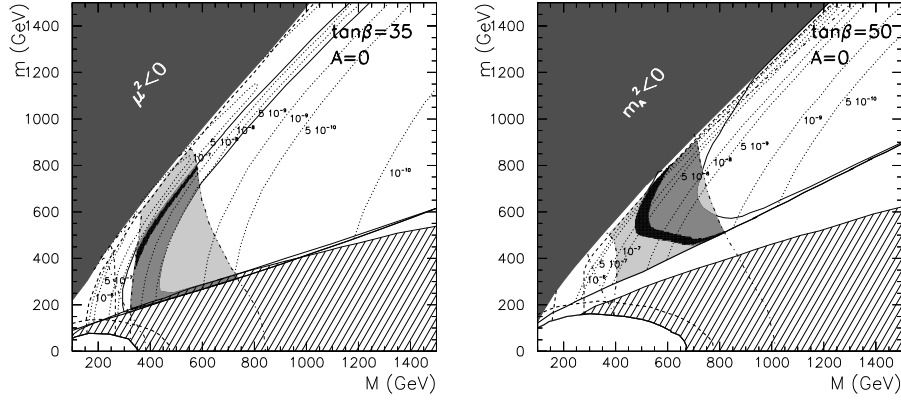


Fig. 20. The same as in Fig. 14 but for the non-universal case *a)* $\delta_1 = 0$, $\delta_2 = 1$, discussed in Eq. (28), with $\tan \beta = 35, 50$ and $A = 0$.

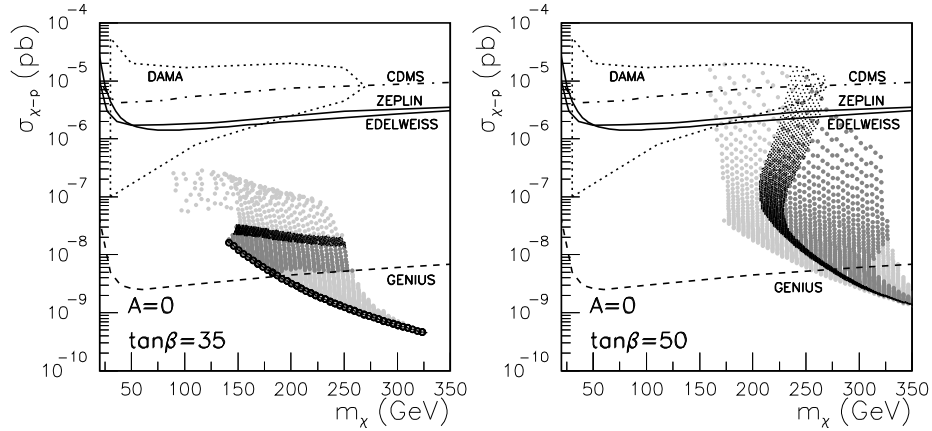


Fig. 21. The same as in Fig. 15 but for the non-universal case *a)* $\delta_1 = 0$, $\delta_2 = 1$, discussed in Eq. (28), with $\tan \beta = 35, 50$ and $A = 0$.

cross section^v.

Thus we will see that, unlike the universal scenario in Subsection 5.2.1., with non-universalities is possible to obtain large values of the cross section, and even some points enter in the DAMA area fulfilling all constraints. Let us analyze three

^vThis effect might also be important when non-universal gaugino masses are taken into account. The contribution of M_3 proportional to the bottom Yukawa coupling in the RGE of $m_{H_d}^2$ will do this smaller if M_3 is large ²²¹.

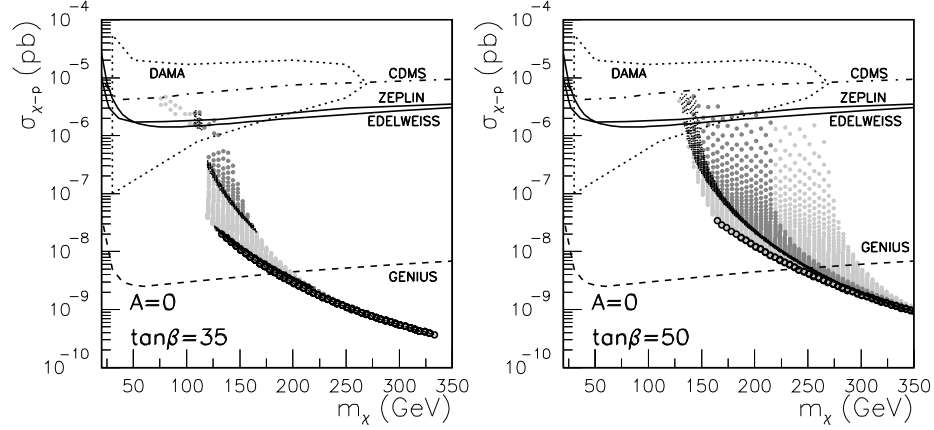


Fig. 22. The same as in Fig. 15 but for the non-universal case $b) \delta_1 = -1, \delta_2 = 0$, discussed in Eq. (28), with $\tan \beta = 35, 50$ and $A = 0$.

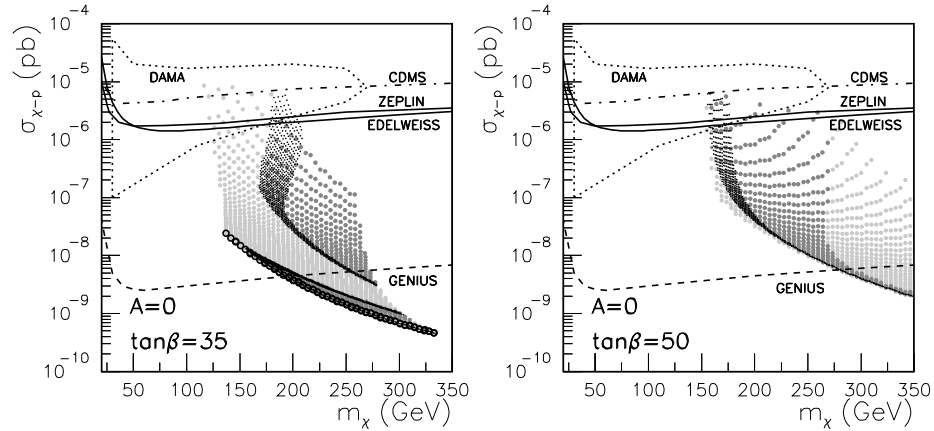


Fig. 23. The same as in Figs. 15 but for the non-universal case $c) \delta_1 = -1, \delta_2 = 1$, discussed in Eq. (28), with $\tan \beta = 35, 50$ and $A = 0$.

representative cases⁶³ with

$$\begin{aligned}
 a) \quad & \delta_1 = 0 \quad , \quad \delta_2 = 1 \quad , \\
 b) \quad & \delta_1 = -1 \quad , \quad \delta_2 = 0 \quad , \\
 c) \quad & \delta_1 = -1 \quad , \quad \delta_2 = 1 \quad .
 \end{aligned} \tag{28}$$

Clearly, the above discussion about decreasing μ^2 applies well to case $a)$, where the variation in $m_{H_u}^2$ through δ_2 is relevant. This is shown in Fig. 20 for $\tan \beta = 35, 50$ and $A = 0$, which can be compared with Fig. 14. Note that now, for $\tan \beta = 35$, there is an important area in the upper left where μ^2 becomes negative due to the increasing in δ_2 with respect to the universal case. A larger area is forbidden for

large values of $\tan \beta$, as e.g. $\tan \beta = 50$, but now because m_A^2 becomes negative. This is similar to what occurs in the universal scenario when $\tan \beta \gtrsim 60$, as discussed in Subsection 5.1. Notice that from Eq. (24) one can write m_A^2 in Eq. (25) as $m_A^2 \approx m_{H_d}^2 - m_{H_u}^2 - M_Z^2$. Since $m_{H_u}^2$ at M_{GUT} increases its negative low-energy contribution becomes less important. In addition, the bottom Yukawa coupling is large and the $m_{H_d}^2$ becomes negative. As a consequence $m_A^2 < 0$.

For $\tan \beta = 35$, although the cross section increases with respect to the universal case, and is generically above the GENIUS lower limit, the present experimental constraints exclude points entering in the DAMA area. This can be seen more clearly comparing Figs. 21 and 15. Notice also that the astrophysical bounds $0.1 \lesssim \Omega_{\tilde{\chi}_1^0} h^2 \lesssim 0.3$ imply $\sigma_{\tilde{\chi}_1^0-p} \approx 10^{-8}$ pb. On the contrary, for $\tan \beta = 50$ there are points entering in the DAMA area, and even part of them fulfil the astrophysical bounds. We have checked that for $A = M$ the figures are similar, although no points enter in the DAMA area, even for $\tan \beta = 50$. On the other hand, the region forbidden by the LSP bound is larger than the one forbidden by the UFB-3 constraint.

We have also checked that larger values of δ_2 , as e.g. $\delta_2 = 1.5$, give rise to similar figures. For small values, $\delta_2 \gtrsim 0.2$ is sufficient to enter in DAMA fulfilling the experimental bounds with $\tan \beta = 50$. In fact, e.g., for $\delta_2 = 0.5, 0.75$ one also gets many points entering in DAMA as for $\delta_2 = 1$, however, they do not fulfil the astrophysical bounds. For the latter one needs $\delta_2 > 0.85$.

Let us finally remark that although $\sin^2(\alpha - \beta)$ is close to 1 in most of the points, some of them can have smaller values when $\tan \beta = 50$. As discussed in Subsection 5.1, these must be points with small values for m_A , and in fact in this case are those close to the region with $m_A^2 < 0$. The same situation occurs for the other cases studied below. Thus, according to our discussion in Subsection 5.1, we use for these points the appropriate bound on the Higgs mass¹⁸⁷. In particular, in Fig. 21, the light grey dots above the CDMS line correspond to these points.

For case *b*) the cross section increases also substantially with respect to the universal case. Now δ_2 is taken vanishing and therefore the value of μ is essentially not modified with respect to the universal case. However, taking $\delta_1 = -1$ produces an increase in the cross section through the decrease in m_A^2 , as discussed previously. As shown explicitly in Fig. 22, for $\tan \beta = 35$ and $A = 0$, there are points in the DAMA region. All of them correspond to $\sin^2(\alpha - \beta)$ not close to 1, and therefore with an experimental bound on the Higgs mass smaller than 114.1 GeV. All points with $\sin^2(\alpha - \beta) \sim 1$ have $\sigma_{\tilde{\chi}_1^0-p} \lesssim 6 \times 10^{-7}$ pb. Note that points with large values of the cross section fulfil in this case the astrophysical bound $\Omega_{\tilde{\chi}_1^0} h^2 \gtrsim 0.1$. Large values of m reduce the resonant effects produced by the Higgs A , and are sufficient to place the relic abundance inside the bounds. For $\tan \beta = 50$, similarly to case *a*), there are points entering in the DAMA area, and part of them fulfil the astrophysical bounds. Those above the ZEPLIN line correspond to $\sin^2(\alpha - \beta)$ not close to 1. For $A = M$ the figures are similar.

We have checked that smaller values of δ_1 , as e.g. $\delta_1 = -1.5, -2$, give also rise to similar figures. For larger values, $\delta_1 \gtrsim -0.4$ is sufficient to enter in DAMA fulfilling the experimental and astrophysical bounds with $\tan \beta = 50$.

Finally, given the above situation concerning the enhancement of the neutralino-proton cross section for *a)* and *b)*, it is clear that the combination of both cases might be interesting. This is carried out in case *c)* where we take $\delta_1 = -1$ and $\delta_2 = 1$. As shown in Fig. 23, cross sections as large as $\sigma_{\tilde{\chi}_1^0-p} \gtrsim 10^{-6}$ pb, entering in DAMA and fulfilling all experimental and astrophysical bounds, can be obtained for $\tan \beta = 35, 50$ and $A = 0$. Those above the ZEPLIN line correspond to $\sin^2(\alpha - \beta)$ not close to 1. On the other hand, for $A = M$ and $\tan \beta = 35$ no points with the correct relic density enter in DAMA. For other cases the results are similar. For example, if we consider $\delta_1 = -0.5$ and $\delta_2 = 1$, one obtains for $\tan \beta = 35$ points entering in DAMA but with $\Omega_{\tilde{\chi}_1^0} h^2 < 0.01$. For $\tan \beta = 50$ a similar plot to the one in Fig. 23 is obtained.

Concerning the restrictions coming from the UFB-3 constraint, we can see in Fig. 20 that these are slightly less important than in the universal scenario (see Fig. 14). Of course, this is not a general result, and different choices of the δ 's can modify the situation. For example, for the same case as in Fig. 20, with $\tan \beta = 35$, but using the opposite choice for the sign of the δ parameters, not only the cross section is smaller, $\sigma_{\tilde{\chi}_1^0-p} < 10^{-8}$ pb, but also the UFB-3 constraint is very restrictive, forbidding all points which are allowed by the experimental and astrophysical constraints.

In summary, when non-universal scalars are allowed in SUGRA, for some special choices of the non-universality, the cross section can be increased a lot with respect to the universal scenario. It is even possible, for some particular values of the parameters, to find points allowed by all experimental and astrophysical constraints with $\sigma_{\tilde{\chi}_1^0-p} \approx 10^{-6}$ pb, and therefore inside the DAMA area. Note however that these points would be basically excluded by the other underground experiments. In any case, the interesting result is that large regions accessible for future experiments are present.

(ii) Non-universal gaugino masses

The effects of the non-universality of gaugino masses on the dark matter relic density in SUGRA scenarios were studied in detail in Refs. 222, 107, 223, 111. Analyses of the neutralino-proton cross section using $SU(5)$ GUT relations for gaugino masses were carried out in Refs. 30, 54, 62, whereas in Refs. 46, 51, 55, 56, 63 generic non-universal soft masses were used. It was also realized that the non-universality in the gaugino masses can increase the cross section.

Let us parameterize this non-universality at M_{GUT} as follows:

$$M_1 = M(1 + \delta'_1), \quad M_2 = M(1 + \delta'_2), \quad M_3 = M(1 + \delta'_3), \quad (29)$$

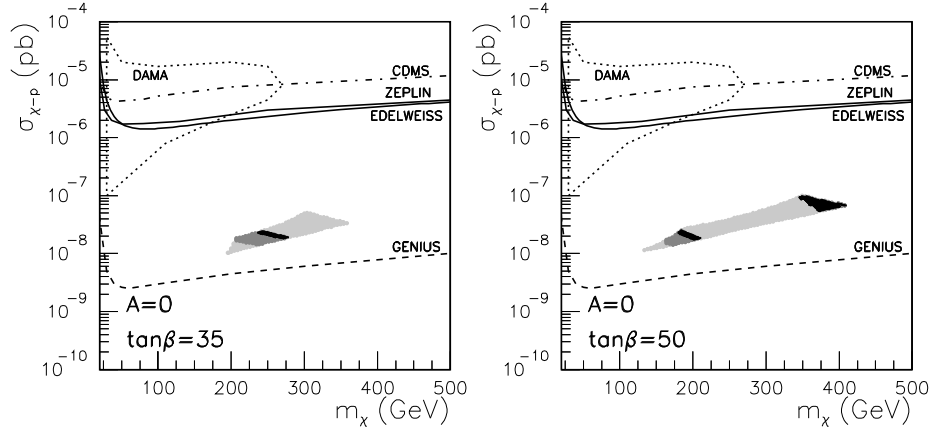


Fig. 24. The same as in Fig. 15 but for the case discussed in Eq. (29) with non-universal soft gaugino masses, $\delta'_{1,2} = 0, \delta'_3 = -0.5$.

where $M_{1,2,3}$ are the bino, wino and gluino masses, respectively. Let us discuss now which values of the parameters are interesting in order to increase the cross section with respect to the universal case $\delta'_i = 0$. In this sense, it is worth noticing that M_3 appears in the RGEs of squark masses, so e.g. their contribution proportional to the top Yukawa coupling in the RGE of $m_{H_u}^2$ will do this less negative if M_3 is small. Although this effect increases the cross section, it is also worth noticing that small values of M_3 also lead to an important decrease in the Higgs mass (we have checked that generically the value of $\sin^2(\alpha - \beta)$ is very close to 1, and therefore we are using the lower bound $m_h = 114.1$ GeV as in the mSUGRA scenario). In addition, $b \rightarrow s\gamma$ and $g_\mu - 2$ constraints are also relevant.

Summarizing, although the cross section increases with respect to the universal case, the present experimental constraints exclude points entering in the DAMA region. This is shown in Fig. 24⁶³ for $\tan\beta = 35, 50$ and $A = 0$, using $\delta'_{1,2} = 0, \delta'_3 = -0.5$, where one can see that there are points allowed by all experimental and astrophysical constraints, but they correspond to $\sigma_{\tilde{\chi}_1^0-p} \lesssim 10^{-7}$ pb.

Finally, as in the previous case with non-universal scalars, increasing the cross section through values at low energy of $m_{H_u}^2$ less negatives implies less important UFB constraints. Now these are not very relevant, and in fact they correspond to the UFB-1 ones.

5.2.4. *Effective MSSM scenario*

In Refs. 16, 25, 36, 37, 38 the authors considered that the uncertainties involved in SUGRA scenarios (such as e.g. the values of the soft parameters, i.e. universality versus non-universality, or the choice of the scale, i.e. M_{GUT} versus M_I) were problematic enough as to work better with a phenomenological SUSY model whose parameters are defined directly at the electroweak scale. This effective scheme of

the MSSM was denoted by effMSSM in Ref. 37. For example, in this work it was imposed for simplicity a set of assumptions at the electroweak scale: a) all trilinear parameters are set to zero except those of the third family, which are unified to a common value A ; b) all squark soft-mass parameters are taken degenerate: $m_{\tilde{q}_i} \equiv m_{\tilde{q}}$; c) all slepton soft-mass parameters are taken degenerate: $m_{\tilde{l}_i} \equiv m_{\tilde{l}}$; d) the gaugino masses, M_1 and M_2 , are assumed to be linked by the GUT relation $M_1 = \frac{5}{3} \tan^2 \theta_W M_2$ (this assumption was relaxed in the fifth and fourth works of Ref. 37 obtaining relic neutralinos significantly lighter than those commonly considered, $m_{\tilde{\chi}_1^0} \gtrsim 50$ GeV). As a consequence, the SUSY parameter space consists of seven independent parameters, chosen them to be: $M_2, \mu, \tan \beta, m_A, m_{\tilde{q}}, m_{\tilde{l}}, A$.

Obviously, the scenarios studied in the previous Subsections, where some boundary conditions at the high scale are imposed and then the RGEs are used in order to obtain the low-energy spectrum, should be a subset of the general effMSSM scenario (i.e. without any assumption). In the effMSSM with the above assumptions, after imposing the experimental and astrophysical constraints, points with cross sections entering in the DAMA area can be obtained. This is similar to the result obtained when non-universal soft scalar masses were considered in the previous Subsection. Note in this sense that varying μ and m_A arbitrarily corresponds to vary m_{H_u} and m_{H_d} .

5.3. Superstring predictions for the neutralino-nucleon cross section

Although the standard model provides a correct description of the observable world, there exist, however, strong indications that it is just an effective theory at low energy of some fundamental one. The only candidate for such a theory is, nowadays, the string theory, which have the potential to unify the strong and electroweak interactions with gravitation in a consistent way.

In the late eighties, working in the context of the (perturbative) $E_8 \times E_8$ heterotic superstring, a number of interesting four-dimensional vacua with particle content not far from that of the supersymmetric standard model were found ²²⁴. Until recently, it was thought that this was the only way in order to construct realistic superstring models. However, in the late nineties, it was discovered that explicit models with realistic properties can also be constructed using D-brane configurations from type I string vacua ²²⁵. We will review below these two superstring constructions concerning dark matter detection.

Such constructions have a natural hidden sector built-in: the complex dilaton field S and the complex moduli fields T_i . These gauge singlet fields are generically present in four-dimensional string models: the dilaton arises from the gravitational sector of the theory and the moduli parameterize the size and shape of the compactified variety. Therefore the auxiliary fields of those multiplets can be the seed of SUSY breaking, solving the arbitrariness of SUGRA where the hidden sector is not constrained. In addition, in superstrings, K and f can be computed explicitly

leading to interesting predictions for the soft parameters, and therefore for the value of the neutralino-proton cross section.

5.3.1. $E_8 \times E_8$ heterotic superstring constructions

For any four-dimensional construction coming from the perturbative 10-dimensional heterotic superstring, the tree-level gauge kinetic function is independent of the moduli sector and is simply given by

$$f_a = k_a S , \quad (30)$$

where usually one takes $k_3 = k_2 = \frac{3}{5}k_1 = 1$. In any case, the values k_a are irrelevant for the tree-level computation since they do not contribute to the soft parameters.

On the other hand, the Kähler potential has been computed for several compactification schemes. This is for example the case of 6-dimensional Abelian orbifolds, where three moduli T_i are generically present. For this class of models the Kähler potential has the form

$$K = -\log(S + S^*) - \sum_i \log(T_i + T_i^*) + \sum_\alpha |C^\alpha|^2 \Pi_i(T_i + T_i^*)^{n_\alpha^i} . \quad (31)$$

Here n_α^i are (zero or negative) fractional numbers usually called “modular weights” of the matter fields C^α .

It is important to know what fields, either S or T_i , play the predominant role in the process of SUSY breaking. This will have relevant consequences in determining the pattern of soft parameters, and therefore the spectrum of physical particles. That is why it is very useful to introduce the following parameterization for the VEVs of dilaton and moduli auxiliary fields ²¹¹

$$\begin{aligned} F^S &= \sqrt{3}(S + S^*)m_{3/2} \sin \theta , \\ F^i &= \sqrt{3}(T_i + T_i^*)m_{3/2} \cos \theta \Theta_i , \end{aligned} \quad (32)$$

where $i = 1, 2, 3$ labels the three complex compact dimensions, $m_{3/2}$ is the gravitino mass, and the angle θ and the Θ_i with $\sum_i |\Theta_i|^2 = 1$, just parameterize the direction of the goldstino in the S, T_i field space.

Using this parameterization and eqs. (30) and (31) one obtains the following results for the soft parameters ²¹¹:

$$\begin{aligned} M_a &= \sqrt{3}m_{3/2} \sin \theta , \\ m_\alpha^2 &= m_{3/2}^2 \left(1 + 3 \cos^2 \theta \sum_i n_\alpha^i \Theta_i^2 \right) , \\ A_{\alpha\beta\gamma} &= -\sqrt{3}m_{3/2} \left(\sin \theta + \cos \theta \sum_i \Theta_i \left[1 + n_\alpha^i + n_\beta^i + n_\gamma^i - (T_i + T_i^*) \partial_i \log Y_{\alpha\beta\gamma} \right] \right) . \end{aligned} \quad (33)$$

Although in the case of the A -parameter an explicit T_i -dependence may appear in the term proportional to $\partial_i \log Y_{\alpha\beta\gamma}$, where $Y_{\alpha\beta\gamma}(T_i)$ are the Yukawa couplings,

it disappears in several interesting cases, and we will only consider this possibility here. Using the above information, one can analyze the structure of soft parameters available in Abelian orbifolds.

In the dilaton-dominated case ($\sin \theta = 1$) the soft parameters are universal, and fulfil

$$m = m_{3/2} , \quad M = \sqrt{3}m_{3/2} , \quad A = -M . \quad (34)$$

Of course, they are a subset of the parameter space of mSUGRA, and therefore one should expect small dark matter cross sections, as discussed in Subsection 5.2.1. However, in general, the soft parameters show a lack of universality due to the modular weight dependence (see scalar masses and trilinear parameters in Eq. (33)). For example, assuming an overall modulus, i.e. $T = T_i$ and $\Theta_i = 1/\sqrt{3}$, one obtains

$$m_\alpha^2 = m_{3/2}^2 (1 + n_\alpha \cos^2 \theta) , \quad A_{\alpha\beta\gamma} = -\sqrt{3}m_{3/2} \sin \theta - m_{3/2} \cos \theta (3 + n_\alpha + n_\beta + n_\gamma) , \quad (35)$$

where we have defined the overall modular weights $n_\alpha = \sum_i n_\alpha^i$, and in the case of Z_n Abelian orbifolds they can take the values -1,-2,-3,-4,-5. Fields belonging to the untwisted sector of the orbifold have $n_\alpha = -1$. Fields in the twisted sector but without oscillators have usually modular weight -2 and those with oscillators have $n_\alpha \leq -3$. Note that e.g. for scalars in the untwisted sector

$$m_\alpha^2 + m_\beta^2 + m_\gamma^2 = M^2 , \quad A = -M . \quad (36)$$

These type of relations between fields in the same Yukawa coupling, for instance $m_{Q_L}^2 + m_{u_R}^2 + m_{H_u}^2 = M^2$, were applied in Ref. 39 to the analysis of dark matter detection, with the final result that the neutralino-proton cross section is very similar to the one of the mSUGRA scenario.

On the other hand, the apparent success of the joining of gauge coupling constants at $M_{GUT} \approx 2 \times 10^{16}$ GeV in the MSSM is not automatic in the heterotic superstring, where the natural unification scale is $M_H = \sqrt{\frac{2}{3}}M_{Planck}$, with $\alpha \approx 1/24$ the gauge coupling. Thus unification takes place at energies around a factor ≈ 12 smaller than expected in the heterotic superstring. This problem might be solved with the presence of large string threshold corrections which explain the mismatch between M_{GUT} and M_H . In a sense, what would happen is that the gauge coupling constants will cross at M_{GUT} and diverge towards different values at M_H . These different values appear due to large one-loop stringy threshold corrections. It was found in Ref. 226 that these corrections can be obtained for restricted values of the modular weights of the fields. In fact, assuming flavour independence, one finds that the simplest possibility corresponds to taking the following values for the standard model fields:

$$n_{Q_L} = n_{d_R} = -1 , \quad n_{u_R} = -2 , \quad n_{L_L} = n_{e_R} = -3 , \quad n_{H_u} + n_{H_d} = -5, -4 , \quad (37)$$

where e.g. u_R denotes the three family squarks $\tilde{u}_R, \tilde{c}_R, \tilde{t}_R$.

The above scenario was studied in Ref. 227 for $n_{H_u} = -3, n_{H_d} = -2$, paying special attention to the calculation of the relic neutralino density. Subsequently, in Ref. 17, the authors estimate the direct detection rate for the same scenario. The conclusion was that this is small and large scale detectors are needed to discover the neutralino.

Although, apparently, gaugino masses are always universal in this superstring construction (see Eq. (33)), this is not in fact completely true. It is true that they are universal at tree level because in this case the gauge kinetic function in Eq. (30) is always proportional to the dilaton. However, threshold corrections turn out to be crucial in the $\sin \theta \rightarrow 0$ limit, when SUSY breaking is not dominated by the dilaton. In this case one can observe that gaugino masses turn out to be non-universal, and a different phenomenology is obtained. The relic neutralino density was analyzed in this scenario in Ref. 228. More recently, the relic density was also analyzed in the general context when the soft Lagrangian is dominated by loop contributions in Ref. 229. For another recent work studying also direct and indirect detection in these scenarios see Ref. 230.

Let us finally remark that an analysis of the dark matter using a specific mechanism for the breaking of SUSY has also been carried out in the literature. In particular, it was pointed out in Ref. 231 that, since scalar masses are much larger than gaugino masses when SUSY is spontaneously broken by non-perturbative hidden-sector gaugino condensates, the relic abundance of the neutralinos is too large and incompatible with the astrophysical observations in most of the parameter space.

Summarizing, in the specific compactification models of the heterotic superstring studied here, although the soft terms can be non-universal, the final cross section is generically small and similar to the one of the mSUGRA scenario.

5.3.2. *D-brane constructions*

D-brane constructions are explicit scenarios where two of the interesting situations studied in Section 5.2, non-universality and intermediate scales, may occur. Concerning the latter, it was recently realized that the string scale may be anywhere between the weak and the Planck scale²²⁵. For instance, embedding the SM inside D3-branes in type I strings, the string scale is given by

$$M_I^4 = \frac{\alpha M_{Planck}}{\sqrt{2}} M_c^3, \quad (38)$$

where α is the gauge coupling and M_c is the compactification scale. Thus one gets $M_I \approx 10^{10-12}$ GeV with $M_c \approx 10^{8-10}$ GeV.

As mentioned in Section 5.2.2, these intermediate scales are interesting from the phenomenological viewpoint²¹⁷. They are also interesting from the theoretical viewpoint. For example, in supergravity models supersymmetry can be spontaneously broken in a hidden sector of the theory and the gravitino mass, which sets

the overall scale of the soft terms, is given by:

$$m_{3/2} \approx \frac{F}{M_{Plank}}, \quad (39)$$

where F is the auxiliary field whose vacuum expectation value breaks supersymmetry. Since in supergravity one would expect $F \approx M_{Plank}^2$, one obtains $m_{3/2} \approx M_{Plank}$ and therefore the hierarchy problem solved in principle by supersymmetry would be re-introduced, unless non-perturbative effects such as gaugino condensation produce $F \approx M_W M_{Plank}$. However, if the scale of the fundamental theory is $M_I \approx 10^{11}$ GeV instead of M_{Plank} , then $F \approx M_I^2$ and one gets $m_{3/2} \approx M_W$ in a natural way, without invoking any hierarchically suppressed non-perturbative effect. In the above example with a D3-brane, with a modest input hierarchy^w between string and compactification scales, $M_I \approx 10^{11}$ GeV and $M_c \approx 10^9$ GeV, one obtains the desired hierarchy $M_W/M_{Plank} \approx 10^{-16}$.

The first attempts to study dark matter within these constructions were carried out in scenarios with the unification scale $M_{GUT} \approx 10^{16}$ GeV as the initial scale^{27,30,32} and dilaton-dominated SUSY-breaking scenarios with an intermediate scale as the initial scale³⁵. However, the important issue of the D-brane origin of the $U(1)_Y$ gauge group as a combination of other $U(1)$'s and its influence on the matter distribution in these scenarios was not included in those analyses. When this is taken into account, interesting results are obtained⁴². In particular, scenarios with the gauge group and particle content of the SUSY standard model lead naturally to intermediate values for the string scale, in order to reproduce the value of gauge couplings deduced from experiments. In addition, the soft terms turn out to be generically non universal. Due to these results, in principle, large cross sections can be obtained.

Let us first recall that there are two possible avenues to construct the supersymmetric standard model with D-branes: (a) The $SU(3)_c$, $SU(2)_L$ and $U(1)_Y$ groups of the standard model come from different sets of Dp -branes. (b) They come from the same set of Dp -branes. In the first scenario, it is worth remarking the difficulty of obtaining three copies of quarks and leptons if the gauge groups are attached to different sets of Dp -branes. Thus whether or not this scenario may arise from different sets of Dp -branes in explicit string constructions is an important issue which is worth attacking in the future. Concerning the other scenario (b), models with the gauge group of the standard model and three families of particles have been explicitly built. Let us concentrate first on scenario (a).

Consider for example a type I string scenario⁴² where the gauge group $U(3) \times U(2) \times U(1)$, giving rise to $SU(3) \times SU(2) \times U(1)^3$, arises from three different types of D-branes as shown schematically in Fig. 25, where open strings starting and ending

^wIt is worth noticing, however, that those values would imply $\text{Re}(S) = 1/\alpha \approx 24$ and $\text{Re}(T) = \frac{1}{\alpha} \left(\frac{M_I}{M_c} \right)^4 \approx 10^9$, i.e. one has again a hierarchy problem but now for the VEVs of the fields that one has to determine dynamically.

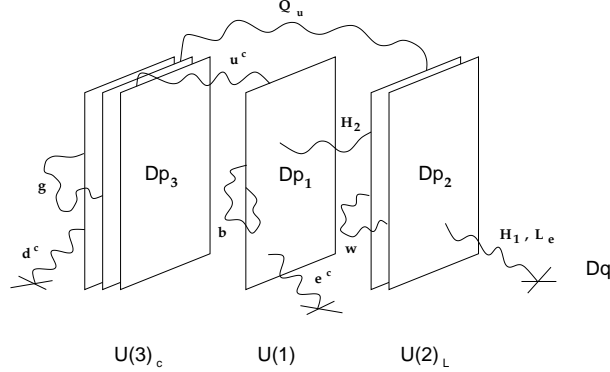


Fig. 25. A generic D-brane scenario giving rise to the gauge bosons and matter of the standard model. It contains three Dp_3 -branes, two Dp_2 -branes and one Dp_1 -brane, where p_N may be either 9 and 5_i or 3 and 7_i . The presence of extra D-branes, say Dq -branes, is also necessary. For each set the Dp_N -branes are in fact on the top of each other.

on the same sets of Dp_N -branes give rise to the gauge bosons of the standard model. For the sake of visualization each set is depicted at parallel locations, but in fact they are intersecting each other. Let us recall that the presence of extra D-branes, say Dq -branes, is also necessary as explained in Ref. 42

Since the standard model gauge group arises from different types of D-branes, the gauge kinetic functions associated with them are different in general, and therefore the gauge couplings are non-universal. On the other hand, $U(1)_Y$ is a linear combination of the three $U(1)$ gauge groups arising from $U(3)$, $U(2)$ and $U(1)$ within the three different D-branes (with the extra $U(1)$'s anomalous and with the associated gauge bosons with masses of the order of the string scale M_I). This implies

$$\frac{1}{\alpha_Y(M_I)} = \frac{2}{\alpha_1(M_I)} + \frac{1}{\alpha_2(M_I)} + \frac{2}{3\alpha_3(M_I)}, \quad (40)$$

where α_k correspond to the gauge couplings of the $U(k)$ branes. As shown in Ref. 42, in order to reproduce the low-energy value of the gauge couplings deduced from experiments, the above equation leads to solutions with the string scale $M_I \approx 10^{10-12}$ GeV. This scenario is shown in Fig. 26 for $M_I = 10^{12}$ GeV. Notice that it is similar to the one shown in Fig. 17a, when discussing intermediate scales in mSUGRA, but with the qualitative difference that the running of the $U(1)_Y$ gauge coupling must fulfil relation (40).

The analysis of the soft terms has been done under the assumption that only the dilaton (S) and moduli (T_i) fields contribute to SUSY breaking and it has been found that these soft terms are generically non-universal. Considering the assignment of gauge bosons and matter of Fig. 25, and using the standard parameterization of Eq. (32), one is able to obtain the following soft terms⁴². The gaugino

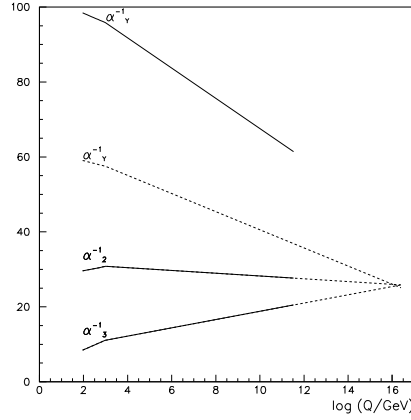


Fig. 26. Running of the gauge couplings of the MSSM with energy Q embedding the gauge groups within different sets of Dp -branes (solid lines). For comparison the running of the MSSM couplings with the usual normalization factor for the hypercharge, $3/5$, is also shown with dashed lines. An overall SUSY scale of 1 TeV is used.

masses associated with the three gauge groups of the standard model are given by

$$\begin{aligned}
 M_3 &= \sqrt{3} m_{3/2} \sin \theta , \\
 M_2 &= \sqrt{3} m_{3/2} \Theta_1 \cos \theta , \\
 M_Y &= \sqrt{3} m_{3/2} \alpha_Y(M_I) \left(\frac{2 \Theta_3 \cos \theta}{\alpha_1(M_I)} + \frac{\Theta_1 \cos \theta}{\alpha_2(M_I)} + \frac{2 \sin \theta}{3 \alpha_3(M_I)} \right) . \quad (41)
 \end{aligned}$$

The soft scalar masses of the three families are given by

$$\begin{aligned}
 m_{Q_L}^2 &= m_{3/2}^2 \left[1 - \frac{3}{2} (1 - \Theta_1^2) \cos^2 \theta \right] , \\
 m_{d_R}^2 &= m_{3/2}^2 \left[1 - \frac{3}{2} (1 - \Theta_2^2) \cos^2 \theta \right] , \\
 m_{u_R}^2 &= m_{3/2}^2 \left[1 - \frac{3}{2} (1 - \Theta_3^2) \cos^2 \theta \right] , \\
 m_{e_R}^2 &= m_{3/2}^2 \left[1 - \frac{3}{2} (\sin^2 \theta + \Theta_1^2 \cos^2 \theta) \right] , \\
 m_{L_L}^2 &= m_{3/2}^2 \left[1 - \frac{3}{2} (\sin^2 \theta + \Theta_3^2 \cos^2 \theta) \right] , \\
 m_{H_u}^2 &= m_{3/2}^2 \left[1 - \frac{3}{2} (\sin^2 \theta + \Theta_2^2 \cos^2 \theta) \right] , \\
 m_{H_d}^2 &= m_{L_L}^2 , \quad (42)
 \end{aligned}$$

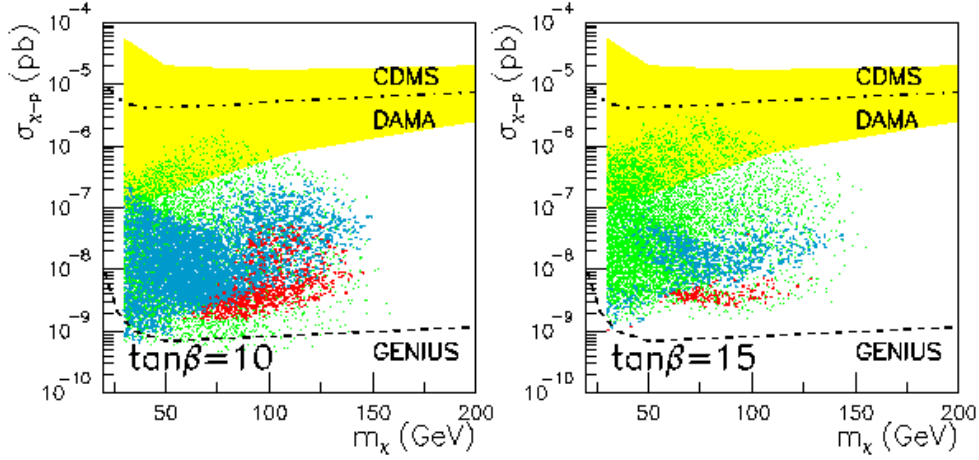


Fig. 27. Scatter plot of the scalar neutralino-proton cross section $\sigma_{\tilde{\chi}_1^0-p}$ as a function of the neutralino mass $m_{\tilde{\chi}_1^0}$ in the D-brane scenario with the string scale $M_I = 10^{12}$ GeV discussed in the text, and for $\tan\beta = 10$ and 15 . Only the big (red and blue) dots fulfil $b \rightarrow s\gamma$ and $g_\mu - 2$ constraints. The red ones correspond to points with $m_h \geq 114$ GeV whereas the blue ones correspond to points with $91 < m_h < 114$ GeV. DAMA and CDMS current experimental limits and projected GENIUS limits are also shown.

where e.g. u_R denotes the three family squarks $\tilde{u}_R, \tilde{c}_R, \tilde{t}_R$. Finally the trilinear parameters of the three families are

$$\begin{aligned} A_u &= \frac{\sqrt{3}}{2} m_{3/2} [(\Theta_2 - \Theta_1 - \Theta_3) \cos \theta - \sin \theta] , \\ A_d &= \frac{\sqrt{3}}{2} m_{3/2} [(\Theta_3 - \Theta_1 - \Theta_2) \cos \theta - \sin \theta] , \\ A_e &= 0 . \end{aligned} \quad (43)$$

Although these formulas for the soft terms imply that one has in principle five free parameters, $m_{3/2}$, θ and Θ_i with $i = 1, 2, 3$, due to relation $\sum_i |\Theta_i|^2 = 1$ only four of them are independent. In the analysis the parameters θ and Θ_i are varied in the whole allowed range, $0 \leq \theta \leq 2\pi$, $-1 \leq \Theta_i \leq 1$. For the gravitino mass, $m_{3/2} \leq 300$ GeV is taken. Concerning Yukawa couplings, their values are fixed imposing the correct fermion mass spectrum at low energies, i.e., one is assuming that Yukawa structures of D-brane scenarios give rise to those values.

Fig. 27 displays a scatter plot of $\sigma_{\tilde{\chi}_1^0-p}$ as a function of the neutralino mass $m_{\tilde{\chi}_1^0}$ for a scanning of the parameter space discussed above⁵¹. Two different values of $\tan\beta$, 10 and 15, are shown. Although the astrophysical and UFB constraints have not been taken into account in the analysis, and $\sin^2(\alpha - \beta)$ has not been computed explicitly, several conclusions can already be drawn. Regions of the parameter space consistent with DAMA limits exist, but the $b \rightarrow s\gamma$ and $g_\mu - 2$ constraints forbid most of them. The latter are shown with small (green) points, and they have $91 <$

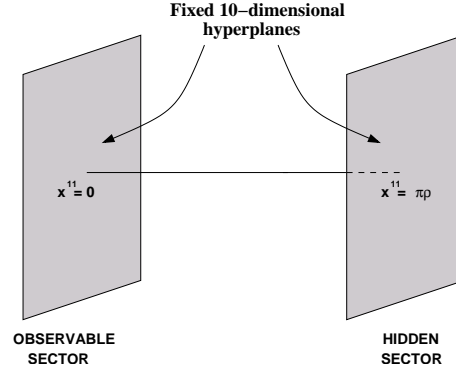


Fig. 28. Schematic of heterotic M-Theory.

$m_h < 114$ GeV. In Fig. 27 only regions with big (red and blue) dots fulfil the above mentioned constraints. The red ones correspond to points with $m_h \geq 114$ GeV whereas the blue ones correspond to points with $91 < m_h < 114$ GeV. It is worth noticing that the larger $\tan\beta$ is, the smaller the regions allowed by the experimental constraints become. For example, increasing $\tan\beta$ the value of $g_\mu - 2$ turns out to be larger and may exceed the experimental bounds^x.

Let us finally mention that other examples with the standard model gauge group embedded in D-branes in a different way, or with larger values of the string scale, can also be found ⁴². The dark matter cross section is qualitatively similar.

Concerning scenario (b), where all gauge groups of the standard model are embedded within the same set of D-branes, and therefore with gauge coupling unification, it can be analyzed similarly to scenario (a). However, in this case the value of the cross section is generically smaller. As mentioned above, in the context of mSUGRA with an intermediate scale, this is due to the different values of α 's at the string scale in both types of scenarios.

Summarizing, in D-brane configurations from type I string non-universal soft terms and intermediate scales arise naturally. Although we saw in Subsection 5.2 that for some values of the parameters this may be interesting in order to increase the value of the cross section, in our case these values are in such a way that the cross section turns out to be essentially below DAMA. However, it is worth noticing that regions accessible for future experiments are present.

5.4. M-Theory predictions for the neutralino-nucleon cross section

The proposal of 11-dimensional M-Theory as a fundamental theory which contains the five 10-dimensional superstring theories, as well as 11-dimensional SUGRA, as

^xHowever, for larger values of the gravitino mass, in some special regions of the parameter space the allowed points may even enter in DAMA ²²¹.

different vacua of its moduli space has motivated a large amount of phenomenological analyses²³². The cornerstone of most of these works is the construction due to Hořava and Witten, who showed that the low-energy limit of M-Theory, compactified on a S^1/Z_2 orbifold with E_8 gauge multiplets on each of the 10-dimensional orbifold fixed planes, was indeed the strong coupling limit of the $E_8 \times E_8$ heterotic string theory. This is shown schematically in Fig. 28.

A resulting 4-dimensional SUGRA can be obtained if six of the remaining dimensions are compactified in a Calabi-Yau manifold. A certain number of virtues were noticed in this theory. The most relevant one was the possibility of tuning the 11-dimensional Planck scale and the orbifold radius so that the GUT-scale, $M_{GUT} \approx 2 \times 10^{16}$ GeV, which is here identified with the inverse of the Calabi-Yau volume, and the Planck scale, $M_{Planck} = 1.2 \times 10^{19}$ GeV, were recovered.

On the other hand, the structure of the soft SUSY-breaking terms has been determined with the result²³³

$$\begin{aligned} M &= \frac{\sqrt{3}m_{3/2}}{1 + \epsilon_O} \left(\sin \theta + \frac{1}{\sqrt{3}}\epsilon_O \cos \theta \right) , \\ m^2 &= m_{3/2}^2 - \frac{3m_{3/2}^2}{(3 + \epsilon_O)^2} \left[\epsilon_O (6 + \epsilon_O) \sin^2 \theta + (3 + 2\epsilon_O) \cos^2 \theta - 2\sqrt{3}\epsilon_O \sin \theta \cos \theta \right] , \\ A &= -\frac{\sqrt{3}m_{3/2}}{3 + \epsilon_O} \left[(3 - 2\epsilon_O) \sin \theta + \sqrt{3}\epsilon_O \cos \theta \right] , \end{aligned} \quad (44)$$

where $-1 < \epsilon_O < 1$, and only one modulus T (also valid in the overall modulus case), with the standard parameterization²¹¹ $F^S = \sqrt{3}(S + S^*)m_{3/2} \sin \theta$, $F^T = (T + T^*)m_{3/2} \cos \theta$, has been assumed. Let us remark that this assumption about the Calabi-Yau compactification leads to interesting phenomenological virtues²³². In particular, the soft SUSY-breaking terms are automatically universal, and therefore the presence of dangerous FCNC is avoided. Examples of such compactifications exist, as e.g. the quintic hypersurface CP^4 . Although these spaces were also known in the context of the weakly-coupled heterotic string, the novel fact in heterotic M-theory is that model building is relatively simple, and the construction of three generation models might be considerably easy.

Using the above results for the soft terms, one can analyze how compatible is the parameter space of heterotic M-theory with the sensitivity of current dark matter detectors. Several analyses of dark matter in M-theory were performed^{234,231,20,235}, paying special attention to the calculation of the relic density. Since in this scenario the soft terms (44) are universal, and it is very unnatural to obtain low scales⁵³, all examples concerning dark matter can be considered as a subset into the parameter space of mSUGRA with a GUT scale. In this sense, one should not expect to obtain high values for $\sigma_{\tilde{\chi}_1^0 - p}$. Let us review this result.

The soft terms are expressed in terms of three free parameters: the gravitino mass $m_{3/2}$, the Goldstino angle, θ , and the parameter ϵ_O . The values of the ϵ_O parameter will be chosen in order to guarantee the correct GUT scale (i.e.,

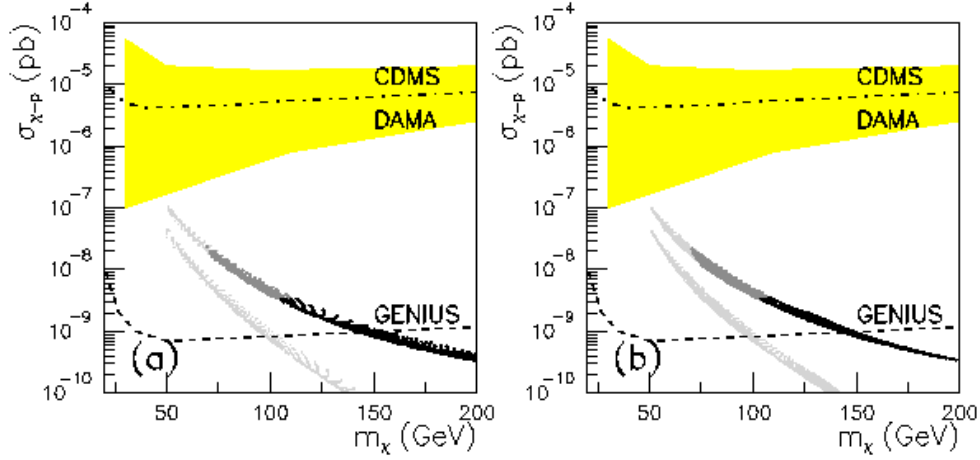


Fig. 29. a) Neutralino-nucleon cross-section versus neutralino mass for $-0.6 \leq \epsilon_O \leq -0.1$. b) The same for $0.1 \leq \epsilon_O < 1$. In both cases only the big (black and dark gray) dots fulfill both $b \rightarrow s\gamma$ and $g_\mu - 2$ constraints. The black ones correspond to points with $m_h \geq 114$ GeV, whereas the dark gray ones correspond to points with $91 \leq m_h \leq 114$ GeV. Current DAMA and CDMS limits and the projected GENIUS limit are shown.

$-0.6 \leq \epsilon_O \leq -0.1$ and $0.1 \leq \epsilon_O < 1$ for non-standard and standard embeddings, respectively). We will take $m_{3/2} = 300$ GeV, and $\tan\beta = 10$, performing a variation of the goldstino angle, θ , in $[0, 2\pi)$. Both cases are depicted in Fig. 29⁵³. Although the astrophysical and UFB constraints have not been taken into account in this analysis, several conclusions can already be drawn. The experimental constraints, $b \rightarrow s\gamma$ and $g_\mu - 2$, put severe bounds, but still neutralinos as light as ~ 100 GeV can be obtained. Once the lower limit on the Higgs mass is applied, the cross-section is as small as $\sigma_{\tilde{\chi}_1^0-p} \sim 3 \times 10^{-9}$ pb, far beyond the reach of present detectors, and close to the lower limit of the projected GENIUS. Let us recall that all the points represented satisfy the experimental constraints on the lower masses of the supersymmetric particles and satisfy $m_h \geq 91$ GeV. Small (light gray) dots represent points not fulfilling the $b \rightarrow s\gamma$ constraint. Large dots do satisfy that constraint, and among these, dark gray points have $91 \text{ GeV} \leq m_h \leq 114 \text{ GeV}$, while black dots satisfy the stronger lower bound for the Higgs mass $m_h > 114$ GeV. Of course, as discussed above, this constraint on the Higgs mass holds in general for the cases with universal soft terms for $\tan\beta \lesssim 50$ and therefore it is the one we should consider here. However, due to the strong restrictions it imposes it is shown explicitly.

Although the predicted values for the cross-section increase, in principle, when larger values of $\tan\beta$ are taken into account, the experimental bounds become much more important in these cases (especially those corresponding to $b \rightarrow s\gamma$ and $g_\mu - 2$), excluding larger regions in the parameter space and thus forbidding large values of $\sigma_{\tilde{\chi}_1^0-p}$.

Finally, it is worth noticing that non-perturbative objects of M-Theory, such as M5-branes, can be shown to survive the orbifold projection of Hořava-Witten construction under certain circumstances, permitting much more freedom to play with gauge groups and with the matter fields that appear. In this context, dark matter implications of vacua with five-branes were investigated in the limit where the five-brane modulus, Z , is the only one responsible for the breaking of supersymmetry⁴³. However, the authors used previous soft-terms computed in the literature, where some corrections were not included²³³. The soft terms are now more involved than those in Eq. (44) and include the F terms associated with S , T and Z . A similar analysis as above, concerning dark matter detection, can be carried out in this case⁵³. The highest value of the cross section, $\sigma_{\tilde{\chi}_1^0-p} \sim 10^{-8}$ pb, can be obtained in the special case in which the five-brane modulus is the only one responsible for SUSY breaking.

Summarizing, as it could be expected from the universality of the soft terms, the predictions of heterotic M-theory with one modulus for the neutralino-nucleon cross section are too low to be probed by the present dark matter detectors. Only future experiments, as e.g. GENIUS, would be able to explore such low values.

6. Conclusions

Nowadays there is overwhelming evidence that most of the mass in the universe (90% and probably more) is some (unknown) non-luminous ‘dark matter’. At galactic and cosmological scales it only manifests through its gravitational interactions with ordinary matter. However, at microscopical scales it might manifest through weak interactions, and this raises the hope that it may be detected in low-energy particle physics experiments.

Plausible candidates for dark matter are Weakly Interacting Massive Particles, the so-called WIMPs. They are very interesting because they can be present in the right amount to explain the observed matter density of the Universe $0.1 \lesssim \Omega h^2 \lesssim 0.3$. The leading candidate for WIMP is the so-called neutralino, a particle predicted by the supersymmetric extension of the standard model. These neutralinos are stable and therefore may be left over from the Big Bang. Thus they will cluster gravitationally with ordinary stars in the galactic halos, and in particular they will be present in our own galaxy, the Milky Way. As a consequence there will be a flux of these dark matter particles on the Earth.

Many underground experiments have been carried out around the world in order to detect this flux. One of them, the DAMA collaboration, even claims to have detected it. They obtain that the preferred range of the WIMP-nucleon cross section is $\approx 10^{-6} - 10^{-5}$ pb for a WIMP mass between 30 and 270 GeV. Unfortunately, this result is controversial because of the negative search result obtained by other experiments like CDMS, EDELWEISS AND ZEPLIN in the same range of parameters. Thus we will have to wait for the next generation of experiments, which are already starting operations or in project, to obtain more information about whether

or not neutralinos, or generically WIMPs, are the evasive dark matter filling the whole Universe. The most sensitive detector, GENIUS, will be able to test a WIMP-nucleon cross section as low as $\approx 10^{-9}$ pb. Indeed such a sensitivity covers a large range of the parameter space of SUSY models with neutralinos as dark matter.

Concerning this point, we have reviewed the known SUSY scenarios, and in particular how big the cross section for the direct detection of neutralinos can be. This analysis is crucial in order to know the possibility of detecting dark matter in the experiments. In particular, we have concentrated on SUGRA and superstring and M-Theory scenarios.

Let us recall that the analysis has been carried out imposing the most recent experimental and astrophysical constraints on the parameter space. Concerning the former, the lower bound on the Higgs mass, the $b \rightarrow s\gamma$ branching ratio, and the muon $g-2$ have been considered. The astrophysical bounds on the matter density mentioned above have also been imposed on the theoretical computation of the relic neutralino density, assuming thermal production. In addition, the constraints that the absence of dangerous charge and colour breaking minima imposes on the parameter space has also been taken into account.

In the usual mSUGRA scenario, where the soft terms are assumed to be universal, and the GUT scale is considered, the cross section is constrained to be $\sigma_{\tilde{\chi}_1^0-p} \lesssim 3 \times 10^{-8}$ pb. Obviously, in this case, present experiments are not sufficient and more sensitive detectors producing further data are needed. A similar conclusion is obtained when an intermediate scale is considered. Although the cross section increases significantly, the experimental bounds impose $\sigma_{\tilde{\chi}_1^0-p} \lesssim 4 \times 10^{-7}$ pb. And, in fact, at the end of the day, the preferred astrophysical range for the relic neutralino density, $0.1 \leq \Omega_{\tilde{\chi}_1^0} h^2 \leq 0.3$, imposes $\sigma_{\tilde{\chi}_1^0-p} \lesssim 10^{-7}$ pb. Still present experiments are not sufficient.

When non-universal scalars are allowed in SUGRA, for some special choices of the non-universality, the cross section can be increased a lot with respect to the universal scenario. It is even possible, for some particular values of the parameters, to find points allowed by all experimental and astrophysical constraints with $\sigma_{\tilde{\chi}_1^0-p} \approx 10^{-6}$ pb, and therefore inside the DAMA area. This is similar to what occurs in the so-called effMSSM scenario. For non-universal gauginos, although the cross section increases, the experimental bounds exclude this possibility.

On the other hand, the low-energy limit of superstring theory and M-theory is SUGRA, and therefore the neutralino will also be a candidate for dark matter in these scenarios. In the context of superstring theory we have reviewed two interesting constructions, the perturbative heterotic superstring and D-branes configurations from type I string, where the soft terms can be computed explicitly in some models. In the former, although the soft terms can be non-universal, the final cross section is similar to the one of the mSUGRA scenario. In the latter, in addition to non-universality, intermediate scales arise naturally, but again the cross section is in general small (although some regions may even be compatible with DAMA).

Finally, due to the universality of the soft SUSY-breaking terms in the heterotic M-Theory scenario analyzed with only one modulus, and the fact that the most natural value for the initial scale is of order 10^{16} GeV, the parameter space can be considered as a subset of mSUGRA. Therefore, the predicted cross-section is very low, $\sigma_{\tilde{\chi}_1^0-p} \lesssim 10^{-8}$ pb, far beyond the reach of the present dark matter experiments.

In summary, underground physics as the one discussed here is crucial in order to detect dark matter. Even if neutralinos are discovered first at future particle accelerators such as LHC, only their direct detection due to their presence in our galactic halo will confirm that they are the sought-after dark matter of the Universe. For that, many new underground experiments are already starting operations or in project, and they will be able to cover an important range of the parameter space of SUSY models.

Acknowledgments

We gratefully acknowledge D.G. Cerdeño for his valuable help, and interesting comments. This work was supported in part by the Spanish DGI of the MCYT under contracts BFM2003-01266 and FPA2003-04597, and under Acción Integrada Hispano-Alemana HA2002-0117; and the European Union under contract HPRN-CT-2000-00148.

References

1. F. Zwicky, *Helv. Phys. Acta* **6** (1933) 110.
2. M.W. Goodman and E. Witten, ‘Detectability of certain dark-matter candidates’, *Phys. Rev. D* **31** (1985) 3059.
3. I. Wasserman, ‘Possibility of detecting heavy neutral fermions in the Galaxy’, *Phys. Rev. D* **33** (1986) 2071.
4. DAMA Collaboration, R. Bernabei et al., ‘Search for WIMP annual modulation signature: results from DAMA/NaI-3 and DAMA/NaI-4 and the global combined analysis’, *Phys. Lett. B* **480** (2000) 23.
5. DAMA Collaboration, R. Bernabei et al., ‘Dark matter search’, *Riv. N. Cim.* **26** (2003) 1 [astro-ph/0307403].
6. CDMS Collaboration, R. Abusaidi et al., ‘Exclusion limits on the WIMP nucleon cross-section from the cryogenic dark matter search’, *Phys. Rev. Lett.* **84** (2000) 5699 [astro-ph/0002471];
D. Abrams, ‘Exclusion limits on the WIMP nucleon cross-section from the cryogenic dark matter search’, *Phys. Rev. D* **66** (2002) 122003 [astro-ph/0203500].
7. EDELWEISS Collaboration, A. Benoit et al., ‘First results of the EDELWEISS WIMP search using a 320-g heat-and-ionization Ge detector’, *Phys. Lett. B* **513** (2001) 15 [astro-ph/0106094]; ‘Improved exclusion limits from the EDELWEISS WIMP search’, *Phys. Lett. B* **545** (2002) 43 [astro-ph/0206271].
8. ZEPLIN Collaboration, N.J.T. Smith et al., ‘Latest results from ZEPLIN I’, talk given at the 4th International Workshop idm2002, York, England, http://www.shf.ac.uk/~phys/idm2002/talks/pdfs/smith_n.pdf.
9. For a review, see H.P. Nilles, ‘Supersymmetry, supergravity and particle physics’, *Phys. Rept.* **110** (1984) 1.

10. For a review, see H.E. Haber and G.L. Kane, ‘The search for supersymmetry: probing physics beyond the standard model’, *Phys. Rept.* **117** (1985) 75.
11. H. Goldberg, ‘Constraint on the photino mass from cosmology’, *Phys. Rev. Lett.* **50** (1983) 1419.
12. J. Ellis, J.S. Hagelin, D.V. Nanopoulos and M. Srednicki, ‘Search for supersymmetry at the $\bar{p}p$ collider’, *Phys. Lett.* **B127** (1983) 233.
13. L.M. Krauss ‘New constraints on ”INO” masses from cosmology (I). Supersymmetric ”inos”’, *Nucl. Phys.* **B227** (1983) 556.
14. J. Ellis, J.S. Hagelin, D.V. Nanopoulos, K.A. Olive and M. Srednicki, ‘Supersymmetric relics from the Big Bang’, *Nucl. Phys.* **B238** (1984) 453.
15. For a review, see G. Jungman, M. Kamionkowski and K. Griest, ‘Supersymmetric dark matter’, *Phys. Rept.* **267** (1996) 195 [hep-ph/9506380].
16. L. Bergström and P. Gondolo, ‘Limits on direct detection of neutralino dark matter from $b \rightarrow s\gamma$ decays’, *Astropart. Phys.* **5** (1996) 263 [hep-ph/9510252];
E.A. Baltz and P. Gondolo, ‘Improved constraints on supersymmetric dark matter from muon $g-2$ ’, *Phys. Rev.* **D67** (2003) 063503 [astro-ph/0207673].
17. S. Khalil, A. Masiero and Q. Shafi, ‘From $b \rightarrow s\gamma$ to the LSP detection rates in minimal string unification models’, *Phys. Rev.* **D56** (1997) 5754 [hep-ph/9704234].
18. A. Bottino, F. Donato, N. Fornengo and S. Scopel, ‘Compatibility of the new DAMA/NaI data on an annual modulation effect in WIMP direct search with a relic neutralino in supergravity schemes’, *Phys. Rev.* **D59** (1999) 095004 [hep-ph/9808459].
19. U. Chattopadhyay, T. Ibrahim and P. Nath, ‘Effects of CP violation on event rates in the direct detection of dark matter’, *Phys. Rev.* **D60** (1999) 063505 [hep-ph/9811362].
20. D. Bailin, G.V. Kraniotis and A. Love, ‘M-Theory dark matter’, *Nucl. Phys.* **B556** (1999) 23 [hep-ph/9812283].
21. R. Arnowitt and P. Nath, ‘Annual modulation signature for the direct detection of Milky Way Wimps and supergravity models’, *Phys. Rev.* **D60** (1999) 044002 [hep-ph/9902237].
22. S. Khalil and Q. Shafi, ‘Supersymmetric CP violating phases and the LSP relic density and detection rates’, *Nucl. Phys.* **B564** (1999) 19 [hep-ph/9904448].
23. T. Falk, A. Ferstl and K.A. Olive, ‘Variations of the neutralino elastic cross-section with CP violating phases’, *Astropart. Phys.* **13** (2000) 301 [hep-ph/9908311].
24. P. Gondolo and K. Freese, ‘CP-violating effects in neutralino scattering and annihilation’, *J. High Energy Phys.* **07** (2002) 052 [hep-ph/9908390];
S.Y. Choi, ‘Neutralino-Nucleus Elastic Scattering in the MSSM with Explicit CP Violation’, hep-ph/9908397.
25. V.A. Bednyakov and H.V. Klapdor-Kleingrothaus, ‘SUSY spectrum constraints on direct dark matter detection’, *Phys. Rev.* **D62** (2000) 043524 [hep-ph/9908427]; ‘Update of the direct detection of dark matter and the role of the nuclear spin’, *Phys. Rev.* **D63** (2001) 095005 [hep-ph/0011233].
26. A. Bottino, F. Donato, N. Fornengo and S. Scopel, ‘Implications for relic neutralinos of the theoretical uncertainties in the neutralino-nucleon cross-section’, *Astropart. Phys.* **13** (2000) 215 [hep-ph/9909228]; ‘Size of the neutralino-nucleon cross-section in the light of a new determination of the pion-nucleon sigma term’, *Astropart. Phys.* **18** (2002) 205 [hep-ph/0111229].
27. S. Khalil, ‘Non universal gaugino phases and the LSP relic density’, *Phys. Lett.* **B484** (2000) 98 [hep-ph/9910408].
28. J. Ellis, A. Ferstl and K.A. Olive, ‘Re-Evaluation of the elastic scattering of supersymmetric dark matter’, *Phys. Lett.* **B481** (2000) 304 [hep-ph/0001005].
29. E. Accomando, R. Arnowitt, B. Dutta and Y. Santoso, ‘Neutralino proton cross sec-

- tions in supergravity models', *Nucl. Phys.* **B585** (2000) 124 [hep-ph/0001019].
30. A. Corsetti and P. Nath, 'Gaugino mass nonuniversality and dark matter in sugra, strings and D-brane models', *Phys. Rev.* **D64** (2001) 125010 [hep-ph/0003186].
31. J.L. Feng, K.T. Matchev and F. Wilczek, 'Neutralino dark matter in focus point supersymmetry', *Phys. Lett.* **B482** (2000) 388 [hep-ph/0004043];
H. Baer and C. Balazs, 'Chi**2 analysis of the minimal supergravity model including WMAP, $g(\mu)$ -2 and $b \rightarrow s$ gamma constraints', *JCAP* **05** (2003) 006 [hep-ph/0303114].
32. R. Arnowitt, B. Dutta and Y. Santoso, 'Neutralino proton cross sections for dark matter in SUGRA and D-brane models', talk given at the Conference 'Sources and Detection of Dark Matter in the Universe', California (2000), hep-ph/0005154.
33. E. Gabrielli, S. Khalil, C. Muñoz and E. Torrente-Lujan 'Initial scales, supersymmetric dark matter and variations of neutralino-nucleon cross sections', *Phys. Rev.* **D63** (2001) 025008 [hep-ph/0006266].
34. J. Ellis, A. Ferstl and K.A. Olive, 'Exploration of elastic scattering rates for supersymmetric dark matter', *Phys. Rev.* **D63** (2001) 065016 [hep-ph/0007113];
J. Ellis, K.A. Olive and Y. Santoso, 'The MSSM parameter space with nonuniversal Higgs masses', *Phys. Lett.* **B539** (2002) 107 [hep-ph/0204192];
J. Ellis, T. Falk, K.A. Olive and Y. Santoso, 'Exploration of the MSSM with nonuniversal Higgs masses', *Nucl. Phys.* **B652** (2003) 259 [hep-ph/0210205];
J. Ellis, A. Ferstl, K.A. Olive and Y. Santoso, 'Direct detection of dark matter in the MSSM with nonuniversal Higgs masses', *Phys. Rev.* **D67** (2003) 123502 [hep-ph/0302032].
35. D. Bailin, G.V. Kraniotis and A. Love, 'Sparticle spectrum and dark matter in type I string theory with an intermediate scale', *Phys. Lett.* **B491** (2000) 161 [hep-ph/0007206].
36. V. Mandic, A.T. Pierce, P. Gondolo and H. Murayama 'The lower bound on the neutralino-nucleon cross section', hep-ph/0008022;
V.A.Bednyakov, 'On possible lower bounds for the direct detection rate of SUSY dark matter', *Phys. Atom. Nucl.* **66** (2003) 490 [hep-ph/0201046].
37. A. Bottino, F. Donato, N. Fornengo and S. Scopel, 'Probing the supersymmetric parameter space by WIMP direct detection', *Phys. Rev.* **D63** (2001) 115009 [hep-ph/0010203]; 'Particle candidates for dark matter: a case for (dominant or subdominant) relic neutralinos', talk given at Les Rencontres de Physique de la Vallée d'Aoste, La Thuile (2001) [hep-ph/0105233]; 'Supersymmetric dark matter', Proceedings of the SPACE PART Conference, La Biodola, Italy (2002), *Nucl. Phys. Proc. Suppl.* **113** (2002) 50 [hep-ph/0208273]; 'Lower bound on the neutralino mass from new data on CMB and implications for relic neutralinos' *Phys. Rev.* **D68** (2003) 043506 [hep-ph/0304080]; 'Light neutralinos and WIMP direct searches', hep-ph/0307303;
A. Bottino, N. Fornengo and S. Scopel, 'Light relic neutralinos', *Phys. Rev.* **D67** (2003) 063519 [hep-ph/0212379].
38. Y.G. Kim, T. Nihei, L. Roszkowski and R. Ruiz de Austri, 'Upper and lower limits on neutralino WIMP mass and spin-independent scattering cross section, and impact of new $(g-2)_\mu$ measurement', *J. High Energy Phys.* **12** (2002) 034 [hep-ph/0208069].
39. M. Drees, Y.G. Kim, T. Kobayashi and M.M. Nojiri, 'Direct detection of neutralino dark matter and the anomalous dipole moment of the muon', *Phys. Rev.* **D63** (2001) 115009 [hep-ph/0011359].
40. M.E. Gomez and J.D. Vergados, 'Cold dark matter detection in SUSY models at large $\tan \beta$ ', *Phys. Lett.* **B512** (2001) 252 [hep-ph/0012020]; 'SUSY cold dark matter detection at large $\tan \beta$ ', Proceedings of CICHEP Conference, Cairo (2001), *Rinton*

- Press* (2001) 248 [hep-ph/0105115].
41. J. Ellis, T. Falk, G. Ganis, K.A. Olive and M. Srednicki, ‘The CMSSM parameter space at large $\tan\beta$ ’, *Phys. Lett.* **B510** (2001) 236 [hep-ph/0102098].
 42. D.G. Cerdeño, E. Gabrielli, S. Khalil, C. Muñoz and E. Torrente-Lujan, ‘Determination of the string scale in D-brane scenarios and dark matter implications’, *Nucl. Phys.* **B603** (2001) 231 [hep-ph/0102270].
 43. D. Bailin, G.V. Kraniotis and A. Love, ‘Dark matter constraints in heterotic M-Theory with five-brane dominance’, *J. High Energy Phys.* **09** (2001) 019 [hep-ph/0103097].
 44. Y.G. Kim and M.M. Nojiri, ‘Implications of muon anomalous magnetic moment for direct detection of neutralino dark matter’, *Prog. Theor. Phys.* **106** (2001) 561 [hep-ph/0104258].
 45. J. Ellis and K.A. Olive, ‘How Finely Tuned is Supersymmetric Dark Matter?’, *Phys. Lett.* **B514** (2001) 114 [hep-ph/0105004].
 46. D.G. Cerdeño, S. Khalil and C. Muñoz, ‘Supersymmetric dark matter and neutralino-nucleon cross section’, Proceedings of CICHEP Conference, Cairo (2001), *Rinton Press* (2001) 214 [hep-ph/0105180].
 47. A. Djouadi, M. Drees, P. Fileviez Perez and M. Muhlleitner, ‘Loop induced Higgs and Z boson couplings to neutralinos and implications for collider and dark matter searches’, *Phys. Rev.* **D65** (2002) 075016 [hep-ph/0109283].
 48. J. Ellis, A. Ferstl and K.A. Olive, ‘Constraints from accelerator experiments on the elastic scattering of CMSSM dark matter’, *Phys. Lett.* **B532** (2002) 318 [hep-ph/0111064].
 49. R. Arnowitt and B. Dutta, ‘Dark matter detection rates in SUGRA models’, talk given at COSMO-01 Conference, Rovaniemi, Finland (2001), hep-ph/0112157.
 50. J. Ellis, K. A. Olive and Y. Santoso, ‘Constraining supersymmetry’, *New. J. Phys.* **4** (2002) 32 [hep-ph/0202110].
 51. D.G. Cerdeño, E. Gabrielli and C. Muñoz, ‘Experimental constraints on the neutralino-nucleon cross section’, talk given at Corfu Conference on Elementary Particle Physics (2001), hep-ph/0204271.
 52. A.B. Lahanas, D.V. Nanopoulos and V.C. Spanos, ‘Supersymmetric dark matter and recent experimental constraints’, talk given at several Conferences, hep-ph/0205225.
 53. D.G. Cerdeño and C. Muñoz, ‘Phenomenology of heterotic M theory with five-branes’, *Phys. Rev.* **D66** (2002) 115007 [hep-ph/0206299].
 54. V. Bertin, E. Nezri and J. Orloff, ‘Neutralino dark matter beyond CMSSM universality’, *J. High Energy Phys.* **02** (2003) 046 [hep-ph/0210034].
 55. R. Arnowitt and B. Dutta, ‘Susy dark matter: closing the parameter space’, talk given at the Conference ‘Beyond the Desert 02’, Oulu, Finland (2002), hep-ph/0210339.
 56. A. Birkedal-Hansen and B.D. Nelson, ‘Relic neutralino densities and detection rates with nonuniversal gaugino masses’, *Phys. Rev.* **D67** (2003) 095006 [hep-ph/0211071]; A. Birkedal-Hansen, ‘rSUGRA: putting nonuniversal gaugino masses on the (W)map’, talk given at SUGRA 20 Conference, Boston (2003), hep-ph/0306144.
 57. J. Ellis, K.A. Olive, Y. Santoso, V.C. Spanos, ‘Supersymmetric dark matter in light of WMAP’, *Phys. Lett.* **B565** (2003) 176 [hep-ph/0303043].
 58. A.B. Lahanas and D.V. Nanopoulos, ‘WMAPing out supersymmetric dark matter and phenomenology’, hep-ph/0303130.
 59. U. Chattopadhyay, A. Corsetti, P. Nath, ‘WMAP constraints, SUSY dark matter and implications for the direct detection of SUSY’, *Phys. Rev.* **D68** (2003) 035005 [hep-ph/0303201].
 60. J.D. Vergados, ‘Theoretical directional and modulated rates for direct SUSY dark matter detection’, *Phys. Rev.* **D67** (2003) 103003 [hep-ph/0303231].

61. R. Dermisek, S. Raby, L. Roszkowski, R. Ruiz De Austri, ‘Dark matter and $B_s \rightarrow \mu^+ \mu^-$ with minimal SO_{10} soft SUSY breaking’, *J. High Energy Phys.* **04** (2003) 037 [hep-ph/0304101].
62. U. Chattopadhyay and D.P. Roy, ‘Higgsino dark matter in a SUGRA model with nonuniversal gaugino masses’, hep-ph/0304108.
63. D.G. Cerdeño, E. Gabrielli, M.E. Gómez and C. Muñoz, ‘Neutralino-nucleon cross section and charge and colour breaking constraints’, *J. High Energy Phys.* **06** (2003) 030 [hep-ph/0304115].
64. H. Baer, C. Balazs, A. Belyaev and J. O’Farril, ‘Direct detection of dark matter in supersymmetric models’, *JCAP* **09** (2003) 007 [hep-ph/0305191].
65. J. Ellis, K.A. Olive, Y. Santoso and V.C. Spanos, ‘Phenomenological constraints on patterns of supersymmetry breaking’, hep-ph/0305212.
66. The LEP Working Group for Higgs Boson Searches, G. Abbiendi et al., ‘Search for the Standard Model Higgs Boson at LEP’, *Phys. Lett.* **B565** (2003) 61 [hep-ex/0306033].
67. For a review, see e.g. S. Bertolini, F. Borzumati, A. Masiero and G. Ridolfi, ‘Effects of supergravity induced electroweak breaking on rare B decays and mixings’, *Nucl. Phys.* **B353** (1991) 591.
68. For a recent review, see e.g. A. Czarnecki and W.J. Marciano, ‘The muon anomalous magnetic moment: a harbinger for new physics’, *Phys. Rev.* **D64** (2001) 013014 [hep-ph/0102122];
S. Narison, ‘Muon and tau anomalies updated’, *Phys. Lett.* **B513** (2001) 53, erratum *ibid.* **B526** (2002) 414 [hep-ph/0103199].
69. See the recent discussion in Ref. 63, and references therein.
70. M.B. Green, J.H. Schwarz and E. Witten, ‘Superstring theory’, Cambridge University Press (1987);
J. Polchinski, ‘String theory’, Cambridge University Press (1998).
71. For a review, see e.g. J.H. Schwarz, ‘From superstrings to M-Theory’, *Phys. Rept.* **315** (1999) 107 [hep-th/9807135].
72. D.P. Roy, ‘Basic constituents of the visible and invisible matter—a microscopic view of the Universe’, physics/0007025.
73. A detailed analysis can be found in M. Persic, P. Salucci and F. Stel, ‘The universal rotation curve of spiral galaxies: I. The dark matter connection’, *Mon. Not. Roy. Astron. Soc.* **281** (1996) 27 [astro-ph/9506004].
74. For a review, see Y. Sofue and V. Rubin, ‘Rotation curves of spiral galaxies’, astro-ph/0010594.
75. For a recent review, see M. Roncadelli, ‘Searching for dark matter’, astro-ph/0307115.
76. A detailed analysis can be found in P. Salucci and M. Persic, ‘Dark matter halos around galaxies’, Proceedings of the Sesto DM1996 Conference, astro-ph/9703027.
77. For a review, see E. Battaner and E. Florido, ‘The rotation curve of spiral galaxies and its cosmological implications’, *Fund. Cosmic Phys.* **21** (2000) 1 [astro-ph/0010475].
78. See e.g. J. Binney and S. Tremaine, ‘Galactic dynamics’, Princeton University Press (1988).
79. For a review, see W.L. Freedman, ‘Determination of cosmological parameters’, *Phys. Scripta* **T85** (2000) 37 [astro-ph/9905222].
80. A. Melchiorri and J. Silk, ‘On the density of Cold Dark Matter’, *Phys. Rev.* **D66** (2002) 041301 [astro-ph/0203200].
81. C.L. Bennett et al., ‘First year Wilkinson microwave anisotropy probe (WMAP) observations: preliminary maps and basic results’, astro-ph/0302207;
D.N. Spergel et al., ‘First year Wilkinson microwave anisotropy probe (WMAP) observations: determination of cosmological parameters’, astro-ph/0302209.

82. A. Finzi, 'On the validity of Newton's law at a long distance', *Mon. Not. R. Astron. Soc.* **127** (1963) 21.
83. See e.g. J. Bekenstein and M. Milgrom, 'Does the missing mass problem signal the breakdown of Newtonian gravity?', *Astrophys. J.* **286** (1984) 7, and references therein.
84. R.H. Sanders, 'Anti-gravity and galaxy rotation curves', *Astron. Astrophys.* **136** (1984) 21.
85. P.D. Mannheim and D. Kazanas, 'Exact vacuum solution to conformal Weyl gravity and galactic rotation curves', *Astrophys. J.* **342** (1989) 635.
86. M. Kenmoku, E. Kitajima and Y. Okamoto and K. Shigemoto, 'Rotation curves of spiral galaxies and large scale structure of Universe under generalized Einstein action', *Int. J. Mod. Phys.* **D2** (1993) 123.
87. S.B. Whitehouse and G.V. Kraniotis, 'A possible explanation of galactic velocity rotation curves in terms of a cosmological constant', astro-ph/9911485.
88. D.N. Vollick, 'Spherically symmetric solutions and dark matter on the brane', *Gen. Rel. Grav.* **34** (2002) 471 [hep-th/0005033].
89. D. Karasik and A. Davidson, 'Geodetic brane gravity', *Phys. Rev.* **D67** (2003) 064012 [gr-qc/0207061].
90. For critical reviews, see D. Scott, M. White, J.D. Cohn and E. Pierpaoli, 'Cosmological difficulties with MODified Newtonian Dynamics (or: la fin du MOND)', astro-ph/0104435;
A. Aguirre, C.P. Burgess, A. Friedland and D. Nolte, 'Astrophysical constraints on modifying gravity at large distances', *Class. Quant. Grav.* **18** (2001) 223 [hep-ph/0105083];
A. Lue and G.D. Starkman, 'Squeezing MOND into a cosmological scenario', astro-ph/0310005.
91. F. Prada et al., 'Observing the dark matter density profile of isolated galaxies', astro-ph/0301360.
92. For a review, see B. Sadoulet, 'Deciphering the nature of dark matter', *Rev. Mod. Phys.* **71** (1999) 197.
93. For recent reviews, see e.g. J.W.F. Valle, 'Neutrinos: summarizing the state-of-the-art', talk given at the Conference 'Dark Matter in Astro and Particle Physics', Cape Town, South Africa (2002), hep-ph/0205216;
P. Aliani, V. Antonelli, R. Ferrari, M. Picariello and E. Torrente-Lujan, 'The solar neutrino puzzle: present situation and future scenarios', talk given at 'Les Rencontres de Physique de la Vallée d'Aoste', 2002, hep-ph/0206308;
S.F. King, 'Neutrino mass models', talk given at Neutrino 2002 Conference, Munich, hep-ph/0208266;
M.C. Gonzalez-Garcia, 'Neutrino masses and mixing: where we stand and where we are going', talk given at SUSY02 Conference, DESY, Hamburg, hep-ph/0211054.
94. R. Cowsik and J. McClelland, 'An upper limit on the neutrino rest mass', *Phys. Rev. Lett.* **29** (1972) 669.
95. R.D. Peccei and H.R. Quinn, 'CP conservation in the presence of instantons', *Phys. Rev. Lett.* **38** (1977) 1440; 'Constraints imposed by CP conservation in the presence of instantons', *Phys. Rev.* **D16** (1977) 1791.
96. J. Ipser and P. Sikivie, 'Are galactic halos made of axions?', *Phys. Rev. Lett.* **50** (1983) 925;
F.W. Stecker and Q. Shafi, 'The evolution of structure in the Universe from axions', *Phys. Rev. Lett.* **50** (1983) 928;
M.S. Turner, F. Wilczek and A. Zee, 'Formation of structure in an axion dominated Universe', *Phys. Lett.* **B125** (1983) 35, erratum *ibid.* **B125** (1983) 519;

- For a review, see M.S. Turner, ‘Windows on the axion’, *Phys. Rept.* **197** (1990) 67.
97. See e.g. M. Kamionkowski and M.S. Turner, ‘Thermal relics: do we know their abundances?’, *Phys. Rev.* **D42** (1990) 3310;
R. Jeannerot, X. Zhang and R.H. Brandenberger, ‘Non-thermal production of neutralino cold dark matter from cosmic string decays’, *J. High Energy Phys.* **12** (1999) 003 [hep-ph/9901357];
T. Moroi and L. Randall, ‘Wino cold dark matter from anomaly-mediated SUSY breaking’, *Nucl. Phys.* **B570** (2000) 455 [hep-ph/9906527];
G. Giudice, E. Kolb and A. Riotto, ‘Largest temperature of the radiation era and its cosmological implications’, *Phys. Rev.* **D64** (2001) 023508 [hep-ph/0005123];
S. Khalil, C. Muñoz and E. Torrente-Lujan, ‘Relic neutralino density in scenarios with intermediate unification scale’, *New J. Phys.* **4** (2002) 27 [hep-ph/0202139];
N. Fornengo, A. Riotto and S. Scopel, ‘Supersymmetric dark matter and the reheating temperature of the Universe’ *Phys. Rev.* **D67** (2003) 023514 [hep-ph/0208072];
S. Profumo and P. Ullio, ‘SUSY dark matter and quintessence’, hep-ph/0309220.
98. K. Griest, ‘Calculations of rates for direct detection of neutralino dark matter’, *Phys. Rev. Lett.* **61** (1988) 666; ‘Cross-sections, relic abundance and detection rates for neutralino dark matter’, *Phys. Rev.* **D38** (1988) 2357, erratum *ibid.* **D39** (1989) 3802.
99. K. Griest, M. Kamionkowski and M.S. Turner, ‘Supersymmetric dark matter above the W mass’, *Phys. Rev.* **D41** (1990) 3565.
100. J. Ellis, L. Roszkowski and Z. Lalak, ‘Higgs effects on the relic supersymmetric particle density’, *Phys. Lett.* **B245** (1990) 545.
101. M. Drees and M.M. Nojiri, ‘The neutralino relic density in minimal N=1 supergravity’, *Phys. Rev.* **D47** (1993) 376 [hep-ph/9207234].
102. K.A. Olive and M. Srednicki, ‘New limits on parameters of the supersymmetric standard model from cosmology’, *Phys. Lett.* **B230** (1989) 78; ‘Cosmological limits on massive LSP’s’, *Nucl. Phys.* **B355** (1991) 208.
103. M. Kamionkowski, *Phys. Rev.* **D44** (1991) 3021;
L. Roszkowski, *Phys. Lett.* **B262** (1991) 59;
J. McDonald, K.A. Olive and M. Srednicki, *Phys. Lett.* **B283** (1992) 80.
104. K. Griest and D. Seckel, ‘Three exceptions in the calculation of relic abundances’, *Phys. Rev.* **D43** (1991) 3191.
105. P. Gondolo and G. Gelmini, ‘Cosmic abundances of stable particles: improved analysis’, *Nucl. Phys.* **B360** (1991) 145;
R. Arnowitt and P. Nath, ‘Susy mass spectrum in $SU(5)$ supergravity grand unification’, *Phys. Rev. Lett.* **69** (1992) 725;
J.L. Lopez, D.V. Nanopoulos and K. Yuan, ‘Accurate neutralino relic density computations in supergravity models’, *Phys. Rev.* **D48** (1993) 2766 [hep-ph/9304216];
M. Drees and A. Yamada, ‘A decisive test of superstring inspired E_6 models’, *Phys. Rev.* **D53** (1996) 1586 [hep-ph/9508254];
M. Srednicki, R. Watkins and K.A. Olive, ‘Calculations of relic densities in the early Universe’, *Nucl. Phys.* **B310** (1988) 693;
T. Nihei, L. Roszkowski and R. Ruiz de Austri, ‘Towards an accurate calculation of the neutralino relic density’, *J. High Energy Phys.* **05** (2001) 063 [hep-ph/0102308];
‘Exact cross sections for the neutralino WIMP pair-annihilation’, *J. High Energy Phys.* **07** (2002) 024 [hep-ph/0206266].
106. S. Mizuta and M. Yamaguchi, ‘Coannihilation effects and relic abundance of Higgsino-dominant LSPs’, *Phys. Lett.* **B298** (1993) 120 [hep-ph/9208251].
107. S. Mizuta, D. Ng and M. Yamaguchi, ‘Phenomenological aspects of supersymmetric standard models without Grand Unification’, *Phys. Lett.* **B300** (1993) 96

- [hep-ph/9208251];
108. J. Ellis, T. Falk and K. A. Olive, ‘Neutralino-stau coannihilation and the cosmological upper limit on the mass of the lightest supersymmetric particle’, *Phys. Lett. B* **444** (1998) 367 [hep-ph/9810360];
J. Ellis, T. Falk, K. A. Olive and M. Srednicki, ‘Calculations of neutralino-stau coannihilation channels and the cosmologically relevant region of MSSM parameter space’, *Astropart. Phys.* **13** (2000) 181, erratum *ibid.* **15** (2001) 413 [hep-ph/9905481];
M. E. Gomez, G. Lazarides and C. Pallis, ‘Supersymmetric Cold Dark Matter with Yukawa Unification’, *Phys. Rev. D* **61** (2000) 123512 [hep-ph/9907261]; ‘Yukawa unification, $b \rightarrow s\gamma$ and bino-stau coannihilation’, *Phys. Lett. B* **487** (2000) 313 [hep-ph/0004028];
A.B. Lahanas, D.V. Nanopoulos and V.C. Spanos, ‘Neutralino relic density in a Universe with a non-vanishing cosmological constant’ *Phys. Rev. D* **62** (2000) 023515 [hep-ph/9909497];
See the work in Ref. 41;
T. Nihei, L. Roszkowski and R. Ruiz de Austri, ‘Exact cross sections for the neutralino-slepton coannihilation’, *J. High Energy Phys.* **07** (2002) 024 [hep-ph/0206266];
See the third work in Ref. 34.
109. J. Edsjö and P. Gondolo, ‘Neutralino Relic Density including Coannihilations’, *Phys. Rev. D* **56** (1997) 1879 [hep-ph/9704361];
R. Arnowitt, B. Dutta and Y. Santoso, ‘Coannihilation effects in supergravity and D-Brane models’, *Nucl. Phys. B* **606** (2001) 59 [hep-ph/0102181];
A. Birkedal-Hansen and B. D. Nelson, ‘The role of wino content in neutralino dark matter’, *Phys. Rev. D* **64** (2001) 015008 [hep-ph/0102075];
H. Baer, C. Balazs and A. Belyaev, ‘Neutralino relic density in minimal supergravity with co-annihilations’, *J. High Energy Phys.* **03** (2002) 042 [hep-ph/0202076];
J. Edsjö, M. Schelke, P. Ullio and P. Gondolo, ‘Accurate relic densities with neutralino, chargino and sfermion coannihilations in mSUGRA’, *JCAP* **04** (2003) 001 [hep-ph/0301106].
110. C. Boehm, A. Djouadi and M. Drees, ‘Light scalar top quarks and supersymmetric dark matter’ *Phys. Rev. D* **62** (2000) 035012 [hep-ph/9911496];
J. Ellis, K. A. Olive and Y. Santoso, ‘Calculations of neutralino-stop coannihilation in the CMSSM’, *Astropart. Phys.* **18** (2003) 395 [hep-ph/0112113].
111. A. Birkedal-Hansen and E. Jeong, ‘Gaugino and Higgsino coannihilations I: Neutralino-neutralino interactions’, *J. High Energy Phys.* **02** (2003) 047 [hep-ph/0210041].
112. S. Profumo, ‘Neutralino dark matter, b-tau Yukawa unification and non-universal sfermion masses’ *Phys. Rev. D* **68** (2003) 015006 [hep-ph/0304071]; ‘Extended coannihilations from non universal sfermion masses’, Talk presented at the XXXVIIIth Rencontres de Moriond, Les Arcs (2003), hep-ph/0305040; ‘Neutralino relic density in supersymmetric GUTs with no-scale boundary conditions above the unification scale’, *J. High Energy Phys.* **06** (2003) 052 [hep-ph/0306119].
113. B.W. Lee and S. Weinberg, ‘Cosmological lower bound on heavy neutrino masses’, *Phys. Rev. Lett.* **39** (1977) 165;
P. Hut, ‘Limits on masses and number of neutral weakly interacting particles’, *Phys. Lett. B* **69** (1977) 85;
M.I. Vysotsky, A.D. Dolgov and Ya.B. Zeldovich ‘Cosmological restriction on neutral lepton masses’, *Pisma Zh. Eksp. Teor. Fiz.* **26** (1977) 200.
114. K. Enqvist, K. Kainulainen and J. Maalampi, ‘Cosmic abundances of very heavy neutrinos’, *Nucl. Phys. B* **317** (1989) 647.

115. S.P. Ahlen et al., ‘Limits on cold dark matter candidates from an ultralow background germanium spectrometer’, *Phys. Lett.* **B195** (1987) 603;
D.O. Caldwell et al., ‘Laboratory limits on galactic cold dark matter’, *Phys. Rev. Lett.* **61** (1988) 510;
D. Reusser et al., ‘Limits on cold dark matter from the Gotthard Ge experiment’, *Phys. Lett.* **B255** (1991) 143;
J. Morales et al., ‘Filtering microphonics in dark matter germanium experiments’, *Nucl. Instrum. Meth.* **A321** (1992) 410;
E. García et al., ‘Dark matter searches with a germanium detector at the Canfranc tunnel’, *Nucl. Phys. B (Proc. Suppl.)* **28A** (1992) 286; ‘Results of a dark matter search with a germanium detector in the Canfranc tunnel’, *Phys. Rev.* **D51** (1995) 1458;
A.K. Drukier et al., ‘Progress report on the search for cold dark matter using ultralow-background germanium detectors at Homestake’, *Nucl. Phys. B (Proc. Suppl.)* **28A** (1992) 293;
M. Beck et al., ‘Searching for dark matter with the enriched detectors of the Heidelberg-Moscow double beta decay experiment’, *Phys. Lett.* **B336** (1994) 141.
116. Kamiokande Collaboration, M. Mori et al., ‘A limit on massive neutrino dark matter from Kamiokande’, *Phys. Lett.* **B289** (1992) 463.
117. G.E. Volovik, ‘Dark matter from $SU(4)$ model’, *JETP Lett.* **78** (2003) 691 [hep-ph/0310006].
118. L.E. Ibañez, ‘The scalar neutrinos as the lightest supersymmetric particles and cosmology’, *Phys. Lett.* **B137** (1984) 160;
J.S. Hagelin, G.L. Kane and S. Raby, ‘Perhaps scalar neutrinos are the lightest supersymmetric partners’, *Nucl. Phys.* **B241** (1984) 638.
119. T. Falk, K.A. Olive and M. Srednicki, ‘Heavy sneutrinos as dark matter’, *Phys. Lett.* **B339** (1994) 248 [hep-ph/9409270].
120. H. Pagels and J.R. Primack, ‘Supersymmetry, cosmology and new TeV physics’, *Phys. Rev. Lett.* **48** (1982) 223;
S. Weinberg, ‘Cosmological constraints on the scale of supersymmetry breaking’, *Phys. Rev. Lett.* **48** (1982) 1303;
See also J. Ellis, K.A. Olive, Y. Santoso and V.C. Spanos, ‘Gravitino dark matter in the CMSSM’, hep-ph/0312262, and references therein.
121. K. Rajagopal, M.S. Turner and F. Wilczek, ‘Cosmological implications of axinos’, *Nucl. Phys.* **B358** (1991) 447;
E.J. Chun, J.E. Kim and H.P. Nilles, ‘Axino mass’, *Phys. Lett.* **B287** (1992) 123.[hep-ph/9205229];
L. Covi, J.E. Kim and L. Roszkowski, ‘Axinos as cold dark matter’, *Phys. Rev. Lett.* **82** (1999) 4180 [hep-ph/9905212].
122. L. Covi, H.B. Kim, J.E. Kim and L. Roszkowski ‘Axinos as dark matter’, *J. High Energy Phys.* **05** (2001) 033 [hep-ph/0101009];
L. Covi, L. Roszkowski and M. Small, ‘Effects of squark processes on the axino CDM abundance’ *J. High Energy Phys.* **07** (2002) 023 [hep-ph/0206119].
123. C.P. Burgess, M. Pospelov and T. ter Veldhuis, ‘The minimal model of nonbaryonic dark matter: a singlet scalar’, *Nucl. Phys.* **B619** (2001) 709 [hep-ph/0011335].
124. A. Birkedal-Hansen and J.G. Wacker, ‘Scalar dark matter from theory space’, hep-ph/0306161.
125. C. Boehm, P. Fayet, ‘Scalar dark matter candidates’, hep-ph/0305261.
126. S. Wolfram, ‘Abundances of stable particles produced in the early Universe’, *Phys. Lett.* **B82** (1979) 65;
C.B. Dover, T.K. Gaisser and G. Steigman, ‘Cosmological constraints on new stable

- hadrons', *Phys. Rev. Lett.* **42** (1979) 1117.
127. J. Bagnasco, M. Dine and S. Thomas 'Detecting technibaryon dark matter', *Phys. Lett.* **B320** (1994) 99 [hep-ph/9310290].
128. For a recent work, see V.L. Teplitz et al., 'SIMP (Strongly Interacting Massive Particle) Search', Proceedings to the 4th UCLA Symposium on Dark Matter DM2000, Marina del Rey, USA, hep-ph/0005111.
129. A. de Rujula, S.L. Glashow and U. Sarid 'Charged dark matter', *Nucl. Phys.* **B333** (1990) 173.
130. D.N. Spergel and P.J. Steinhardt 'Observational evidence for selfinteracting cold dark matter' *Phys. Rev. Lett.* **84** (2000) 3760 [astro-ph/9909386].
131. W.B. Lin, D.H. Huang, X. Zhang and R. H. Brandenberger, 'Non-thermal production of WIMPs and the subgalactic structure of the Universe', *Phys. Rev. Lett.* **86** (2001) 954 [astro-ph/0009003].
132. See e.g. E.W. Kolb, D.J.H. Chung, A. Riotto, 'WIMPZILLAS!', hep-ph/9810361, and references therein.
133. G. Servant and T.M.P. Tait, 'Is the lightest Kaluza-Klein particle a viable dark matter candidate?', *Nucl. Phys.* **B650** (2003) 391 [hep-ph/0206071]; 'Elastic scattering and direct detection of Kaluza-Klein dark matter' *New J. Phys.* **4** (2002) 99 [hep-ph/0209262];
H.-C. Cheng, J.L. Feng and K.T. Matchev, 'Kaluza-Klein dark matter', *Phys. Rev. Lett.* **89** (2002) 211301 [hep-ph/0207125];
D. Hooper and G.D. Kribs, 'Probing Kaluza-Klein dark matter with neutrino telescopes', *Phys. Rev.* **D67** (2003) 055003 [hep-ph/0208261];
G. Bertone, G. Servant and G. Sigl, 'Indirect detection of Kaluza-Klein dark matter', *Phys. Rev.* **D68** (2003) 044008 [hep-ph/0211342].
134. J.L. Feng, A. Rajaraman and F. Takayama, 'Superweakly interacting massive particles', *Phys. Rev. Lett.* **91** (2003) 011302 [hep-ph/0302215].
135. D.J. Gross, J.A. Harvey, E.J. Martinec and R. Rohm, 'The heterotic string', *Phys. Rev. Lett.* **54** (1985) 502.
136. E.W. Kolb, D. Seckel and M.S. Turner 'The shadow world', *Nature* **314** (1985) 415.
137. J. Ellis, J.L. Lopez and D.V. Nanopoulos, 'Confinement of fractional charges yields integer-charged relics in string models', *Phys. Lett.* **B247** (1990) 257.
138. A.E. Faraggi, M. Pospelov, 'Self-interacting dark matter from the hidden heterotic-string sector', *Astropart. Phys.* **16** (2002) 451 [hep-ph/0008223].
139. J.A.R. Cembranos, A. Dobado and A.L. Maroto, 'Brane world dark matter', *Phys. Rev. Lett.* **90** (2003) 241301 [hep-ph/0302041];
G. Shiu and L.-T. Wang, 'D-matter', hep-ph/0311228.
140. S. Ansoldi, A. Aurilia and E. Spallucci, 'Vacuum bubbles nucleation and dark matter production through gauge symmetry rearrangement', *Phys. Rev.* **D64** (2001) 025008 [hep-ph/0104212];
B.A. Bassett, M. Kunz, D. Parkinson and C. Ungarelli 'Condensate cosmology—dark energy from dark matter', *Phys. Rev.* **D68** (2003) 043504 [astro-ph/0211303];
R.N. Mohapatra and A. Perez-Lorenzana, 'Neutrino mass, proton decay and dark matter in TeV scale universal extra dimension models', *Phys. Rev.* **D67** (2003) 075015 [hep-ph/0212254];
A.Yu. Ignatiev and R.R. Volkas, 'Mirror dark matter and large scale structure', *Phys. Rev.* **D68** (2003) 023518 [hep-ph/0304260].
141. K. Freese and P. Gondolo, 'On the direct detection of extragalactic WIMPs', *Phys. Rev.* **D64** (2001) 123502 [astro-ph/0106480].
142. See e.g. the discussion in the Introduction of the review by P.F. Smith and J.D.

- Lewin, ‘Dark matter detection’, *Phys. Rep.* **187** (1990) 203, and in particular Fig. 1.1.
143. J.I. Collar, ‘Clumpy cold dark matter and biological extinctions’, *Phys. Lett.* **B368** (1996) 266 [astro-ph/9512054].
144. K. Zioutas, ‘Evidence of dark matter from biological observations’, *Phys. Lett.* **B242** (1990) 257.
145. S. Abbas and A. Abbas, ‘Volcanogenic dark matter and mass extinctions’, *Astropart. Phys.* **8** (1998) 317 [astro-ph/9612214];
S. Abbas, A. Abbas and S. Mohanty, ‘Double mass extinctions and the volcanogenic dark matter scenario’, astro-ph/9805142.
146. Z.K. Silagadze, ‘TeV scale gravity, mirror universe, and ... dinosaurs’, *Acta Phys. Polon.* **B32** (2001) 99 [hep-ph/0002255]; ‘Mirror objects in the solar system?’, *Acta Phys. Polon.* **B33** (2002) 1325 [astro-ph/0110161].
147. J. Ellis, R.A. Flores and J.D. Lewin, ‘Rates for inelastic nuclear excitation by dark matter particles’, *Phys. Lett.* **B212** (1988) 375;
H. Ejiri, K. Fushimi and H. Ohsumi, ‘Search for spin-coupled dark matter by studying the axial-vector excitation of nuclei’, *Phys. Lett.* **B317** (1993) 14.
148. G.D. Starkman and D.N. Spergel, ‘Proposed new technique for detecting supersymmetric dark matter’, *Phys. Rev. Lett.* **74** (1995) 2623.
149. J.D. Vergados, P. Quentin and D. Strottman, ‘Direct detection of supersymmetric dark matter-Theoretical rates for transitions to excited states’, hep-ph/0310365.
150. Heidelberg-Moscow Collaboration, L. Baudis et al., ‘New limits on dark-matter weakly interacting particles from the Heidelberg-Moscow experiment’, *Phys. Rev.* **D59** (1999) 022001 [hep-ex/9811045].
151. IGEX Collaboration, A. Morales et al., ‘New constraints on WIMPs from the Canfranc IGEX dark matter search’, *Phys. Lett.* **B489** (2000) 268 [hep-ex/0002053].
152. A.K. Drukier, K. Freese and D.N. Spergel, ‘Detecting cold dark-matter candidates’, *Phys. Rev.* **D33** (1986) 3495;
K. Freese, J. Frieman and A. Gould, ‘Signal modulation in cold-dark matter detection’, *Phys. Rev.* **D37** (1988) 3388;
K. Griest, ‘Effect of the Sun’s gravity on the distribution and detection of dark matter near the Earth’, *Phys. Rev.* **D37** (1988) 2703.
153. J.D. Vergados, ‘The role of ionization electrons in direct neutralino detection’, hep-ph/0401151.
154. DAMA Collaboration, R. Bernabei et al., ‘New limits on WIMP search with large-mass low-radioactivity NaI(Tl) set-up at Gran Sasso’, *Phys. Lett.* **B389** (1996) 757.
155. P. Belli, R. Cerulli, N. Fornengo and S. Scopel, ‘Effect of the galactic halo modeling on the DAMA/NaI annual modulation result: an extended analysis of the data for WIMPs with a purely spin-independent coupling’, *Phys. Rev.* **D66** (2002) 043503 [hep-ph/0203242].
156. P. Ullio and M. Kamionkowski, ‘Velocity distributions and annual-modulation signatures of weakly-interacting massive particles’, *J. High Energy Phys.* **03** (2001) 049 [hep-ph/0006183];
A.M. Green, ‘The WIMP annual modulation signal and non-standard halo models’, *Phys. Rev.* **D63** (2001) 043005 [astro-ph/0008318]; ‘A potential WIMP signature for the caustic ring halo model’, *Phys. Rev.* **D63** (2001) 103003 [astro-ph/0012393];
G. Gelmini and P. Gondolo, ‘WIMP annual modulation with opposite phase in late-infall halo models’, *Phys. Rev.* **D64** (2001) 023504 [hep-ph/0012315].
157. A.M. Green, ‘Effect of realistic astrophysical inputs on the phase and shape of the WIMP annual modulation signal’, *Phys. Rev.* **D68** (2003) 023004 [astro-ph/0304446].
158. R. Bernabei et al., ‘On the investigation of possible systematics in WIMP annual

- modulation search', *Eur. Phys. J.* **C18** (2000) 283.
159. R. Bernabei et al., 'DAMA results', talk given at Neutrino Telescopes Conference, Venice (2003), astro-ph/0305542.
160. D.S. Akerib et al., 'New results from the cryogenic dark matter search experiment', hep-ex/0306001.
161. P. Ulloa, M. Kamionkowski and P. Vogel, 'Spin-dependent WIMPs in DAMA?', *J. High Energy Phys.* **07** (2001) 044 [hep-ph/0010036];
D. Smith and N. Weiner, 'Inelastic dark matter', *Phys. Rev.* **D64** (2001) 043502 [hep-ph/0101138]; 'Inelastic dark matter at DAMA, CDMS and future experiments', talk given at DM 2002 Conference, Marina del Rey, California (2002), astro-ph/0208403;
R. Bernabei et al., 'Investigating the DAMA annual modulation data in the framework of inelastic dark matter', *Eur. Phys. J.* **C23** (2002) 61;
G. Prezeau, A. Kurylov, M. Kamionkowski and P. Vogel, 'New contribution to WIMP-nucleus scattering', astro-ph/0309115.
162. C.J. Copi and L.M. Krauss, 'Comparing WIMP interaction rate detectors with annual modulation detectors', *Phys. Rev.* **D67** (2003) 103507 [astro-ph/0208010].
163. IGEX Collaboration, A. Morales et al., 'Improved constraints on WIMPs from the international germanium experiment IGEX', *Phys. Lett.* **B532** (2002) 8 [hep-ex/0110061].
164. HDMS Collaboration, H.V. Klapdor-Kleingrothaus et al., 'First results from the HDMS experiment in the final setup', *Astropart. Phys.* **18** (2003) 525 [hep-ph/0206151].
165. A. Morales, 'Searching for WIMP dark matter: the case for Germanium ionization detectors', talk given at the 29th International Meeting on Fundamental Physics, Sitges, Barcelona (2001), [hep-ex/0111089].
166. CRESST Collaboration, M. Bravin et al., 'The CRESST dark matter search', *Astropart. Phys.* **12** (1999) 107 [hep-ex/9904005];
M. Altmann, 'Results and plans of the CRESST dark matter search', talk given at LP 01 Conference, Rome (2001), astro-ph/0106314.
167. GENIUS Collaboration, H.V. Klapdor-Kleingrothaus et al., 'GENIUS - a Supersensitive Germanium Detector System for Rare Events', hep-ph/9910205.
168. H.V. Klapdor-Kleingrothaus, 'Search for neutrino mass and dark matter in underground experiments', talk given at Non-Accelerator Astroparticle Physics Conference, ICTP (2001), hep-ph/0211033.
169. C. Tomei, A. Dietz, I. Krivosheina and H.V. Klapdor-Kleingrothaus, 'Searching for the annual modulation of dark matter signal with the GENIUS-TF experiment', hep-ph/0306257.
170. D.N. Spergel, 'The motion of the Earth and the detection of WIMPs', *Phys. Rev.* **D37** (1988) 1353.
171. J.D. Vergados, 'The directional rate and the modulation effect for direct supersymmetric dark matter detection', *Part. Nucl. Lett.* **106** (2001) 74 [hep-ph/0010151].
172. DRIFT Collaboration, M.J. Lehner et al., 'The DRIFT project: searching for WIMPs with a directional detector', talk given at Dark 98 Conference, Heidelberg (1998), astro-ph/9905074.
173. For a review, see J.L. Feng, K. T. Matchev and F. Wilczek, 'Prospects for indirect detection of neutralino dark matter', *Phys. Rev.* **D63** (2001) 045024 [astro-ph/0008115].
174. For recent works, see e.g. J. Ellis, J.L. Feng, A. Ferstl, K.T. Matchev and K.A. Olive, 'Supersymmetric dark matter detection at post-LEP benchmark points', contribution to Snowmass 2001 [hep-ph/0111294];
V. Bertin, E. Nezri and J. Orloff, 'Neutrino indirect detection of neutralino dark matter

- in the CMSSM', *Eur. Phys. J. C* **26** (2002) 111 [hep-ph/0204135].
175. I.P. Lopes, J. Silk, S.H. Hansen, 'Helioseismology as a new constraint on SUSY dark matter', astro-ph/0111530.
176. A. Falvard et al., 'Supersymmetric dark matter in M31: can one see neutralino annihilation with CELESTE?', astro-ph/0210184;
L. Pieri and E. Branchini, 'On dark matter annihilation in the Local Group', astro-ph/0307209.
177. See e.g. A. Morselli et al., 'Search for dark matter with GLAST', Proceedings of the SPACE PART Conference, La Biodola, Italy (2002), *Nucl. Phys. Proc. Suppl.* **113** (2002) 213 [astro-ph/0211327];
A. Cesarini et al., 'The galactic center as a dark matter gamma-ray source', astro-ph/0305075.
178. See e.g. G.L. Kane, L.-T. Wang and J.D. Wells, 'Supersymmetry and the positron excess in cosmic rays', *Phys. Rev. D* **65** (2002) 057701 [hep-ph/0108138];
E.A. Baltz, J. Edsjö, K. Freese and P. Gondolo, 'The cosmic ray positron excess and neutralino dark matter', *Phys. Rev. D* **65** (2002) 063511 [astro-ph/0109318].
179. See also Refs. 19 and 23 for a summary.
180. See the first work in Ref. 36.
181. See also Refs. 23 and 28 for a summary.
182. V.A. Bednyakov, 'Aspects of spin-dependent dark matter search', hep-ph/0310041.
183. See the second work in Ref. 25.
184. S. Ambrosanio, A. Dedes, S. Heinemeyer, S. Su and G. Weiglein, 'Implications of the Higgs boson searches on different soft SUSY-breaking scenarios', *Nucl. Phys. B* **624** (2002) 3 [hep-ph/0106255].
185. J.F. Gunion and H.E. Haber, 'Higgs bosons in supersymmetric models.1.' *Nucl. Phys. B* **272** (1986) 1, erratum *ibid.* **B402** (1993) 567; 'Higgs bosons in supersymmetric models. 2. Implications for phenomenology', *Nucl. Phys. B* **278** (1986) 449; 'Higgs bosons in supersymmetric models. 3. Decays into neutralino and charginos', *Nucl. Phys. B* **307** (1988) 445.
A. Djouadi, J. Kalinowski and P.M. Zerwas, 'Exploring the SUSY Higgs sector at e^+e^- linear colliders: a synopsis', *Z. Phys. C* **57** (1993) 569.
186. See e.g. the discussion in A. Bottino, N. Fornengo and S. Scopel, 'Implications of a possible 115 GeV supersymmetric Higgs boson on detection and cosmological abundance of relic neutralinos', *Nucl. Phys. B* **608** (2001) 461 [hep-ph/0012377].
187. ALEPH Collaboration, R. Barate et al., 'Searches for neutral Higgs bosons in e^+e^- collisions at center-of-mass energies from 192 GeV to 202 GeV', *Phys. Lett. B* **499** (2001) 53 [hep-ex/0010062].
188. S. Heinemeyer, W. Hollik and G. Weiglein, 'FeynHiggs: a program for the calculation of the masses of the neutral CP even Higgs bosons in the MSSM', *Comput. Phys. Commun.* **124** (2000) 76 [hep-ph/9812320]; 'FeynHiggsFast: a program for a fast calculation of masses and mixing angles in the Higgs sector of the MSSM', hep-ph/0002213;
M. Frank, S. Heinemeyer, W. Hollik and G. Weiglein, 'FeynHiggs 1.2: hybrid \overline{MS} /on-shell renormalization for the CP-even Higgs boson sector in the MSSM', hep-ph/0202166;
See also the web page <http://www.feynhiggs.de>
189. J.S. Lee, A. Pilaftsis, M. Carena, S.Y. Choi, M. Drees, J. Ellis and C.E.M. Wagner, 'CPsuperH: a Computational tool for Higgs phenomenology in the minimal supersymmetric standard model with explicit CP violation', hep-ph/0307377;
See also the web page <http://theory.ph.man.ac.uk/~jslee/CPsuperH.html>
190. G. Rodrigo and A. Santamaria, 'QCD matching conditions at thresholds', *Phys. Lett.*

- B313** (1993) 441 [hep-ph/9305305];
G. Rodrigo, A. Pich and A. Santamaria, ‘ $\alpha_s(M_Z)$ from τ decays with matching conditions at three loops’, *Phys. Lett.* **B424** (1998) 367 [hep-ph/9707474];
H. Baer, J. Ferrandis, K. Melnikov and X. Tata, ‘Relating bottom quark mass in $\bar{D}R$ and $\bar{M}S$ regularization schemes’, *Phys. Rev.* **D66** (2002) 074007 [hep-ph/0207126].
191. L.J. Hall, R. Rattazzi and U. Sarid, ‘The top quark mass in supersymmetric $SO(10)$ unification’ *Phys. Rev.* **D50** (1994) 7048 [hep-ph/9306309];
M. Carena, S. Pokorski, M. Olechowski and C.E.M. Wagner, ‘Electroweak symmetry breaking and bottom-top Yukawa unification’, *Nucl. Phys.* **B426** (1994) 269 [hep-ph/9402253];
D.M. Pierce, J.A. Bagger, K.T. Matchev and R.-J. Zhang, ‘Precision corrections in the minimal supersymmetric standard model’ *Nucl. Phys.* **B491** (1997) 3 [hep-ph/9606211].
192. Joint LEP 2 supersymmetry working group,
http://lepsusy.web.cern.ch/lepsusy/www/inos_moriond01/charginos_pub.html
193. Joint LEP 2 supersymmetry working group,
http://alephwww.cern.ch/~ganis/SUSYWG/SLEP/sleptons_2k01.html
194. CLEO Collaboration, S. Chen et al., ‘Branching fraction and photon energy spectrum for $b \rightarrow s\gamma$ ’ *Phys. Rev. Lett.* **87** (2001) 251807 [hep-ex/0108032].
195. BELLE Collaboration, H. Tajima et al., ‘Belle B physics results’, *Int. J. Mod. Phys.* **A17** (2002) 2967 [hep-ex/0111037].
196. G. Belanger, F. Boudjema, A. Pukhov and A. Semenov, ‘micrOMEGAs: a program for calculating the relic density in the MSSM’, *Comput. Phys. Commun.* **149** (2002) 103 [hep-ph/0112278]; ‘MicrOMEGAs: recent developments’, Talk presented at the 4th International Workshop idm2002, York, England, hep-ph/0210327;
G. Belanger, ‘micrOMEGAs and the relic density in the MSSM’, Talk at CPP2001, Tokyo, Japan, hep-ph/0210350;
See also the web page <http://wwwlapp.in2p3.fr/lapth/micromegas>
197. M.E. Gomez, G. Lazarides and C. Pallis, ‘On Yukawa quasi-unification with $\mu < 0$ ’, *Phys. Rev.* **D67** (2003) 097701 [hep-ph/0301064].
198. G. D’Ambrosio, G.F. Giudice, G. Isidori, A. Strumia, ‘Minimal flavour violation: an effective field theory approach’, *Nucl. Phys.* **B645** (2002) 155 [hep-ph/0207036].
199. Muon $g - 2$ Collaboration, G.W. Bennet et al., ‘Measurements of the positive muon anomalous magnetic moment to 0.7 ppm’ *Phys. Rev. Lett.* **89** (2002) 101804 [hep-ex/0208001], erratum *ibid.* **89** (2002) 129903.
200. M. Davier, S. Eidelman, A. Hocker and Z. Zhang, ‘Confronting spectral functions from e^+e^- annihilation and τ decays: consequences for the muon magnetic moment’, *Eur. Phys. J.* **C27** (2003) 497 [hep-ph/0208177];
K. Hagiwara, A.D. Martin, D. Nomura and T. Teubner, ‘The SM prediction of $g-2$ of the muon’, *Phys. Lett.* **B557** (2003) 69 [hep-ph/0209187].
201. CDF Collaboration, F. Abe et al., ‘Search for the decay $B_d^0 \rightarrow \mu^+\mu^-$ and $B_s^0 \rightarrow \mu^+\mu^-$ in $p\bar{p}$ collisions at $\sqrt{s} = 1.8$ TeV’, *Phys. Rev.* **D57** (1998) 3811.
202. See e.g. J.K. Mizukoshi, X. Tata and Y. Wang, ‘Higgs-mediated leptonic decays of B_s and B_d mesons as probes of supersymmetry’, *Phys. Rev.* **D66** (2002) 115003 [hep-ph/0208078], and references therein.
203. Particle Data Group, K. Hagiwara et al., *Phys. Rev.* **D66** (2002) 010001;
For a review, see M.L. Perl, P.C. Kim, V. Halyo, E.R. Lee, I.T. Lee, D. Loomba and K.S. Lackner, ‘The search for stable, massive, elementary particles’, *Int. J. Mod. Phys.* **A16** (2001) 2137 [hep-ex/0102033].
204. For an analysis of this possibility, see the first and second work in Refs. 34 and 37,

respectively;

See also G. Gelmini, ‘Dark matter searches: looking for the cake or its frosting? (detectability of a subdominant component of the CDM)’, hep-ph/0310022.

205. G. Jungman, M. Kamionkowski and K. Griest, ‘Neutdriver’, <http://t8web.lanl.gov/people/jungman/neut-package.html>;
P. Gondolo, J. Edsjö, L. Bergström, P. Ullio and T. Baltz, ‘DarkSUSY’, <http://www.physto.se/~edsjo/darksusy/index.html>;
P. Gondolo, J. Edsjö, P. Ullio, L. Bergström, M. Schelke and E. A. Baltz, ‘DarkSUSY - A numerical package for supersymmetric dark matter calculations’, Proceedings of the 4th International Workshop idm2002, York, England, astro-ph/0211238.
206. A. Pukhov, E. Boos, M. Dubinin, V. Edneral, V. Ilyin, D. Kovalenko, A. Kryukov, V. Savrin, S. Shichanin, A. Semenov, ‘CompHEP: a package for evaluation of Feynman diagrams and integration over multi-particle phase space. User’s manual for version 33’, hep-ph/9908288;
See also the web page <http://www.ifh.de/~pukhov/comphep.html>
207. A. Djouadi, J. Kalinowski and M. Spira, ‘Hdecay: a program for Higgs boson decays in the standard model and its supersymmetric extension’, *Comput. Phys. Commun.* **108** (1998) 56 [hep-ph/9704448];
See also the web page <http://www.desy.de/~spira/hdecay>.
208. M.E. Gomez, G. Lazarides and C. Pallis, ‘Yukawa quasi-unification’, *Nucl. Phys.* **B638** (2002) 165 [hep-ph/0203131];
M.E. Gomez and C. Pallis, ‘Yukawa quasi-unification and neutralino relic density’, hep-ph/0303098.
209. For a review, see e.g. C. Muñoz, ‘Charge and color breaking in supersymmetry and superstrings’, talk given at several Conferences, hep-ph/9709329.
210. J.A. Casas, A. Lleyda and C. Muñoz, ‘Strong constraints on the parameter space of the MSSM from charge and colour breaking minima’, *Nucl. Phys.* **B471** (1996) 3 [hep-ph/9601357].
211. For a review, see A. Brignole, L.E. Ibañez and C. Muñoz, ‘Soft supersymmetry-breaking terms from supergravity and superstring models’, in the book ‘Perspectives on Supersymmetry’, Ed. G. Kane, *World Scientific* (1998) 125 [hep-ph/9707209].
212. L.E. Ibañez and C. López, ‘N=1 supergravity, the weak scale and the low-energy particle spectrum’, *Nucl. Phys.* **B233** (1984) 511;
L.E. Ibañez, C. López and C. Muñoz, ‘The low-energy supersymmetric spectrum according to N=1 supergravity GUTs’ *Nucl. Phys.* **B256** (1985) 218.
213. R.G. Roberts and L. Roszkowski, ‘Implications for minimal supersymmetry from grand unification and the neutralino relic abundance’, *Phys. Lett.* **B309** (1993) 329 [hep-ph/9301267];
G. Kane, C.F. Kolda, L. Roszkowski and J.D. Wells, ‘Study of constrained minimal supersymmetry’, *Phys. Rev.* **D49** (1994) 6173 [hep-ph/9312272].
214. See also, P. Nath and R. Arnowitt, ‘Top quark mass and Higgs mass limits in the standard $SU(5)$ supergravity unification’, *Phys. Lett.* **B289** (1992) 368.
215. H. Baer and M. Brhlik, ‘Cosmological relic density from minimal supergravity with implications for collider physics’, *Phys. Rev.* **D53** (1996) 597 [hep-ph/9508321]; ‘Neutralino dark matter in minimal supergravity: direct detection vs. collider searches’ *Phys. Rev.* **D57** (1998) 567 [hep-ph/9706509];
H. Baer, M. Brhlik, M.A. Diaz, J. Ferrandis, P. Mercadante, P. Quintana and X. Tata, ‘Yukawa unified supersymmetric $SO(10)$ model: cosmology, rare decays and collider searches’, *Phys. Rev.* **D63** (2001) 015007 [hep-ph/0005027];
A.B. Lahanas, D.V. Nanopoulos and V.C. Spanos, ‘Neutralino dark matter elastic

- scattering in a flat and accelerating Universe' *Mod. Phys. Lett.* **A16** (2001) 1229 [hep-ph/0009065].
216. J.L. Feng, K.T. Matchev and T. Moroi, 'Multi-TeV scalars are natural in minimal supergravity', *Phys. Rev. Lett.* **84** (2000) 2322 [hep-ph/9908309]; 'Focus points and naturalness in supersymmetry' *Phys. Rev.* **D61** (2000) 75005 [hep-ph/9909334]
217. See e.g. the discussion in Ref. 46, and references therein.
218. M. Olechowski, S. Pokorski, 'Electroweak symmetry breaking with non-universal scalar soft terms and large $\tan\beta$ solutions', *Phys. Lett.* **B344** (1995) 201 [hep-ph/9407404].
219. V. Berezinsky, A. Bottino, J. Ellis, N. Fornengo, G. Mignola and S. Scopel, 'Neutralino dark matter in supersymmetric models with non-universal scalar mass terms', *Astropart. Phys.* **5** (1996) 1 [hep-ph/9508249]; 'Searching for relic neutralinos using neutrino telescopes', *Astropart. Phys.* **5** (1996) 333 [hep-ph/9603342].
220. R. Arnowitt and P. Nath, 'Non-universal soft SUSY breaking and dark matter', *Phys. Rev.* **D56** (1997) 2820 [hep-ph/9701301]; 'Limits on SUSY particle spectra from proton stability and dark matter constraints', *Phys. Lett.* **B437** (1998) 344 [hep-ph/9801246].
221. D.G. Cerdeño and C. Muñoz, in preparation.
222. K. Griest and L. Roszkowski, 'Effect of relaxing grand unification assumptions on neutralinos in the minimal supersymmetric model' *Phys. Rev.* **D46** (1992) 3309–251.
223. See the fourth work in Ref. 109.
224. See the recent discussion in C. Muñoz, 'A kind of prediction from superstring model building', *J. High Energy Phys.* **12** (2001) 015 [hep-ph/0110381], and references therein.
225. See e.g. the discussion in Ref. 42, and references therein.
226. L.E. Ibañez, D. Lust and G.G. Ross, 'Gauge coupling running in minimal $SU(3) \times SU(2) \times U(1)$ superstring unification', *Phys. Lett.* **B272** (1991) 251 [hep-th/9109053]; L.E. Ibañez and D. Lust, 'Duality anomaly cancellation, minimal string unification and the effective low-energy Lagrangian of 4-D strings', *Nucl. Phys.* **B382** (1992) 305 [hep-th/9202046].
227. S. Khalil, A. Masiero and Q. Shafi, 'Sparticle and Higgs masses within minimal string unification', *Phys. Lett.* **B397** (1997) 197 [hep-ph/9611280].
228. C.-H. Chen, M. Drees and J.F. Gunion, 'A non-standard string/SUSY scenario and its phenomenological implications', *Phys. Rev.* **D55** (1997) 330 [hep-ph/9607421], erratum *ibid.* **D60** (1999) 039901 [hep-ph/9902309].
229. P. Binetruy, A. Birkedal-Hansen, Y. Mambrini and B.D. Nelson, 'Phenomenological aspects of heterotic orbifold models at one loop', hep-ph/0308047.
230. P. Binetruy, Y. Mambrini and E. Nezri, 'Direct and indirect detection of dark matter in heterotic orbifold models', hep-ph/0312155.
231. Y. Kawamura, H.P. Nilles, M. Olechowski and M. Yamaguchi, 'Relic abundance of neutralinos in heterotic string theory: weak coupling vs. strong coupling', *J. High Energy Phys.* **06** (1998) 008 [hep-ph/9805397].
232. For a review, see e.g. C. Muñoz, 'Effective supergravity from heterotic M-Theory and its phenomenological implications', Proceedings of the Corfu Conference on Elementary Particle Physics (1998), *JHEP PRHEP-corfu98/065* (1999) 1 [hep-th/9906152].
233. See e.g. the discussion in Ref. 53, and references therein.
234. D. Bailin, G.V. Kraniotis and A. Love, 'Sparticle spectrum and dark matter in M-Theory', *Phys. Lett.* **B432** (1998) 90 [hep-ph/9803274].
235. S. Khalil, G. Lazarides and C. Pallis, 'Cold dark matter and $b \rightarrow s\gamma$ in the Horava-Witten theory', *Phys. Lett.* **B508** (2001) 327 [hep-ph/0005021].